59 Copies

NASA CR-66543

EVALUATION TESTING OF ZERO GRAVITY HUMIDITY CONTROL SYSTEM

Prepared Under Contract No. NAS 1-5622
by
Biotechnology Organization
Lockheed Missiles & Space Company
Sunnyvale, California

NATIONAL AERONAUTICS AND SPACE ADMINISTRATION
LANGLEY RESEARCH CENTER
LANGLEY STATION
HAMPTON, VIRGINIA

NASA CR-66543

EVALUATION TESTING OF ZERO GRAVITY HUMIDITY CONTROL SYSTEM

Prepared Under Contract No. NAS 1-5622
by
Biotechnology Organization
Lockheed Missiles & Space Company
Sunnyvale, California

Thomas M. Olcott
and
Richard A. Lamparter
25 October 1967

NATIONAL AERONAUTICS AND SPACE ADMINISTRATION
LANGLEY RESEARCH CENTER
LANGLEY STATION
HAMPTON, VIRGINIA

LIST OF CONTRIBUTORS

Name	Area of Contribution
T. M. Olcott	Project Leader
R. B. Jagow	Model Trade-Off Studies
R. A. Lamparter	Experimental Evaluation
J. W. Brunner	Report Preparation

NASA Technical Monitor

C. Saunders

Life Support Section
Flight Instrumentation Division
NASA Langley Research Center

CONTENTS

ILLUSTRATIONS

EVALUATION TESTING OF ZERO GRAVITY HUMIDITY CONTROL SYSTEM

Prepared by

Thomas M. Olcott
and
Richard A. Lamparter
Biotechnology Organization
Lockheed Missiles & Space Company

SUMMARY

A test and evaluation program was conducted on a Zero Gravity Humidity Control System to establish data for the development of optimum design criteria for the hydrophobic/hydrophilic type humidity control system. The system tested was built by Lockheed and delivered to NASA/LRC under contract NAS 1-5622. The humidity control system was subsequently returned to Lockheed along with associated test equipment for a test and evaluation program. The program was conducted in four separate phases, as follows:

- o Phase One - Development of evaluation criteria and test plan.
- o Phase Two - System integration and checkout, initial steady state tests, and test plan modification.
- o Phase Three - Final steady state and performance evaluation testing and test data analysis.
- o Phase Four - Development of optimum design criteria.

These are described below.

Development of Evaluation Criteria and Test Plan

An optimization trade-off methodology was developed in Phase One to evaluate the various configurations of the humidity control system by developing total equivalent weights, considering weight/power penalties, as a function of performance. These values of total equivalent weight as a function of performance (determined by water removal capability and efficiency) can then be compared for each condition of test of configuration to assess the optimum design and performance parameters.

The procedure for evaluating the humidity control system performance is presented in Appendix A and was used as a basis for developing the test plan also shown in Appendix A. The objective of the test program is to develop data for a trade-off analysis to show the optimum configuration

of the spinner and coalescer in the water separator. Because of test program limitations, no test evaluation of hydrophobic cone mesh sizes or cone geometries was planned.

System Integration and Checkout, Initial Steady State Test, and Test Plan Modification

During system integration and checkout, in the horizontal mode, it was observed that the moisture was coalescing on the plate fin surface of the condensing heat exchanger and gravitating to the lower portions of the heat exchanger/water separator and not reaching the hydrophobic cone. From this observation it was determined that the optimum attitude for simulating zero gravity test conditions was the vertical mode. The test apparatus was reoriented to the vertical mode where initial tests verified that the coalescing function was being performed by the condensing heat exchanger and that the water separator performed at 100 percent efficiency without the coalescer in place.

In addition, it was observed that the hydrophobic cone performance was sensitive to varying water removal rates particularly at high flow rates. Based on these observations, testing was stopped and the test program re-evaluated. It was concluded that the optimum water separator configuration was with no coalescer in place. The coalescer evaluation testing was eliminated from the program and additional cone mesh sizes evaluated. The test plan was modified in accordance with Appendix B and additional hydrophobic cones of 325 mesh screen with finer wire and a 230 mesh screen were selected for fabrication and test evaluation. These cone materials were chosen as optimum based on commercial availability thereby avoiding high cost and schedule delay of special weaves.

Final Steady State and Performance Evaluation Testing and Test Data Analysis

Performance evaluation testing was conducted on three hydrophobic cone materials and three spinner configurations in this phase of the program. The test data, reduced to parametric form, was then plotted in curve form to evaluate the comparative unit performance and select the optimum configuration for additional evaluation testing to determine the effects of varying humidity loads and response to transient conditions. The results showed that the 230 mesh screen hydrophobic cone with no spinner performed with 100 percent water removal efficiency over the entire test range at the lowest power penalty. Additional testing resulted in no performance efficiency change at varying inlet and outlet humidity loads and fast response to transient conditions. The performance data was then normalized to define the pressure/density relationship versus mass flow per unit area for use at all cabin pressures and hydrophobic cone areas.

Development of Optimum Design Criteria

As demonstrated in the sample systems parameters below, the objective of the test and evaluation program to develop optimum design criteria for the zero gravity humidity control system was accomplished. By applying the optimization methodology developed in Phase One (Reference Appendix A), and the reduced data from the test and evaluation program (Reference Design Criteria Section), optimum design criteria can be developed for other systems with water removal requirements up to 0.012 lbs. H_2O/lb. air at flows up to 140 CFM (maximum tested values). Given system flow requirements as in the case in the temperature controlled ECS, optimum cone area and weight can be determined. Given outlet humidity requirements as in the case in the humidity controlled ECS, optimum air flow corresponding to cone areas and weights can be determined.

By assuming values for critical system parameters, optimum design criteria were established for a humidity control system regulated by humidity requirements and for one regulated by temperature control requirements.

Test program results showing the 230 mesh hydrophobic cone with no spinner as the optimum configuration for both the humidity controlled and temperature controlled systems were confirmed in the analysis using normalized data.

The following is a summary of the optimum design criteria established for two sample humidity control systems:

PARAMETER	SAMPLE SYSTEM		REMARKS
	Humidity Controlled	Temperature Controlled	
1. System Power Penalty (lb/kw)	600	600	Assumed
2. System Flow (CFM)	88 (Calculated)	100 (Assumed)	
3. Cone Area (in^3)	28.9 (Assumed)	33.6 (Calculated)	
4. Weight (lbs.)	8.75 (Assumed)	9.8 (Calculated)	
5. System Pressure (psia)	10	10	Assumed
6. Water Removal Rate (-lbs. H_2O/lb.air)	0.012 (Optimum)	Variable up to 0.012 maximum	Maximum measured value from test data. Temperature controlled ECS varies with temperature requirements.

INTRODUCTION

The NASA-Langley Research Center, recognizing future manned space program requirements, directed the Lockheed Missiles & Space Company to conduct a test program on a hydrophobic/hydrophilic type humidity control system to evaluate system performance and establish optimum design criteria. A number of zero gravity water separator concepts are currently under evaluation including rotating units, integrated wick heat exchangers, elbow-wick units, and the Lockheed hydrophobic/hydrophilic design. The Lockheed separator has the advantage of no moving parts, outside of the water pumping system, low pressure loss, ease of maintenance, and large surface areas to prevent clogging. These features have made it a desirable unit for developmental studies. Recognizing these features NASA directed Lockheed to produce a four-man humidity control system of the hydrophobic/hydrophilic type. This unit included a fan and aluminum plate-fin condensing heat exchanger. The system was produced and delivered to NASA as part of contract NAS 1-5622.

In an attempt to evaluate the Lockheed Humidity Control System and gain design data on this type of unit, NASA designed and built a test stand for the gathering of data on the system. The specific purpose of this program is to evaluate the hydrophobic/hydrophilic water separator system in the NASA test stand.

The tasks involved in the program are to:

- o Perform a model trade-off study to establish test parameters and optimization methodology for the experiment.
- o Conduct steady state tests for the purpose of evaluating the unit.
- o Conduct dynamic tests to determine the recovery rate from an upset condition.
- o Conduct tests on the humidity control system at various attitudes.
- o Reduct test data and provide an optimum design criteria for generalized application to future spacecraft.

The program was modified after preliminary testing in the following manner:

- o Modify initial test plan.
- o Fabricate additional hydrophobic cones of different mesh for testing.
- o Delete attitude tests.

This report describes in detail the results of the evaluation testing of the Lockheed Humidity Control System

APPARATUS

The test apparatus consisted of the hydrophobic/hydrophilic humidity control system designed and fabricated by Lockheed for the NASA/LRC, the closed circuit test stand designed and built by the LRC and furnished to Lockheed, and the supporting instrumentation and controls required to run the test. The test set-up,including instrumentation is shown in fig. 1. A schematic of this test system is shown in fig. 2. This schematic includes location of the sensing points for the instrumentation.

Description

The test apparatus is designed to evaluate the operation and performance of the Lockheed humidity control system. The system is a closed air circulating loop with the hydrophobic/hydrophilic humidity control system, reheat chamber, steam feed, and mixing chamber. The hydrophobic/hydrophilic humidity control system components are a fan, condensing heat exchanger, and a water separator. The water separator components are a hydrophobic cone, a coalescer, a spinner, and a hydrophilic sump system consisting of a pump, valves, bladder tank, and a control sensing system. The system is described in Appendix C of this report.

Equipment

The major pieces of supporting equipment consisted of:

- γ_1 measurement - Cambridge Systems Model 992 Dew Point Hygrometer
- γ_1 recorder - Honeywell Electronic 18
- γ_2 and γ_3 measurement Cambridge Systems Model 992 Dew Point Hygrometer
- γ_2 and γ_3 recorder - Leeds and Northrup Speedomax-H
- Flow measurement - Hastings Precision Air Meter
- Pressure measurement - Wallace and Tiernan Gauge
- Pressure loss measurement - Dwyer No. 1425 Hook Gauge
- Steam supply - Hotshot Electric Steam Boiler
- Steam feed control - Honeywell Electr-O-Volt Controller and Control Valve
- Coolant supply - Acme Chiller
- Power supply -0 -28 volt for fan

Fig. 1 - Water Separator Test Apparatus

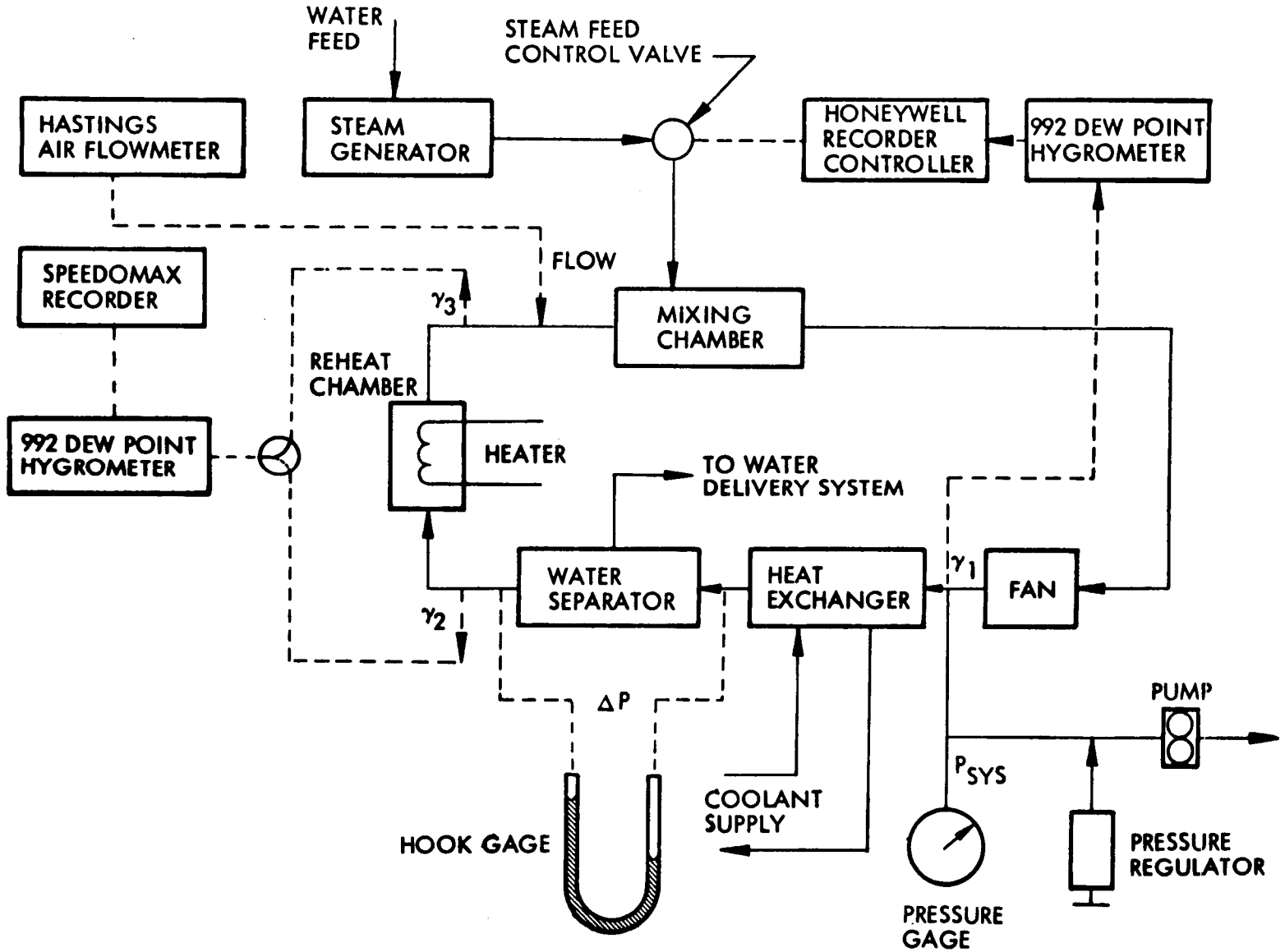

Fig. 2 - Schematic - Water Separator Test System

o Pressure regulator - Fairchild Hiller Strators Vacuum Regulator
o Air pump - Air Control Inc., Dia-Pump

Procedures

Humid air first enters the fan of the humidity control system from the mixing chamber. This component provides the impetus required to circulate the air stream in the closed system. A portion of the air leaving the fan is then sampled to determine the humidity control system inlet dew point (γ_1). The pump which maintains the system at the desired pressure is also connected to the system downstream of the fan. The major portion of the air leaving the fan then passes through the condensing heat exchanger which removes a portion of the inlet water content by condensation. The heat exchanger uses a cold glycol-water solution as a heat sink. Free water and chilled saturated air leaving the heat exchanger then enter the hydrophobic/ hydrophilic water separator. The air is free to pass through the hydrophobic cone while the free water is deflected to the hydrophilic sumps where it is pumped from the system. Air will not pass through the sumps when they are wet. The water separator also includes a coalescer material and a spinner which provides a rotational velocity to the air stream to improve the capability of free water removal. A small portion of the air stream leaving the water separator is sampled to determine the air outlet dew point (γ_2). The water separator outlet stream then passes through a reheat chamber where any free moisture in the air stream can be re-evaporated. A small portion of the air leaving the reheat chamber is sampled to determine the outlet dew point (γ_3).

This measurement also provides the total water passing through the water separator. A Hastings flow meter in the duct downstream of the reheat chamber measures the circulating velocity of the air stream. Steam is fed into the circulating air stream at this point through the test apparatus humidity control system to make up for the free water condensed in the heat exchanger and removed by the water separator. The steam and air mixture then pass through a mixing chamber back to the humidity control system fan inlet.

The humidity sensed by the humidity control system is sampled downstream of the fan. The signal from the dew point sensor is recorded on a Honeywell recorder and used by the Honeywell Electr-O-Volt Controller to maintain the inlet humidity (γ_1) at the proper level. Steam for the unit is generated in a Hotshot Electric Boiler. The samples for recording the water separator outlet and reheat chamber outlet humidity are selected by a 2-way valve. These samples are measured by a second 992 Dew Point Hygrometer and recorded on a Leeds & Northrup Speedomax-H recorder.

The air flow, in feet per minute, is measured by a Hastings Precision Air Meter. This probe is located just upstream of the steam feed and mixing chamber. The measurements of this probe are converted from flow velocity in feet per minute to CFM using the known duct area (3.75 in^2).

The water separator pressure loss which varies from .1 to 3.0 inches of water is measured within an accuracy of 0.01 in. H_2O with a Hook Gauge.

A system tap at the fan outlet is used to maintain the system pressure at the proper level. A Fairchild Hiller Stratos Pressure Regulator is used to control to the proper level and an Air-Control Inc. Dia-Pump is used to maintain pressure. A pressure gauge is used to monitor system pressure at this point.

An Acme Chiller provided the cold water/glycol mixture used as a coolant in the heat exchanger.

During operation of the test apparatus, a number of system characteristics were observed. These characteristics resulted in the following rules of operation to acquire reliable data.

- During massive water break through of the hydrophobic cone, total re-evaporation did not take place in the reheat chamber. As a result, Y_3 was only an indication of break through, not a measure of it.

- In order to get good humidity control at the low steam feed levels for this test, boiler pressure was maintained below 5.0 psig.

- Condensation takes place in the steam feed lines. To prevent injection of free water into the test set-up, a heated steam trap was inserted at the test apparatus inlet.

- To assure complete water removal by the hydrophilic sumps the delta pressure switch setting was maintained between 7 and 8 inches of water.

- Operation of the water collection system air pump caused a step in the pressure differential measurement. As a result, measurements were taken only after the system had settled out after a pulse.

- The unit has a capacity for considerable amounts of free water. This must be removed from the sumps at the start of each run.

- The Honeywell Electr-O-Volt control is difficult to adjust. Recommended settings are:

Reset	.1
Rate	.1
Prop Band	8.5

TEST PROGRAM

A Hydrophobic/Hydrophilic Humidity Control System Model Trade-Off Study and Test Plan (Appendix A) was developed by Lockheed and approved by NASA/LRC for system test and evaluation to establish optimum design criteria.

The primary humidity control system component is the water separator. The test program was designed to evaluate the effects on system performance of the coalescer (3 densities), the spinner (3 vane configurations), and the 325 Mesh Coarse Wire hydrophobic cone.

Initial testing was devoted to familiarization with the humidity control system, test apparatus, and associated instrumentation, and to the development of data acquisition requirements in accordance with the plan of test. Following system checkout, initial steady state testing was performed at varying conditions, configurations, and orientations to determine the optimum test configuration, and to define the scope of the important test parameters. The initial steady state tests showed a need for significant modification of the plan of test including the added scope to evaluate various hydrophobic cone configurations. The testing was stopped, test plans were modified, and two new cone configurations were selected and fabricated. Upon delivery of the two new hydrophobic cones, the test program was conducted in accordance with the modified test plan (Appendix B). In the final phase of the program, the test data was reduced and analyzed to evaluate the humidity control system performance and establish optimum design criteria. The following paragraphs provide a detailed technical discussion and evaluation of the test program. The tabulated data points, taken from the test data log books, which were used to generate the figures in the report are presented in Appendix D. A summary of the significant conclusions from the test program is as follows:

1. The optimum attitude to simulate "zero g" conditions for the water separator is the vertical mode.

2. The optimum configuration of water separator is the 230 Mesh hydrophobic cone with no spinner and no coalescer.

Initial Steady State Tests

System Integration and Checkout.- Upon completion of the test apparatus/instrumentation integration and system checkout, tests were run on the water separator to evaluate separator performance in the horizontal mode.

Initial testing at high air flow rates and low ΔP switch settings showed that an intermittent massive water breakthrough occurred indicating inadequate water removal capacity by the sumps. System testing was then stopped and testing was conducted on sump water flow rate as a function of differential pressure switch setting to determine the optimum water separator/sump ΔP switch settings within the range of test parameters (Appendix D- Run No. 1). The curve showing the relationship of these parameters

is presented in fig.3. The conclusions from this testing are as follows:

- o At low ΔP switch settings, flow falls off rapidly approaching zero at switch settings of 5 inches H_2O ΔP. (Region of inadequate sump water removal capacity resulting in water breakthrough at the separator cone.)

- o At a switch setting of 8 inches H_2O ΔP the sump breaks through and passes air.

As a result, the ΔP switch was set at just below 8 inches H_2O to cover the full test range of water flows with no air flow breakthrough at the sump.

Horizontal Runs.-Continued runs in the horizontal mode (Appendix D Run No. A1 and A2) showed unpredictable performance of the water removal system. Further investigation revealed that the spinner acted as a dam in the horizontal mode, causing water to build up upstream of the spinner resulting in major water pulses when the overflow point was reached. To prevent this condition from occurring, the spinner was removed. This change in configuration resulted in a 100 percent water separator efficiency at conditions up to 115 cfm (Appendix D Run No. A3), which represents a flow well beyond the test design flow of 70 cfm. (The 115 cfm flow was the maximum test apparatus output with the 28 VDC supply.) Heat exchanger studies show that it is characteristic of condensing heat exchangers for water to leave the core in the form of large drops. In the horizontal mode these drops under the influence of the air stream, gravitate from the downstream face of the plate fin core and collect at the bottom of the heat exchanger. Any remaining free water that was carried over by the air stream was trapped by the coalescer where it in turn gravitated to the low spot of the water separator casing. It was felt that the objective of the experiment was not being accomplished in the horizontal mode because water separation was performed primarily by the heat exchanger and coalescer and not by the hydrophobic cone.

To eliminate this test deficiency, the vertical mode was selected for future testing to most closely assimulate "zero g" conditions. In the vertical mode with flow in the direction of gravity, the total free moisture flow is delivered to the hydrophobic cone, thereby placing more than maximum load on the cone because of the added one "g" velocity increment. In addition, the vertical mode causes no effective disturbances to the radial flow distribution. At this point the test apparatus was rotated and set up for operation in the vertical mode.

Vertical Runs.- Initial tests in the vertical mode resulted in 100 percent water separation efficiency within the range of the moisture and velocity load requirements of the plan of test. At conditions above 100 CFM air flow, massive water breakthrough occurred. During breakthrough conditions, the reheat chamber was not able to totally re-evaporate the

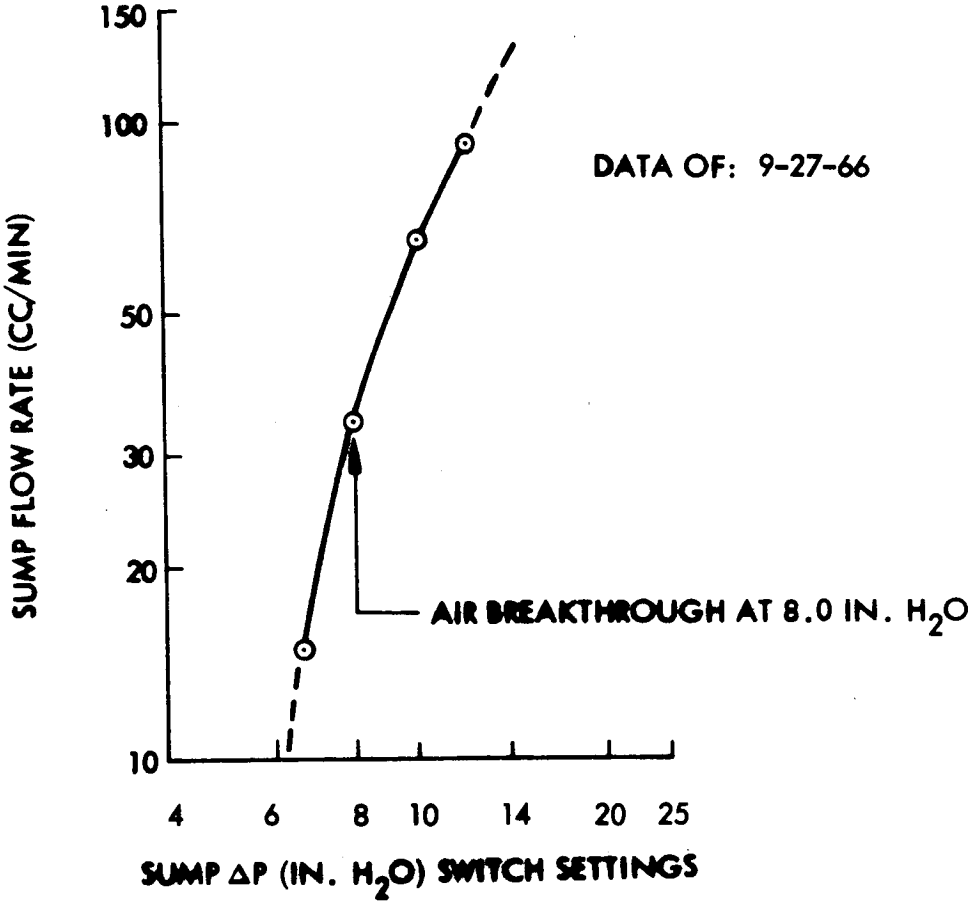

Fig. 3- Typical Hydrophilic Sump Characteristics

free moisture and therefore no measure of water separator efficiency was possible. Based on the fact that water condensation occurs on the metal surface of the heat exchanger and leaves in the form of droplets under the combined influence of gravity and the air stream (thereby performing the function of the coalescer), the coalescer was removed from the water separator. Tests were then run to evaluate the humidity control system performance with the coalescer removed. Comparative data, from both the test with the low density coalescer in place (Appendix D Run A4), and with no coalescer in the water separator (Appendix D Run A5), showing pressure loss as a function flow at a fixed moisture removal rate is presented in fig.4 for reference. Although the additional pressure drop caused by the coalescer represented less than 10 percent of the total system pressure loss, the significant result was that no difference in separator efficiency was observed when the coalescer was removed. The unit functioned at 100 percent water separation efficiency to above the test requirement condition of 100 CFM (duct velocity 880 ft/min on fig. 4) before breakthrough occurred. In the test, with the water separator in the vertical mode and the spinner and coalescer removed, the chiller used was not capable of maintaining the required dew points at high flow rates.

Therefore the inlet humidity was increased with flow to maintain a nearly constant specific water removal rate. Figure 4 shows that the sharp increase in the rate of pressure rise occurs in the region (above velocity of 900 ft/min) that water breakthrough was initially observed. It was then postulated that at some high pressure difference across the screen, water is forced into the mesh and held causing increased pressure loss as area is blocked and ultimately resulting in breakthrough. This theory is fortified by observations of pressure loss data taken as the flow rate was reduced from high flow rates. The data shows that the higher than expected pressure loss which is attributed to screen blockage by water accumulated at the higher flow, purges itself from the screen with time and the pressure loss is restored to the data level recorded at increasing flow rates. As a result of these observations, a new set of tests was developed which would show the effect of water flow on pressure at some fixed value of flow.

Water Removal Effects.- The final tests in the initial series consisted of testing to determine pressure loss for fixed values of flow with variable water removal rates (Appendix D Runs No. A6, A7 & B7). This data is presented in fig. 5. At each of the test points several readings were obtained to assure that the pressure loss had achieved a stable steady state value. The data shows a marked increase in pressure loss with water removal at 101 CFM. At low air flow rates water removal efficiency was 100 percent. However, as water flow was increased beyond .042 pounds per minute, breakthrough occurred. This curve clearly shows the effect of increasing water flow rate on water separator pressure drop, and indicates that the important parameters (lbs.H_2O/lb. air flow), is missing from fig.4.

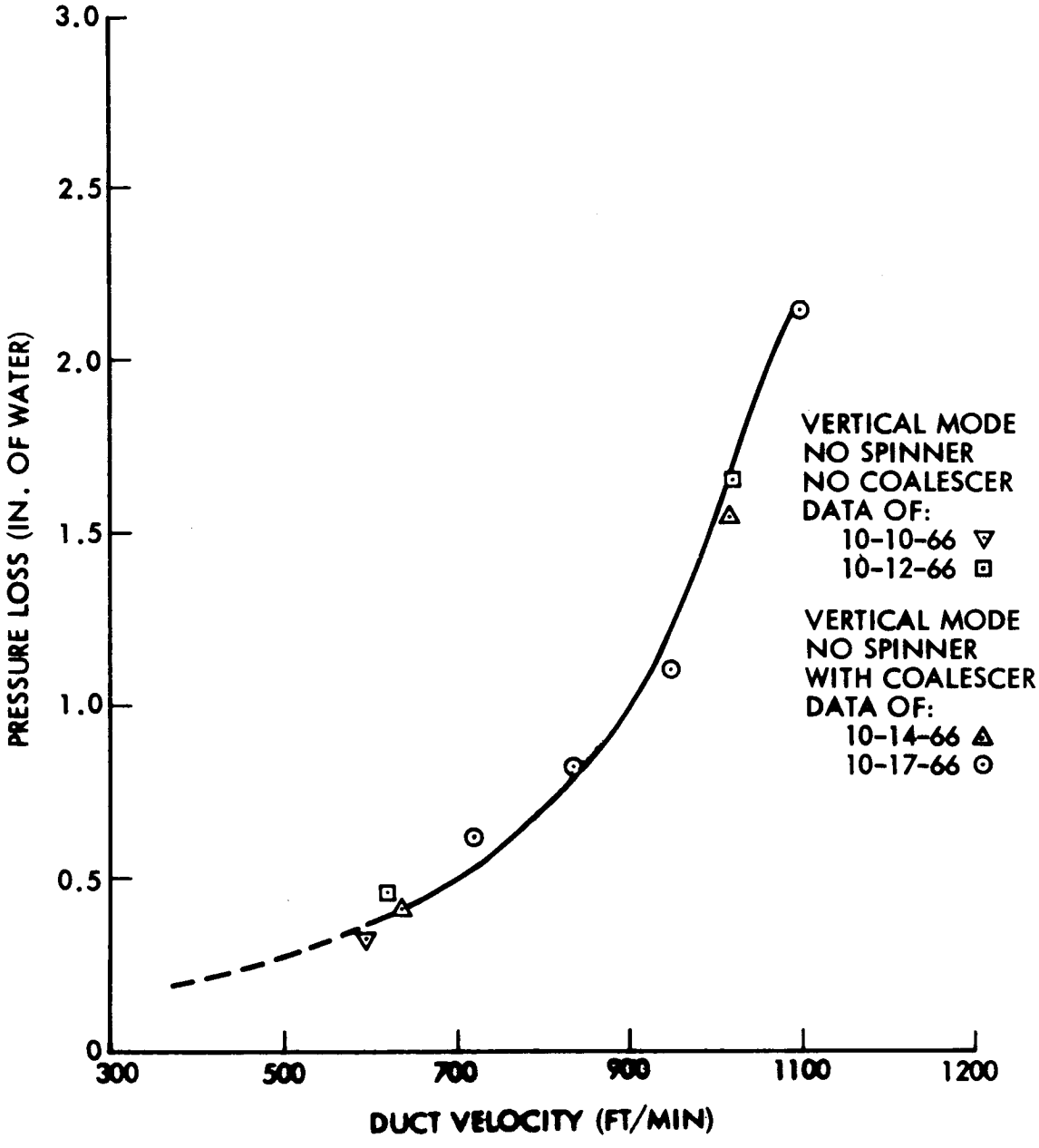

Fig. 4 - Mesh Coares Wire Pressure Loss

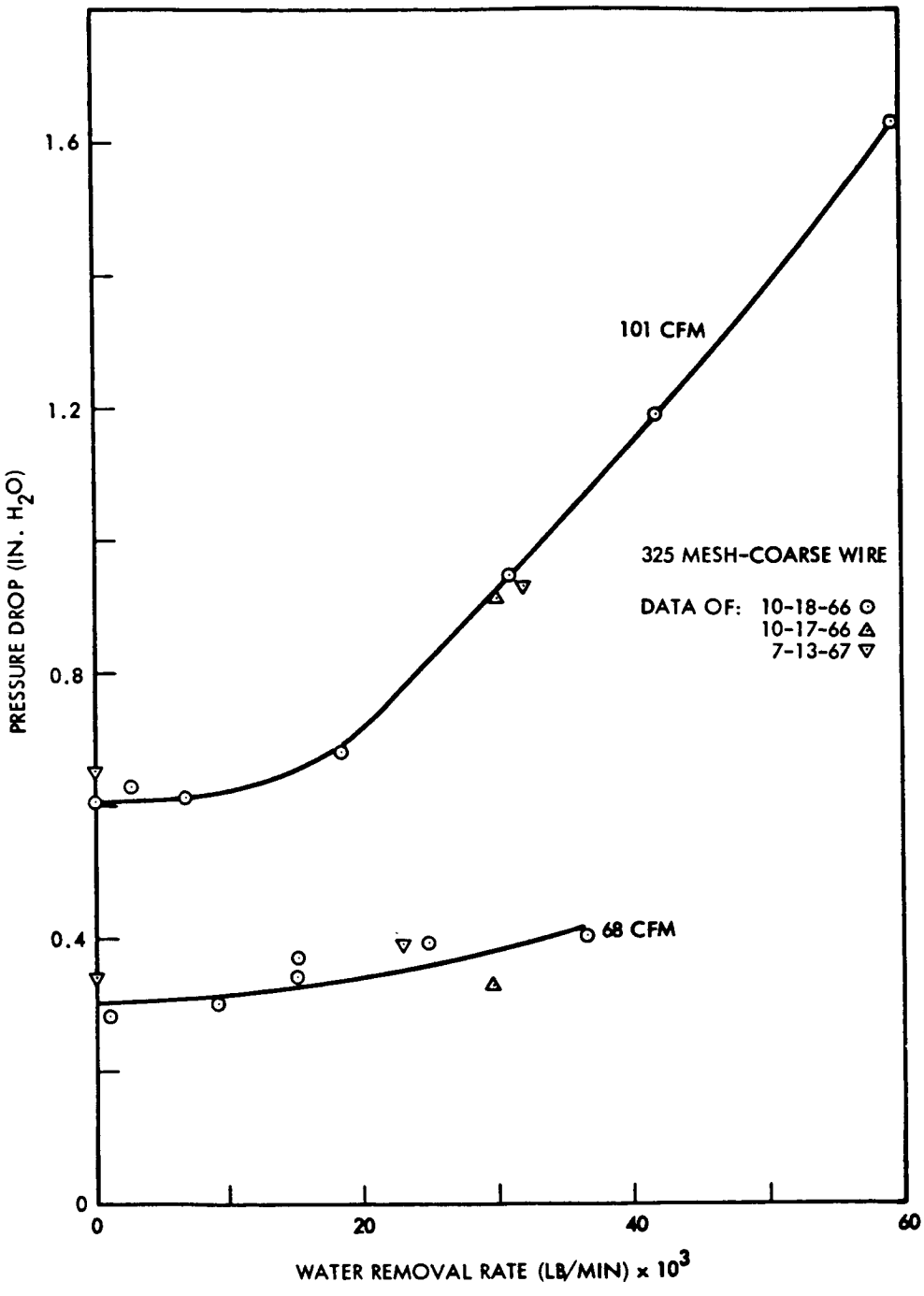

Fig. 5 - Effects of Specific Water Removal Rate

A repeat of this test procedure at 68 CFM shows only a slight increase in pressure drop with water flow (Reference Appendix D Run No. A8). A possible explanation of this effect is that the lower pressure difference across the cone at the lower flow rate was not enough to cause water on the surface to be held.

Test Plan Modification

The results of the initial steady state tests indicated a need for revising the plan of test. The following conclusions were made from analysis of the initial steady state test data:

1. The objective of the first phase of the steady state tests was to determine the performance of the water separator in a series of nine test runs with three different coalescer densities and three spinner configurations. An optimum configuration for the spinner and coalescer then was to be established for further test and evaluation. The initial steady state tests indicated that the water separator performed at 100% separation efficiency for the test conditions with no spinner and no coalescer. This accomplished the objective for determining the optimum configuration for the coalescer and spinner configurations within the water separator. The test plan was then modified to establish the optimum configuration for the hydrophobic cone screen size and to further evaluate spinner configurations. It was thought that configurations which encompass larger screen apertures would tend to reduce water separator efficiency and pressure drop.

2. Evaluation of the data from the initial steady state tests indicates that the heat exchanger upstream of the water separator serves as a coalescer and thus the coalescer is redundant. Therefore, variation in coalescer density was deleted from the test plan.

3. Operation of the system in a vertical downward rather than a horizontal attitude during the steady state test runs was most representative of a zero gravity situation. The performance of the separator was affected in the horizontal mode by the tendency for water to drop to the bottom of the separator. Testing in a vertical mode eliminated this affect and produced a more rigorous and realistic operational test of the hydrophobic cone.

4. In step 1 of the initial steady state test plan, the configuration trade-off studies were performed at a single air flow rate. Based on observed test data it was considered desirable to include the parametric variation of air flow with the configuration variations. This increases the number of data points to be taken in the steady state tests and improves the probability of defining the true optimum configurations.

Based upon these observations, the test plan was modified for the final phase testing. The revised test plan is presented in Appendix B.

Screen Selection

In the selection of new hydrophobic screens to be tested, three major areas of importance were considered. These were mesh, wire diameter, and finally open area which is a result of the first two. The remaining parameter, cone angle, was held constant. These parameters are related as discussed below.

Theory of Operation.- Theoretical consideration of two capillary phenomena are important to the design of a hydrophobic/hydrophilic phase-separation humidity control system. These are: (1) the pressure differential existing across a stable liquid-gas interface in a porous material, and (2) the velocity which will cause a liquid droplet, striking a porous hydrophobic surface, to penetrate that surface.

The porous material used in the humidity control system is a fine-mesh stainless steel screen. This material is used in the uncoated form on the hydrophilic sumps. Coated with Teflon, it behaves as a hydrophobic material and is used on the hydrophobic cone.

Analytical models available for prediction of the low-gravity phase separation capabilities of woven screens are far from exact. For this reason a fairly simple model was used, recognizing that inaccuracies in performance predictions would result. The variance between predicted and actual performance shows that an analytical model chosen can be used at least to estimate the order of magnitude of performance.

Stability of the Liquid-Gas Interface.- The conditions for stability of a liquid-gas interface in a porous material are shown in fig. 6. For example, if liquid droplets on the gas side of the porous plate shown in the illustration reach the stable liquid-gas interface, they will enter the liquid phase. In this way liquid is extracted selectively from a two-phase medium with a hydrophilic screen mesh surface.

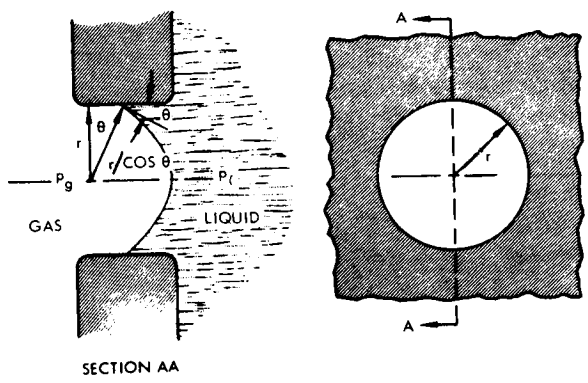

Fig.6- Stability of Liquid Gas Interface in a Cylindrical Hole

The model used for predicting the pressure differential existing across a stable gas-liquid interface is shown in fig.6. The analytical expression for the pressure differential across the interface is given by the capillary pressure rise equation attributed to Laplace:

$$p_g - p_l = \sigma\left(\frac{1}{r_1} + \frac{1}{r_2}\right) \qquad (1)$$

where

p_g = pressure on gas side

p_l = pressure on liquid side

σ = surface tension

r_1 and r_2 = principal radii of curvature of the liquid-gas interface.

For a cylindrical hole as shown in the model, the principal radii of curvature are identical and equal to

$$\frac{r}{\cos\theta}$$

where

r = radius of cylindrical hole

θ = contact angle

Substituting $r_1 = r_2 = r/\cos\theta$ in Eq. (1) gives

$$p_g - p_l = \frac{2\sigma\cos\theta}{r} \qquad (2)$$

The geometry of interest, a woven screen however, is roughly approximated by the square opening shown in fig.7; for the lack of a better model, this approximation was used.

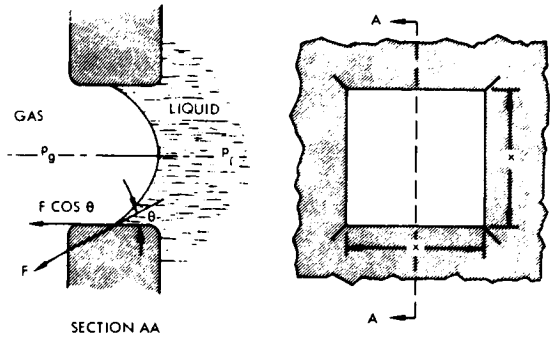

Fig. 7- Stability of Liquid-Gas Interface in a Square Hole

To apply the solution for the round opening to the square configuration the hydraulic radius, r_h, was substituted for the term r/2 in Eq. (2), giving

$$p_g - p_l = \frac{\sigma \cos \theta}{r_h} \qquad (3)$$

where r_h = area/wetted perimeter. This approach appears to be justified on the basis of a force balance on the liquid surface as depicted in fig. 7. The sum of the forces acting parallel to the axis of the opening contributes to the pressure difference:

$$(p_g - p_l) = \frac{\Sigma F}{A} = \frac{4\sigma x \cos 0}{x^2} = \frac{4\sigma \cos \theta}{x} \qquad (4)$$

The hydraulic radius of the square opening is:

$$r_h = \frac{x^2}{4x} = \frac{x}{4}$$

Substituting in Eq. (4) gives an expression identical to Eq. (3)

Using Eq. (3), pressure differential calculations were made for the hydrophilic (uncoated stainless steel) screen with θ = 45 deg, and for the hydrophobic (Teflon-coated) screen with θ = 105 deg.

Droplet Penetration Velocity.- For a hydrophobic screen it is interesting to note that if gas with entrained liquid droplets were to flow to the screen, it would be possible to stop the liquid droplets from passing the screen mesh while the air was allowed to continue through. One requirement for this type of separation is that the droplet must be larger than the screen porosities. Additionally, when the liquid droplet contacts the hydrophobic screen, a liquid stagnation will develop at the region of impact. As long as the pressure difference developed across the screen results in a stable interface the liquid droplet will not pass through the screen.

To estimate the maximum velocity that a droplet may have and still be stopped by a hydrophobic screen, consider the schematic diagram of fig.8. With the liquid droplets approaching the hydrophobic screen at a velocity V, the difference between the stagnation and static pressures of the liquid drop is:

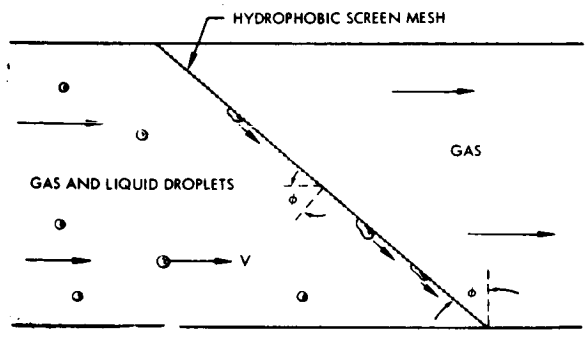

Fig.8-Separation of Liquid Droplets from a Gaseous Stream by a Hydrophobic Surface

$$p_{stab.} - p_{static} = \frac{\rho V^2}{2g_c}$$

where

ρ = liquid density

V = approach velocity

g_c = gravitational constant

If the radii of the droplets are large compared with the screen opening, then the static pressure of liquid in a drop will be equal to the pressure of the gas surrounding it; that is $p_{stat} = p_g$. Hence the difference between the stagnation pressure of the moving liquid droplets and the gas-stream pressure may be expressed by:

$$p_{stag} - p_g = \frac{\rho V^2}{2g_c}$$

If, as shown in fig. 8, the angle between the normal to the screen surface and the direction of the gas-liquid droplet flow steam is ϕ, then only a fraction of the stagnation pressure will be developed on the hydrophobic screen as a liquid droplet impinges. The difference between liquid and gas pressures at the point of impact may be expressed by

$$p_l - p_g = \frac{\rho V^2}{2g_c} \cos \phi$$

The maximum stable pressure difference ($p_l - p_g$) that can be supported across a hydrophobic screen can be estimated from Eq. (3), thereby allowing calculation of the impingement velocity below which penetration should not occur.

In evaluating the driving force for passing water through a hydrophobic screen material, the pressure difference across the screen must also be considered. Water on the surface of the screen will be subjected to the full pressure loss across the screen. In the case of the 325 mesh screen tested in the initial steady state tests, this pressure difference, at high air flow rates, constitutes a large part of the pressure difference indicated by equation (3). Thus, lowering unit pressure loss may, even if the effective hydraulic radius is increased, reduce the possibility of water breakthrough.

Final Hydrophobic Screen Selection.- Examination of the 325 mesh coarse wire hydrophobic cone tested showed that the initial uncoated free area of 30 percent is reduced significantly by coating. However, the reduced free area increases the air pressure loss across the cone significantly. As water is held upon the surface of the cone, free area decreases and consequently the air pressure loss increases still further.

In an attempt to reduce the humidity control system pressure loss penalty, a search was made for screens which would have a lower pressure loss and at the same time provide high unit performance. Standard screen material available on the market have open areas, generally less than 50 percent. This results from using larger diameter wire as mesh is reduced. A 230 mesh (with .0014 m diameter wire) stainless steel screen represented the optimum size screen within the commercially available screen sizes providing the minimum hydraulic radius and the maximum free area. This had an uncoated area of 46 percent. The 325 mesh screen (with .0011 m diameter fine wire) selected also had a smaller hydraulic radius but had an uncoated area of only slightly less than 42 percent because of the closer weave. Other special screens may be more desirable but were ruled out because of the high cost and schedule penalty of special mill runs. A summary of the three screens chosen for the final tests is shown below:

Screen	Mesh	Wire Diameter (M)	Relative Rh	Uncoated Open Area (%)	Referred To As
1	325	.0014	min.	30	325 mesh coarse wire
2	325	.0011	--	42	325 mesh fine wire
3	230	.0014	max.	46	230 mesh

Hydrophobic cones were manufactured to the original 325 mesh specification dimensional configuration for screens 2 and 3 and used in the final steady state test plan presented in Appendix B.

Final Steady State Tests

Upon receiving the new hydrophobic cones from manufacturing, the test apparatus was again checked out and a new chiller, which would provide a more stable outlet humidity at all flows, was integrated into the system. The final steady tests consisted of the following:

- Performance on each of the three hydrophobic cones - 325 mesh coarse wire, 325 mesh fine wire, and 230 mesh.
- Performance on each of the spinner configurations - 0, 1.0, and 1.5 plates.
- Effects of variable inlet and outlet humidity levels for the optimum configuration.
- Dynamic tests

A summary of this data appears in tabular form in Appendix D Runs No. B1 - B15 and is presented in the figures that follow in this section.

Test Data Runs.- Final steady state testing was started on the 325 mesh with coarse wire, no spinner and no coalescer. These tests showed a much higher pressure loss and earlier water breakthrough than the previous tests conducted during the initial steady state test phase. The unit was disassembled and examination of the 325 mesh showed a large buildup of oil and dirt which had accumulated from the initial runs and storage. The screen was cleaned in Freon and prepared for future runs. In cleaning, dirt collected appeared to be carbon dust as might originate from the fan motor brushes.

Hydrophobic Cone Ratings.- The first acceptable complete run was conducted on the 230 mesh hydrophobic cone. The data is presented in Appendix D Run B1, and is plotted in fig. 9. Data taken on the test runs (Reference Appendix D Runs No. B2 and B3) at later dates are also shown on this curve. This is significant as it shows reproducibility after the unit had been disassembled for testing of other configurations. Additional performance on this screen was taken at the maximum test apparatus air velocity at a fan voltage of 28 volts to evaluate the 230 mesh configuration at the maximum stress condition. Flow measurements were off scale, preventing an accurate determination of flow; however, estimates based on pressure loss show the flow to be above 140 CFM with efficiency remaining at 100 percent and no breakthrough. This is better performance than was achieved with the original 325 mesh coarse wire screen. The lower air pressure loss across the screen, as discussed in the screen selection section, provided less potential for driving water through the hydrophobic cone material. The 325 mesh coarse wire unit showed a pressure loss in excess of 1.0 inch of water at breakthrough while the 230 mesh cone never showed a loss greater than .5

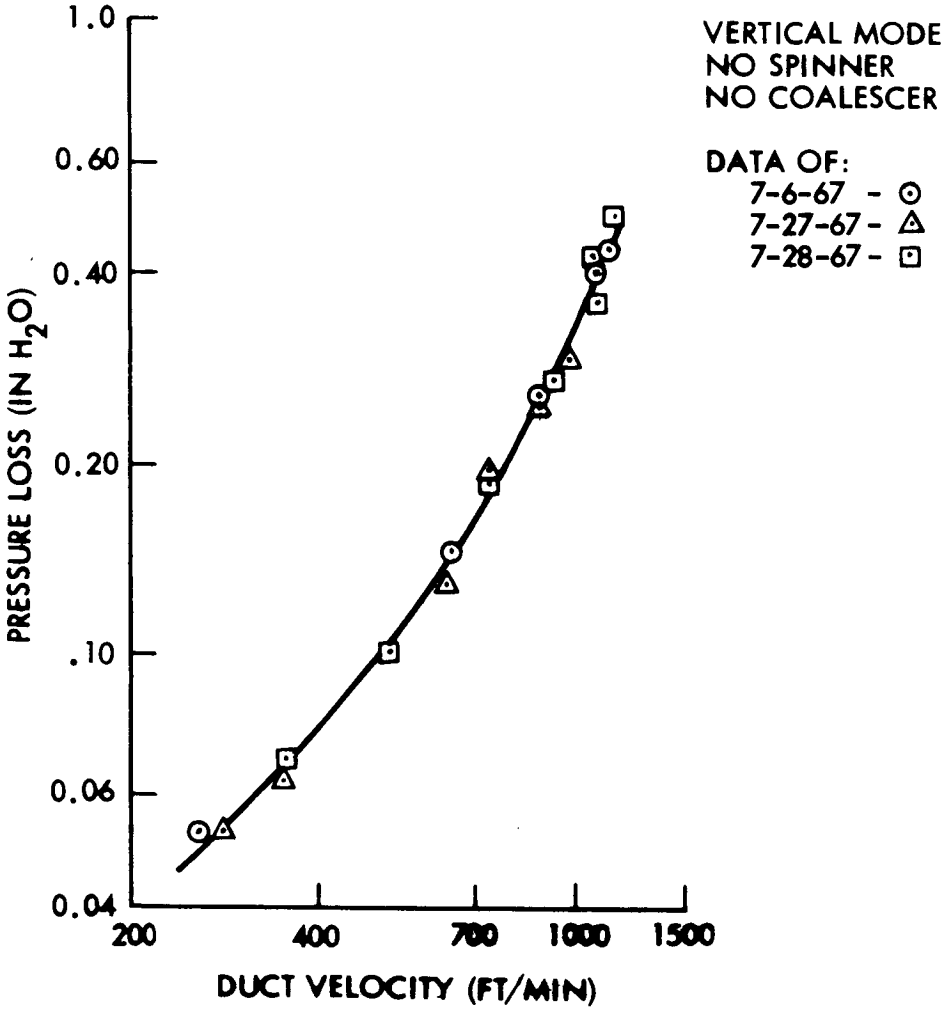

Fig. 9 - 230 Mesh Pressure Loss Data

inches of water even at the maximum test system flow condition. After the initial run on the 230 mesh cone configuration, the new 325 mesh cone with the fine wire weave was installed in the unit for testing.

The performance data for the 325 mesh fine wire weave is shown in fig. 10 (Appendix D Runs No. B8 & B9). This configuration showed a 100 percent removal efficiency up to the maximum test capacity air flow at 28 volts fan motor supply. The pressure loss over the flow range was higher than the 230 mesh unit. The higher pressure loss is attributed to the decrease in free area. This unit does, however, have improved performance over the original 325 mesh design in both pressure loss and water removal efficiency. The final test on the hydrophobic cone configurations was with the original 325 mesh coarse wire cone, which had been cleaned after initial high pressure loss characteristics.

Data on the 325 mesh coarse wire cone is shown on fig. 11 (Appendix D Runs No. B4, B5 & B6). As was the case during the original steady state test, breakthrough was found at high flow conditions over 900 ft/min. It is important to note that data taken after the screen was cleaned, closely reproduces the original data. This can be seen from fig. 11 where both sets of data are plotted. The effect of water removal rate on pressure loss for this cone is evident from the steeper slope of the pressure loss versus flow relationship.

Summary.- Once data on the three hydrophobic cones were gathered, it was analyzed to determine the optimum screen configuration. The 230 mesh was determined to be optimum as it had the lowest pressure loss and maintained a 100 percent removal efficiency throughout its operating range. A brief comparison of pressure loss data at the original design point of 70 CFM (velocity 620 ft/min) is shown below for the three screens tested:

Hydrophobic Cone	Pressure Loss
230 mesh	.135 inches water
235 mesh fine wire	.265 inches water
325 mesh coarse wire	.41 inches water

As a result this screen was chosen for testing of inlet and outlet humidity effects, and for the dynamic test runs.

Effects of Inlet Humidity.- The first test condition on the 230 mesh screen was run with the steady state test inlet and outlet humidities to confirm the data (Appendix D Runs No. B2 and B3). The data is plotted on fig. 9 and shows that the performance is reproducible. Tests were then conducted to determine the effects of high and low humidity level on water separator performance.

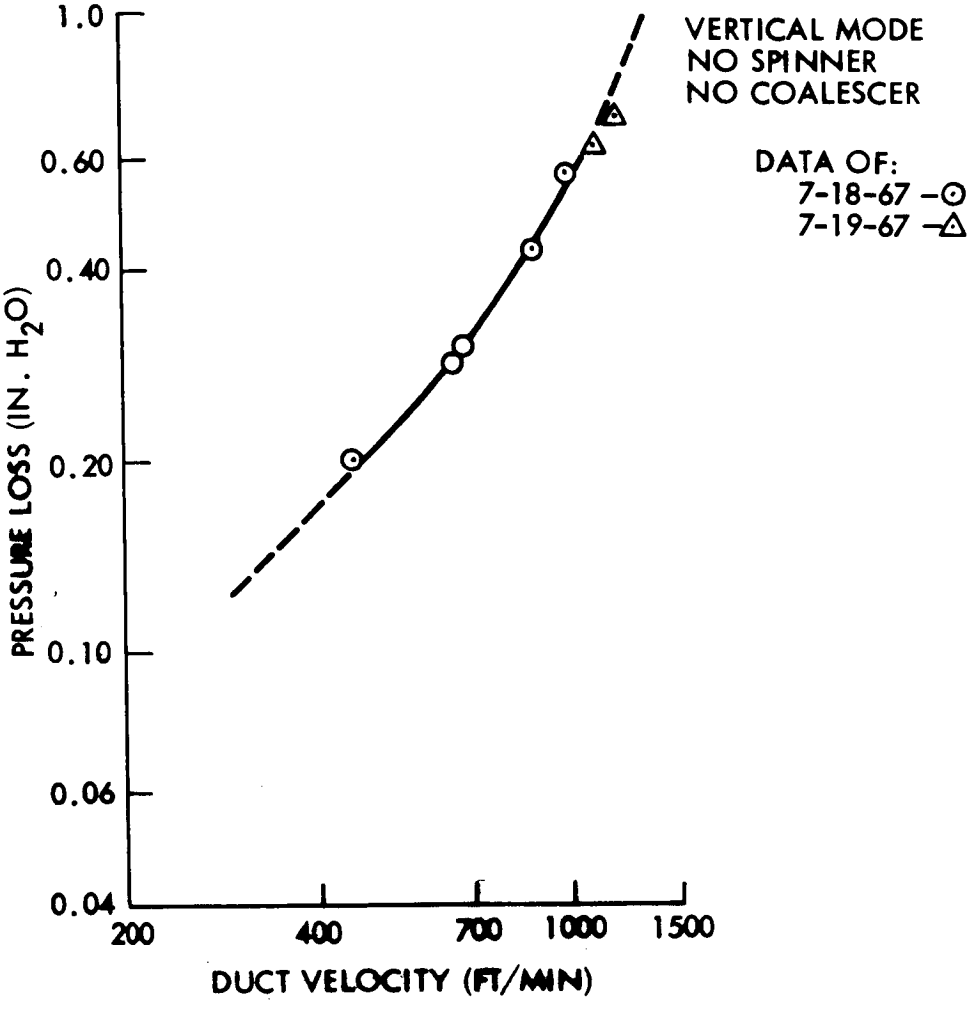

Fig. 10 - Mesh Fine Wire Pressure Loss Data

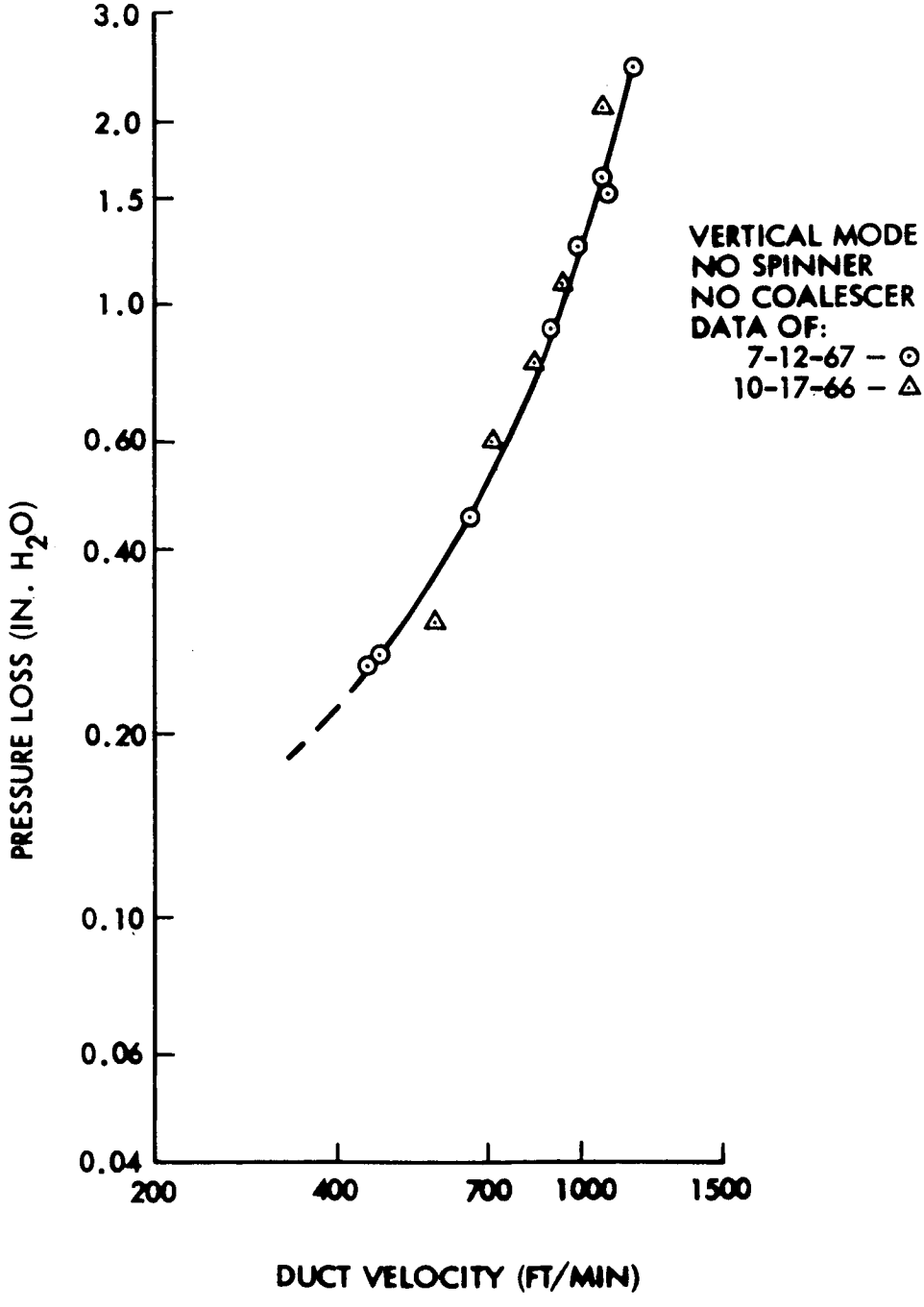

Fig. 11 - 325 Mesh Coarse Wire Pressure Loss Data

The steady state tests were run with an inlet humidity of .0137 lb H_2O/lb air and an outlet humidity of .0071 lb. H_2O/lb air. In order to assess the importance of both inlet and outlet humidity levels, the plan of test required runs with other values of inlet and outlet humidity. The initial series of steady state tests demonstrated the possible importance of water removal rate as shown in fig. 5. This effect would be of great importance to a designer as latent heat loads (which vary over a wide range of work conditions) and available heat sink temperature are important design considerations for relative humidity control. These two parameters have a direct effect on the humidity levels of the humidity control system. Data was taken on the 230 mesh hydrophobic cone without spinner or coalescer for two additional values of inlet humidity. These were .0191 lb. H_2O/lb.air (Appendix D Runs No. B 10 & B11), and .0082 lb. H_2O/lb. air (Appendix D Run No. B12). This data is presented in figs. 12 and 13. Comparison of figs. 12 and 13 with fig. 9 at .0137 lb. H_2O/lb. air shows that for the 230 mesh hydrophobic cone, there is no variation of pressure loss with changes in inlet humidity level, and water removal efficiency was 100 percent within the range of the experiment.

Effects of Outlet Humidity.-Following the test to determine the effects of inlet humidity on pressure loss and water separator performance, tests were run (Appendix D Run B13) to determine the effect of outlet humidity on performance. The outlet humidity rates were changed by varying heat exchanger coolant inlet temperatures. Figure 14 shows no variation in pressure loss with changing outlet humidity for the 230 mesh cone at an inlet humidity of .0137 lb.H_2O/lb.air, and a flow of 107 CFM. As might be expected from the study on effect of inlet humidity, there is no effect on pressure loss due to changing outlet humidity level. These tests showed no effect on the 230 mesh cone water separator performance efficiency either in humidity level or pressure loss. This is contrary to the original steady state tests on the 325 mesh coarse wire cone where increase in outlet humidity level caused a significant increase in ΔP and breakthrough. In this test program it was not possible to define the reasons for the difference. However, it is felt that the lower pressure loss in the 230 mesh unit is the reason. This is justified on the basis of the 68 CFM data shown on fig. 5 which shows minimal effect of water removal rate on the 325 mesh unit where the pressure loss is low.

Spinner Losses.- In order to evaluate the effect of the spinner on the water separator pressure loss, flow tests were run to determine spinner loss data with the hydrophobic cone removed. The initial test was run with no spinner which confirmed that system losses were negligible and the base was considered as zero loss. A pressure loss versus flow test was then conducted on the spinner with 1.5 plates (Appendix D Run No. B14). This unit was then cut down to 1.0 plates and rerun (Appendix D Run No. B15). Figure 15 shows the results of these tests. The small difference between these two

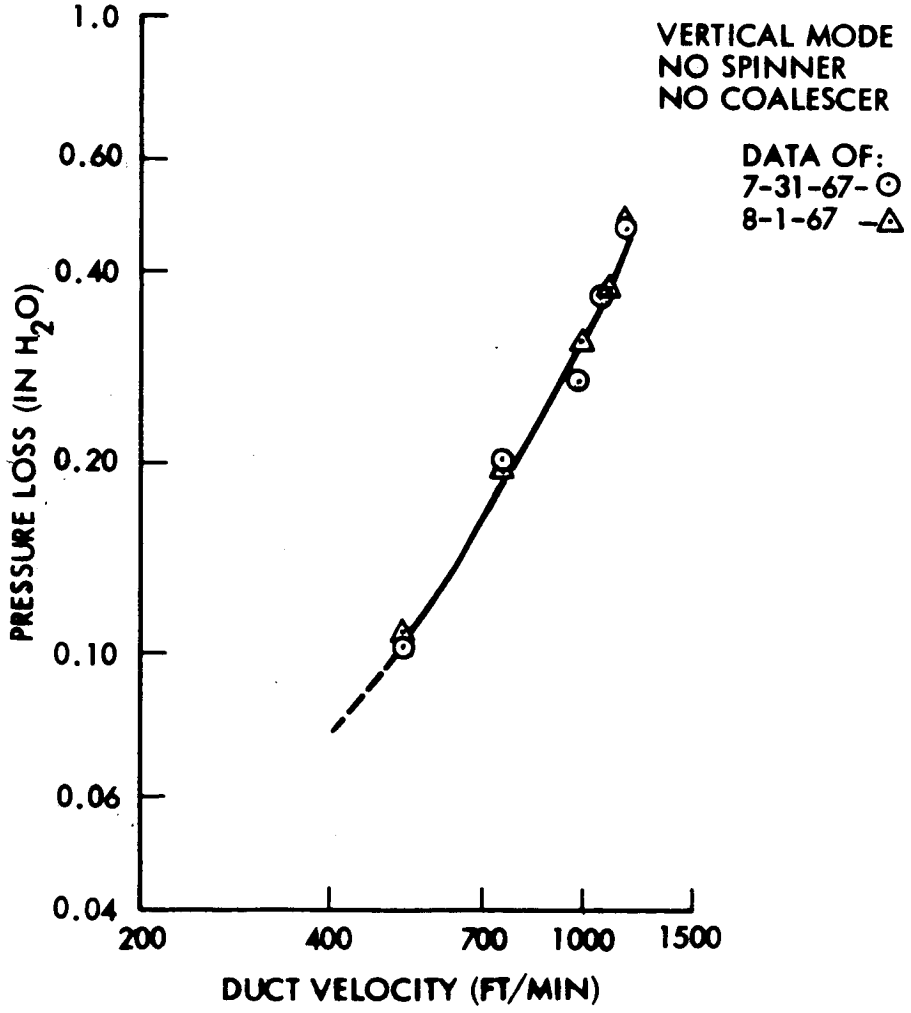

Fig. 12- 230 Mesh High Inlet Humidity Data

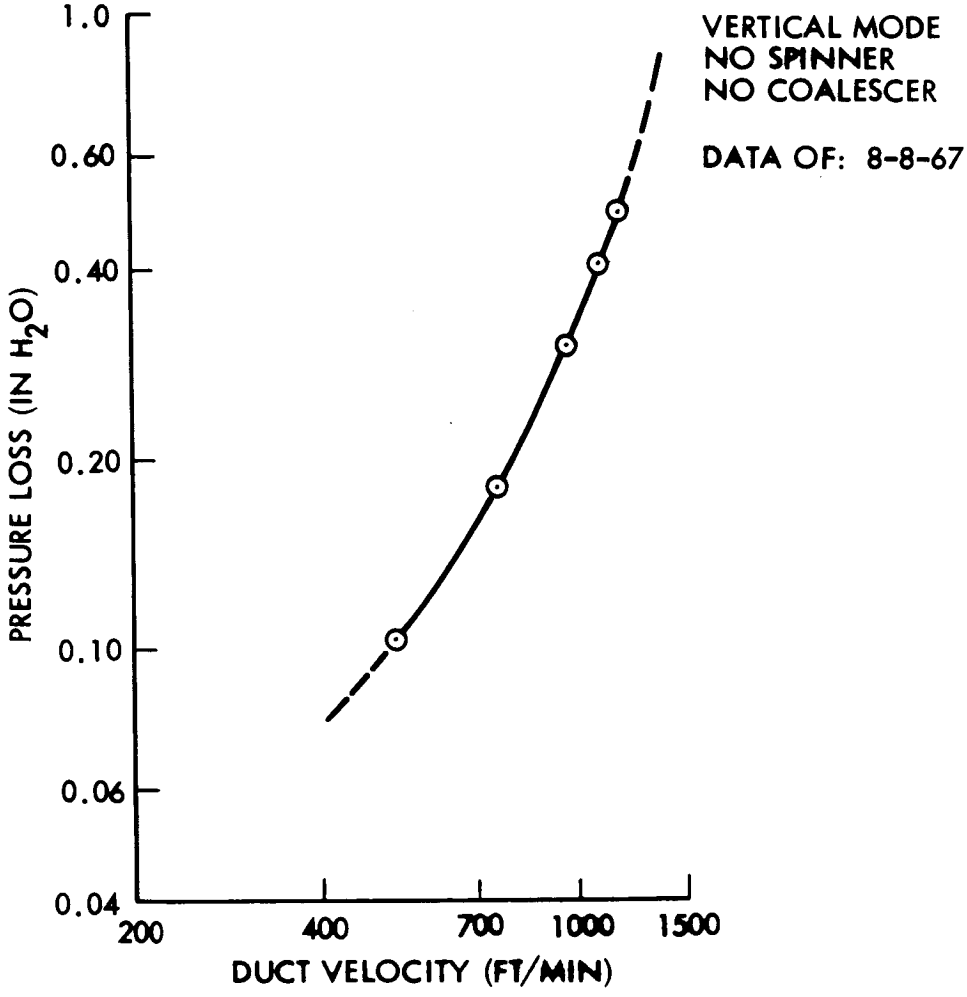

Fig. L3 - 230 Mesh Low Inlet Humidity Data

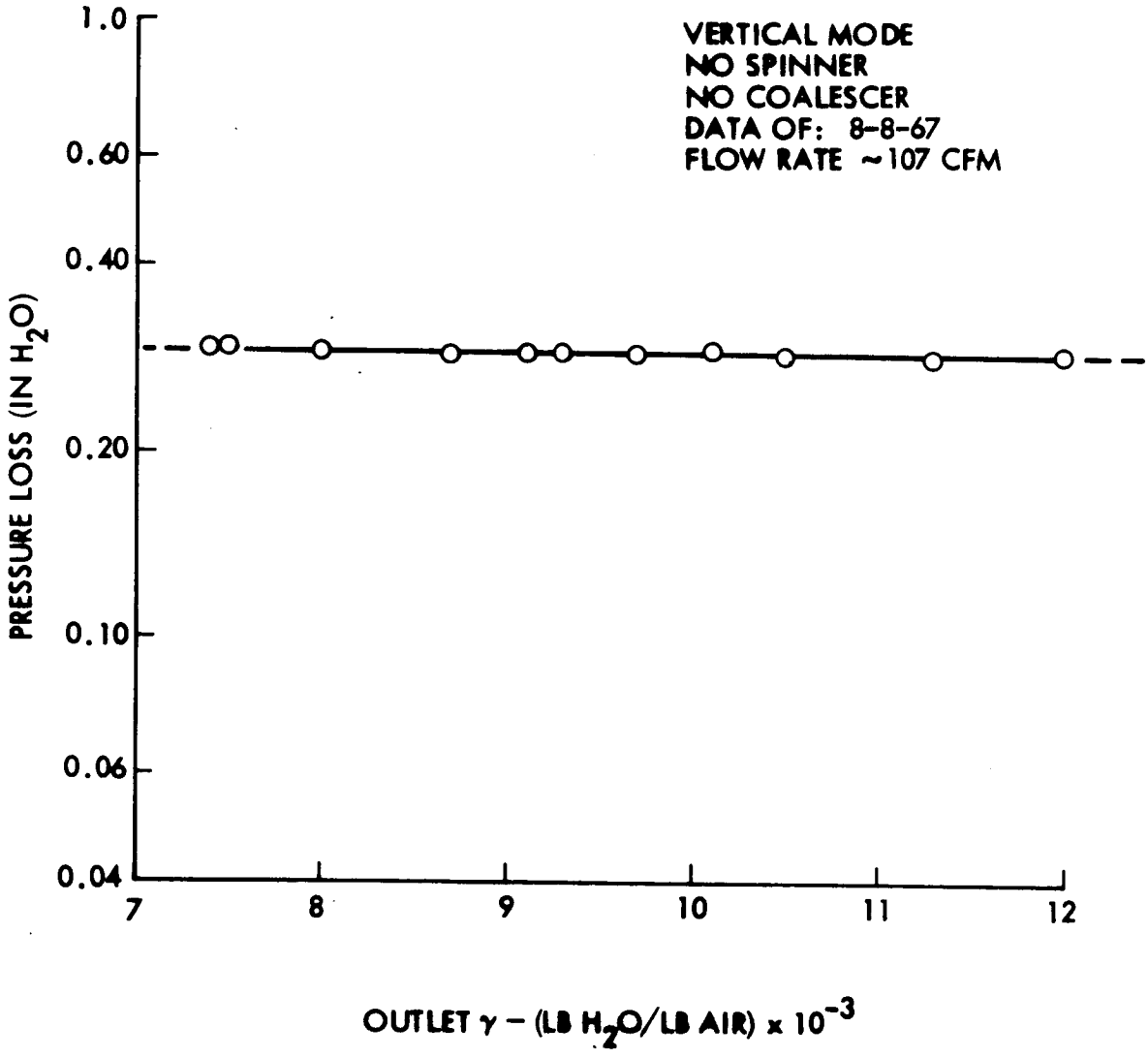

Fig. 14 - 230 Mesh Variable Outlet Humidity Data

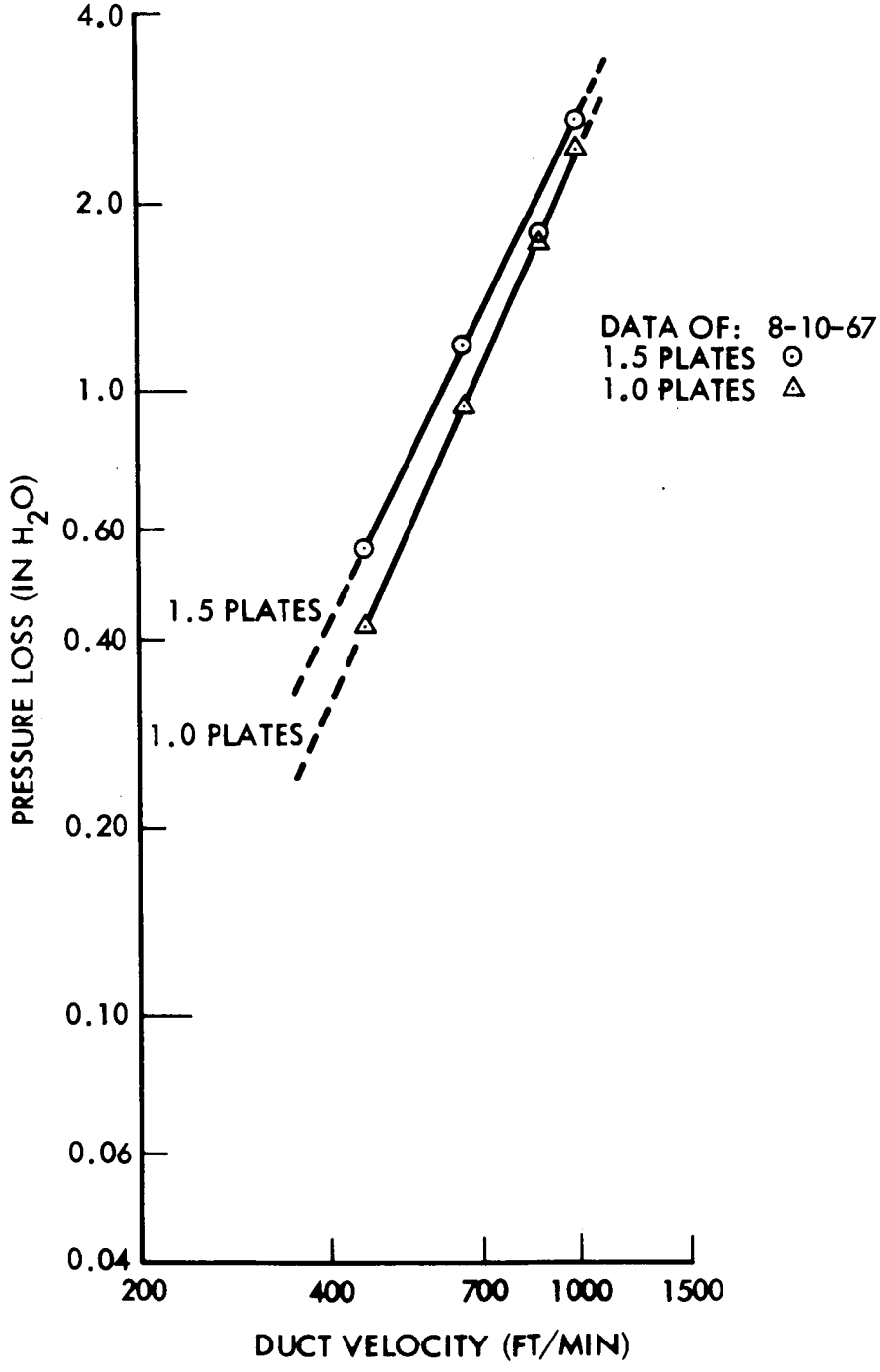

Fig. 15 - Pressure Loss Data - Water Separator Spinner

configurations is explained by the fact that the cross section area for flow was large and had little loss while the entrance and exit losses constituted the major loss.

Test Data Reduction

The test data presented in figs. 9 through 15, was then reduced to determine water separator design criteria. The data as plotted in figs. 9 through 15 is valid only for the pressure, temperature and cone tested. Pressure loss data may be presented in the form of $\sigma \Delta P$ where σ is the ratio of density to standard density of .0765 lb/cubic foot. The duct velocity measurements were converted to true velocity by a pressure conversion then reduced to $lb/min/ft^2$. Although characteristics of pressure loss may vary with cone geometry, it appears from this testing that cone area is the best possible parameter in the absence of more complete data. Spinner losses are additive to screen losses in the evaluation of total system performance data for screen configurations with spinner. Data showing the cumulative system pressure loss versus mass velocity flow per unit area for each of the hydrophobic cones is presented in figs. 16 through 19. These data can then be used in any combination of pressure/density relationships for evaluating system design parameters for each screen mesh configuration shown in figs. 16 through 19.

Dynamic Performance Tests

Dynamic tests were performed on the humidity control system to determine the recovery rate of an upset condition produced from a sudden increase in inlet humidity level caused by some emergency. The test was accomplished by establishing a high humidity level, in excess of a 70°F. dew point, by controlling the level with the automatic steam controller. At a period in time a manual step change was made to the steam feed valve which resulted in dew point of about 58° F. The rate of system recovery from the elevated dew point to the lower was recorded on the Honeywell recorder for inlet humidity δ 1. This procedure was repeated three times to assure consistency at each flow of 40, 70 and 100 CFM. The initial rate of recovery indicated a problem of instrument response time. Thus, an attempt was made to measure this response. Saturated air was fed to the dew point sampling system. At a point in time a step was made to lower dew point air and the response recorded. The results of the instrument check are shown in fig. 20, and the data taken at each of the flows in figs. 21 through 23. The data from the chart has been reduced to show the dew point temperature as a function of time.

As might be expected with systems of small volume and high flow rate, the figures show a rapid recovery rate. The small difference in time between the instrument and system response is most likely due to an unmeasureable characteristic of the steam feed system.

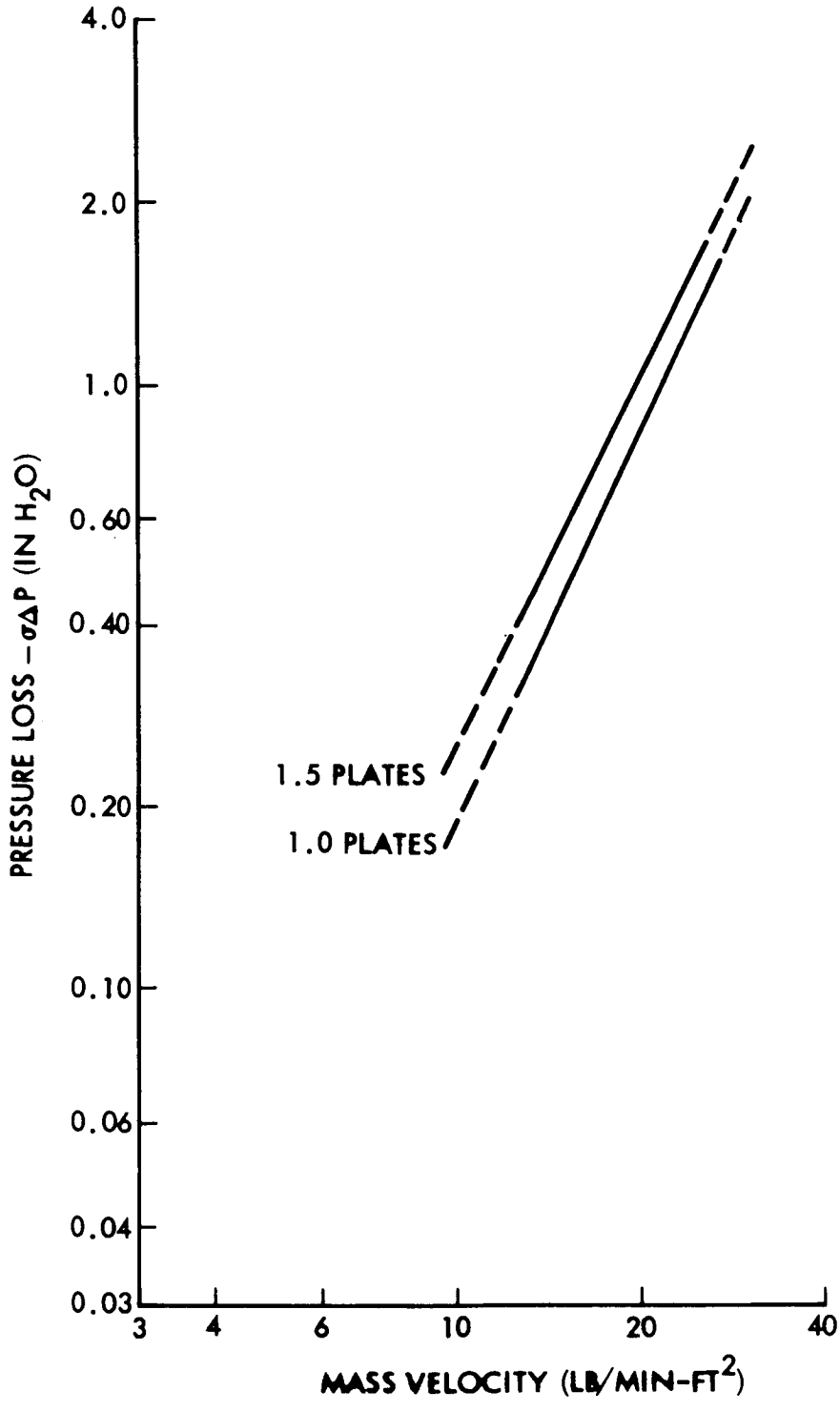

Fig. 16 - Water Separator Spinner Pressure Loss Characteristics

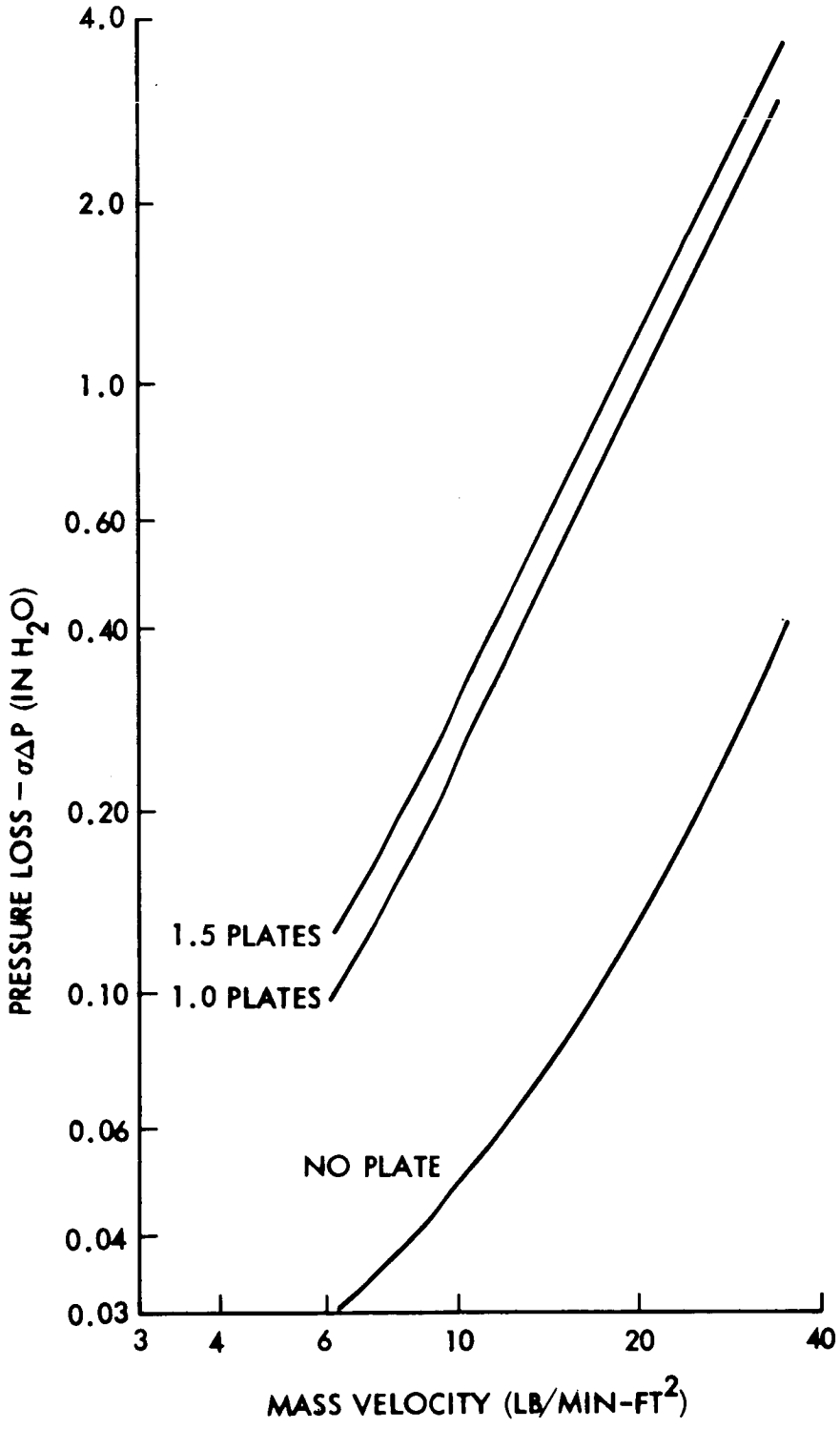

Fig. 17 - 230 Mesh Pressure Loss Characteristics

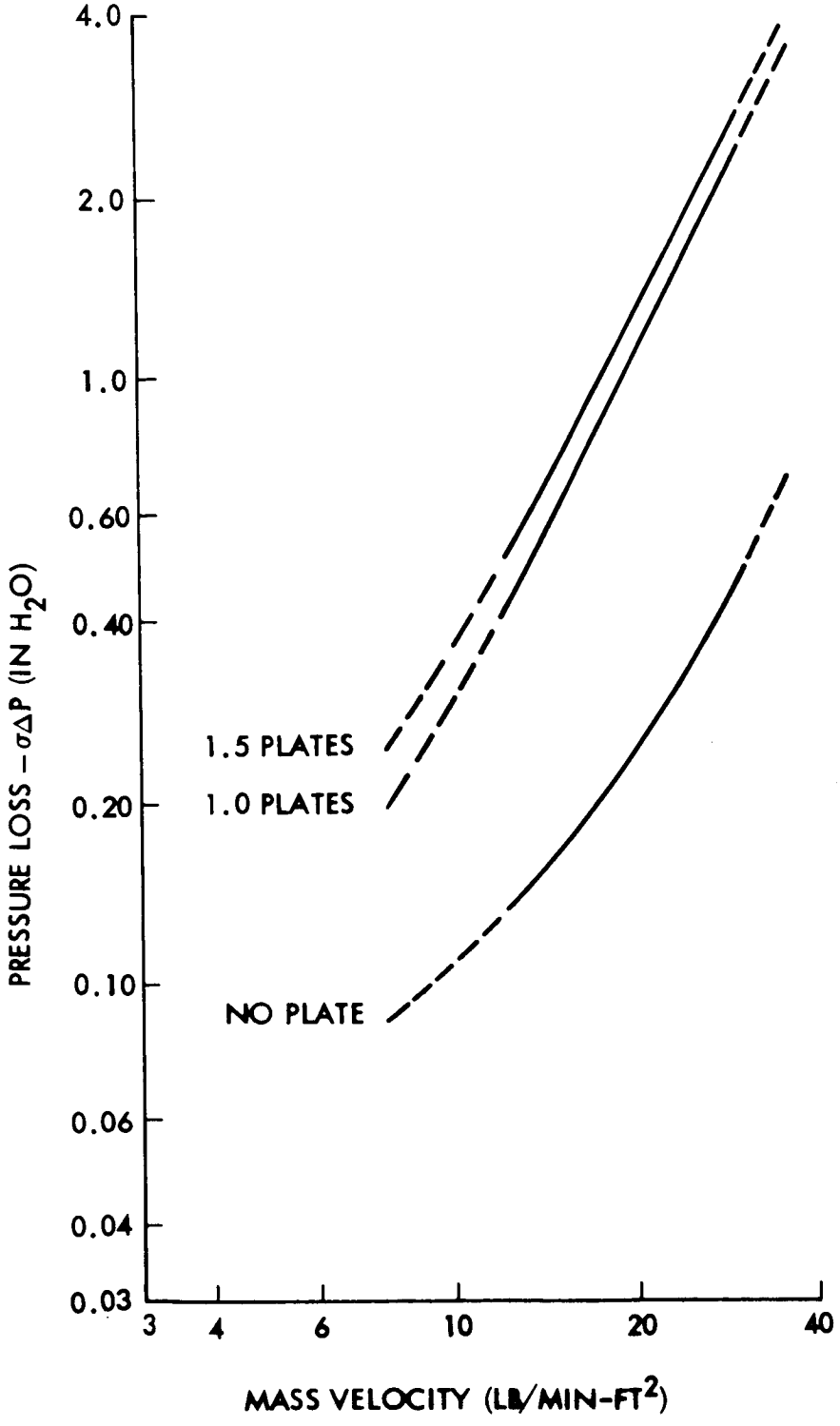

Fig. 18 - Mesh Fine Wire Pressure Loss Characteristics

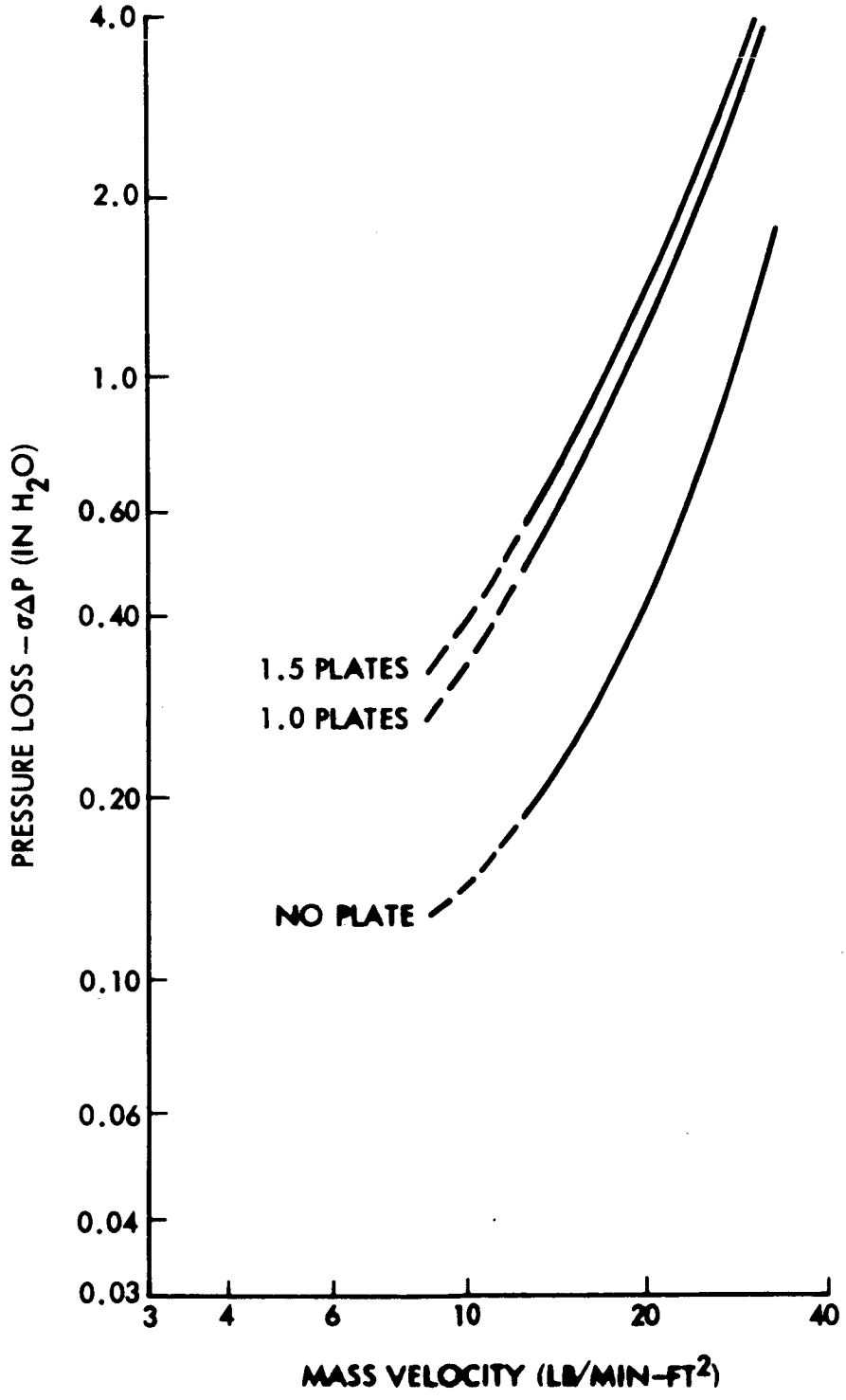

Fig. 20 - Response of Humidity Control System Instrumentation

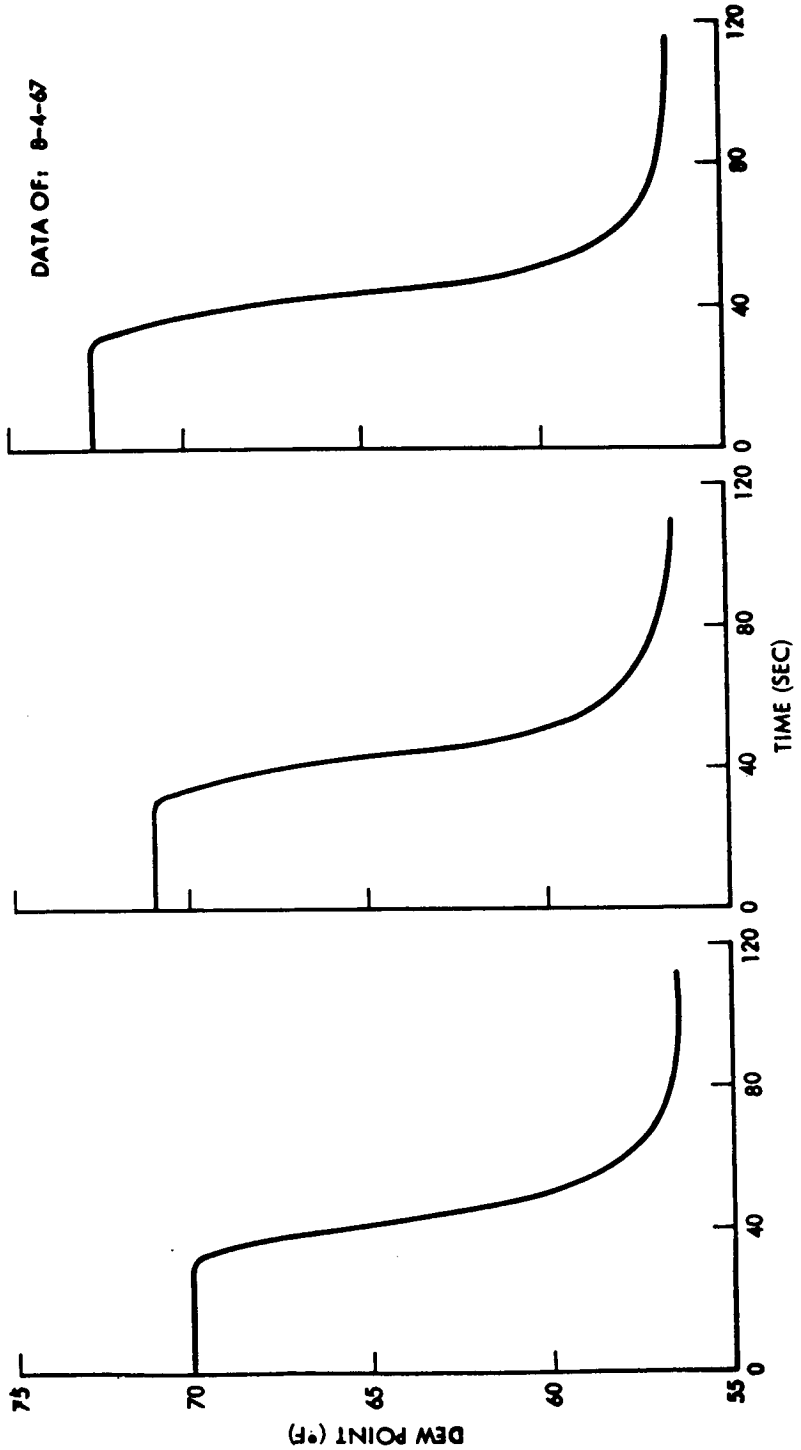

Fig. 20 - Response of Humidity Control System Instrumentation

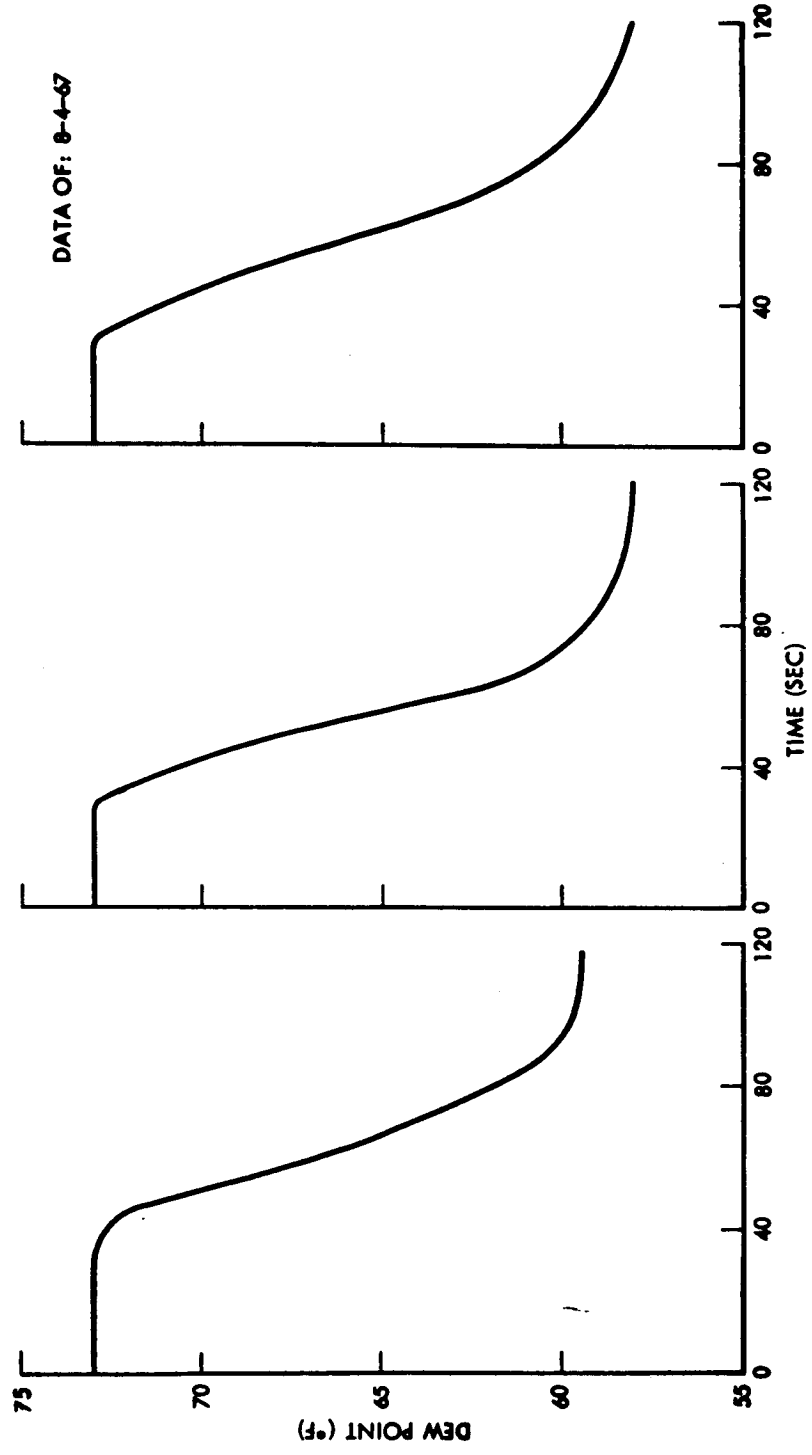

Fig. 21 - Dynamic System Response at 40 CFM

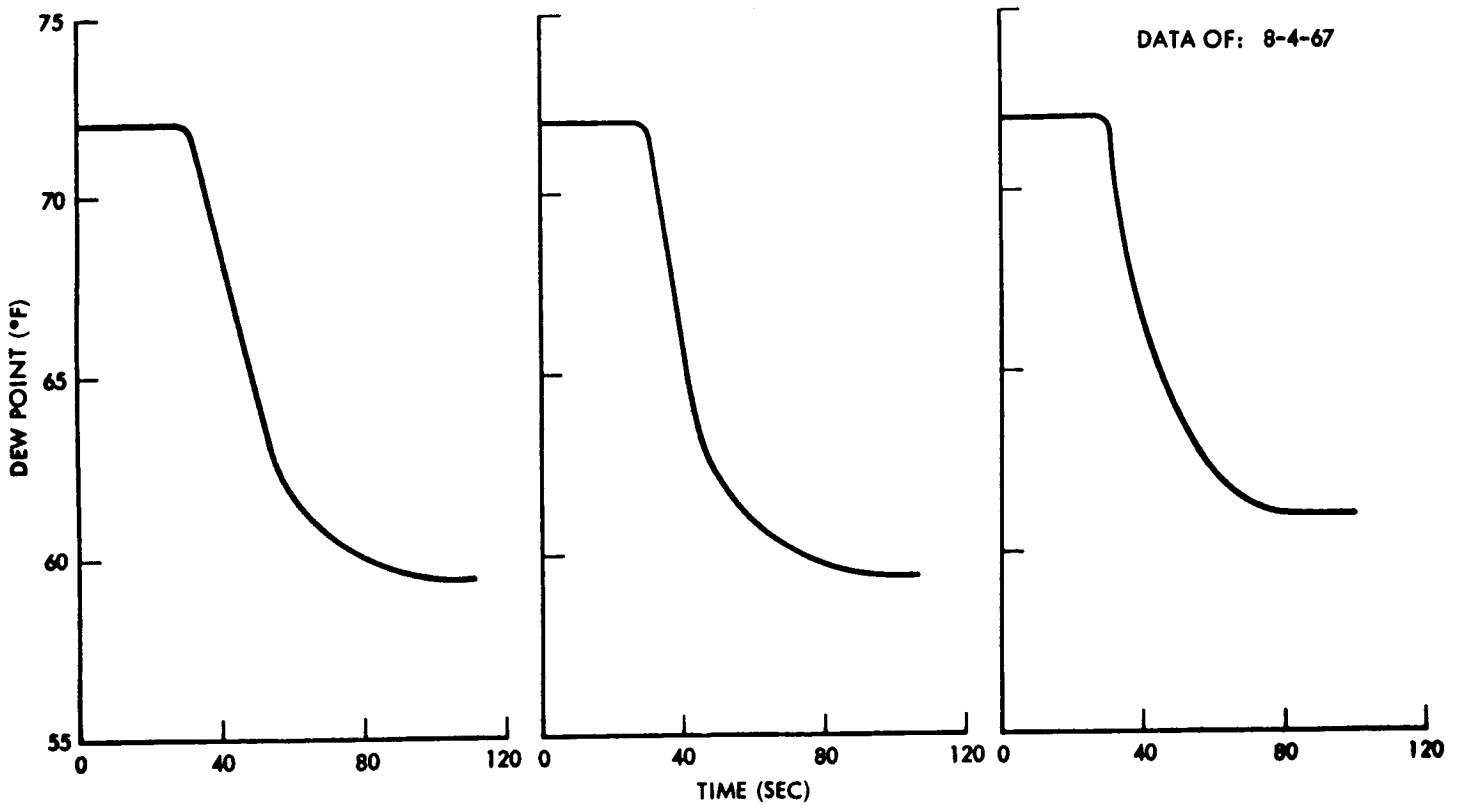

Fig. 22 - Dynamic System Response at 70 CFM

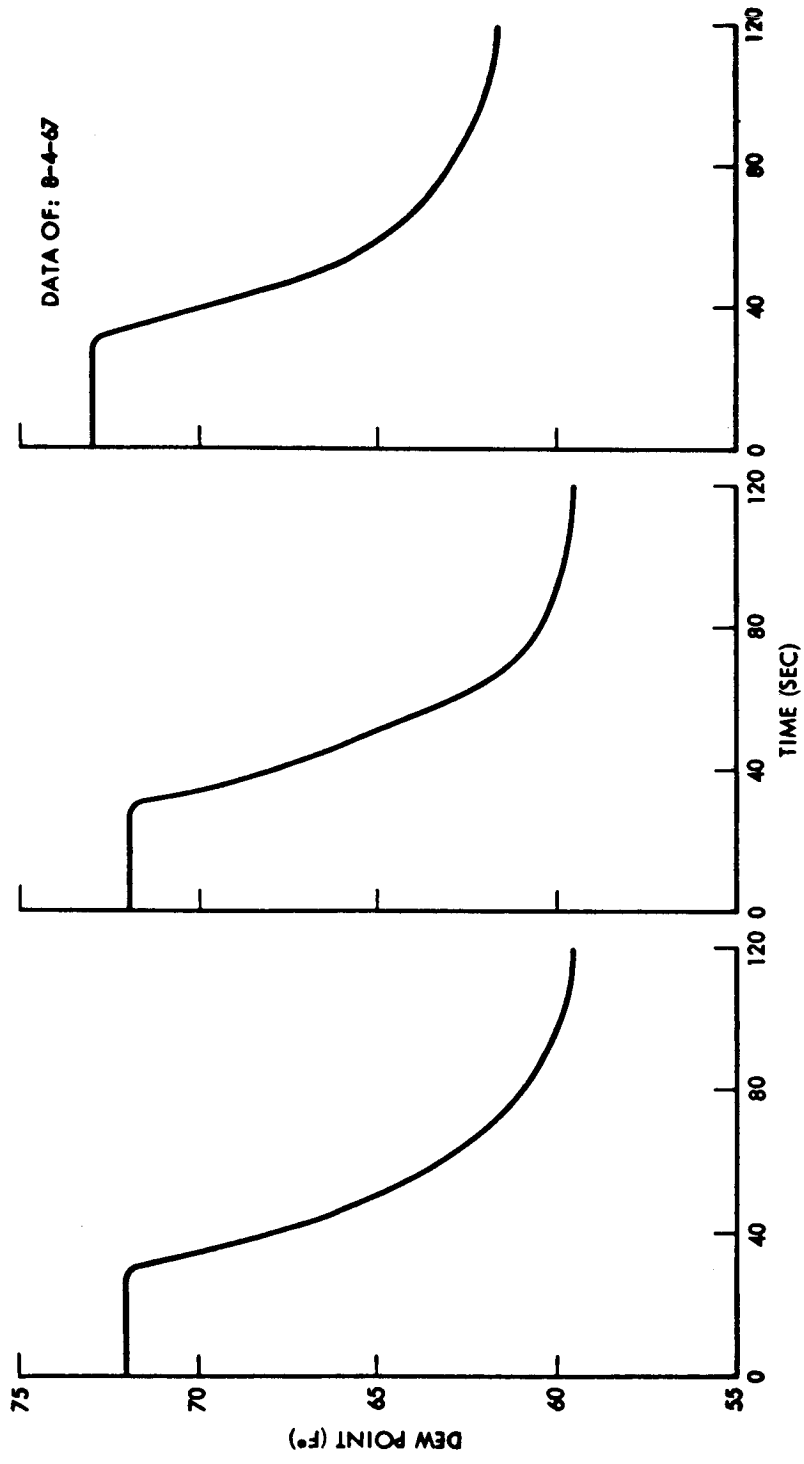

Fig. 23 - Dynamic System Response at 100 CFM

DESIGN CRITERIA

The optimization of the humidity control subsystem for a space vehicle depends upon a number of vehicle parameters and a definition of complete environmental system requirements. The following major parameters were considered for this optimization analysis:

- Subsystem reliability requirements
- Subsystem maintainability requirements
- Vehicle power penalty
- Available sink temperature
- Water generation rate
- Allowable humidity level
- System pressure
- System integration concept

The task of generating a concise optimization of the water separator subsystem design criteria, including the consideration of the total variables in the above list, is not practical at this point in system evaluation testing without defined system parameters and performance requirements. However, by assigning values to certain variables, a system approach can be established for evaluating an optimum humidity control subsystem design. Two major environmental control system integration arrangements were examined for the design optimization analysis; one, utilizing the basic assumption that water separator flow is established by humidity control requirements; and the other, that water separator flow is fixed as established by thermal control requirements.

The humidity control system used in the test program was evaluated as a basis to illustrate selection of an optimum configuration for a system whose water separator flow is established by humidity control requirements. The second system optimization consisted of a fixed flow system as established by thermal control requirements and is presented as a sample system. Other systems with different requirements may be evaluated in the same manner as these two illustrations.

Figure 24 was developed for environmental control systems which may require a water separator of different size from the test unit. This figure presents water separator weight for the optimum configuration showing weight as a function of cone area. The curve is based on the 230 mesh test unit

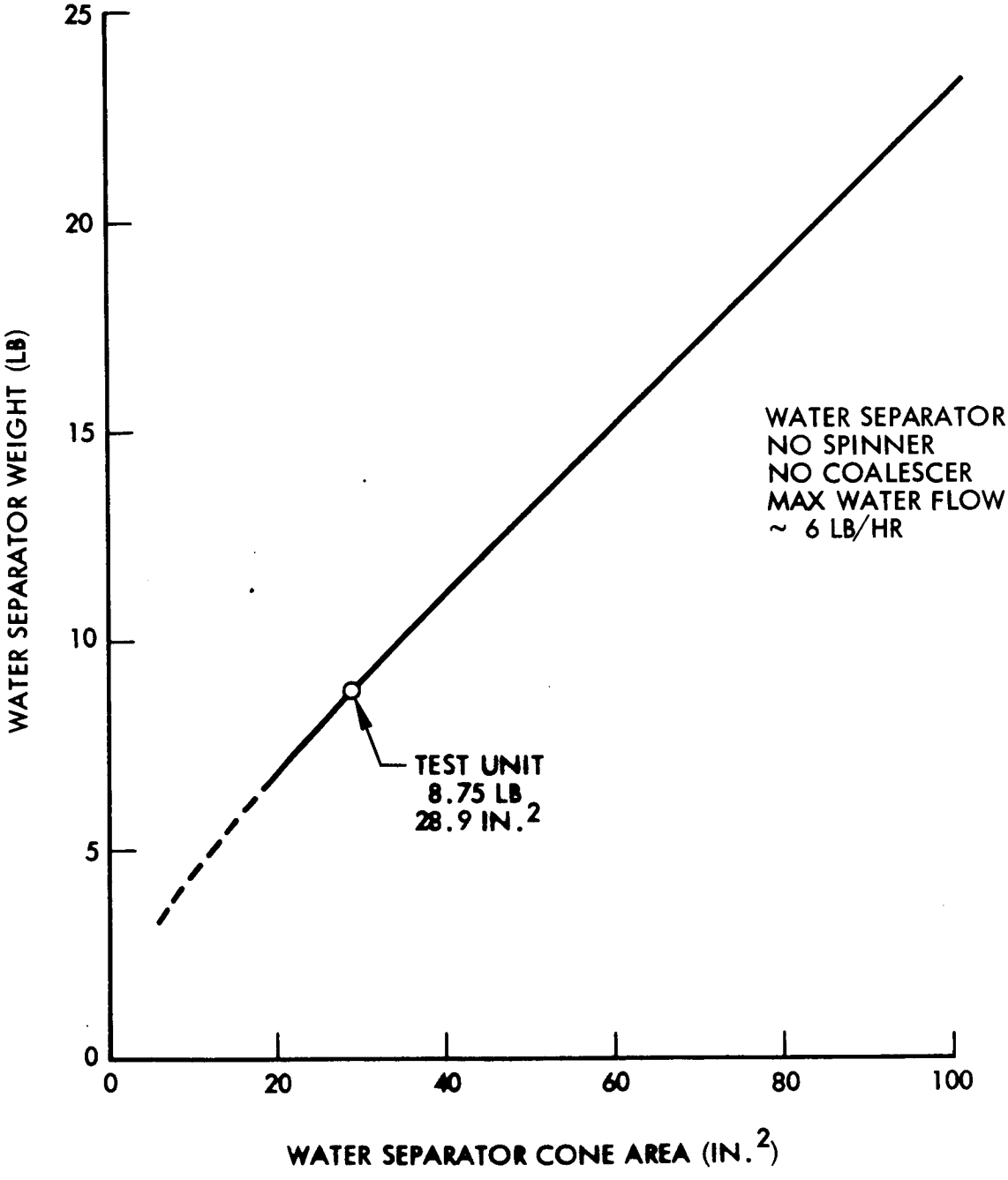

Fig. 24 - Water Separator Fixed Weight

with individual components and is scaled proportionately for other sizes. For reference, the cone area of the test unit water separator is 28.9 square inches and the unit weighs 8.75 lbs.

The performance data from the water separator test program shown in fig. 17-19 was reduced to the common system denominators of pressure/density/flow per unit area relationship. The reduced performance data together with the weight/area relationship shown in fig. 24 for the water separator configuration, serve as a basis for establishing design criteria in this report.

Reliability and Maintainability

The Lockheed hydrophobic/hydrophilic water separator contains no moving parts and is, therefore, completely passive in nature except for a water delivery system which is common to all water separator concepts. The test program, though limited in duration, showed no loss of unit performance with time. Further, the hydrophobic cone which became contaminated during storage was easily restored to its original performance when cleaned. The hydrophilic sumps are also easily removed and cleaned. It was concluded from this test program, that the high inherent reliability and the demonstrated characteristics of total recovery after simple cleaning procedures compares favorably with all other water separator concepts. These parameters of reliability and maintainability are applicable to both the humidity control and the thermal control systems and were not considered further in the establishment of design criteria.

System Integration

In addition to assuming the environmental control system integration concepts of either humidity or temperature control, the following values were assumed for the vehicle parameters considered in the design optimization of the two humidity control subsystem concepts:

VEHICLE PARAMETER	VALUE	REMARKS
o Power Penalty	600 lb/kw	Typical of Advanced Solar Cell Technology
o Sink Temperature-Humidity Controlled System	38°F	Practical Minimum to Avoid Freezing in Heat Exchanger
o Sink Temperature-Temperature Controlled System	Variable	Function of Temperature Control
o Operating Pressure	10 psia	Assumed to Correlate Test Data

VEHICLE PARAMETER	VALUE	REMARKS
o Humidity Level	50% at 70° F	Typical Design Criteria for Cabin
o Volume	Not Considered	Function of Cone Area and System Flow
o Flow-Humidity Controlled System	To be Calculated	
o Flow-Temperature Controlled System	100 cfm	Typical System Value
o Cone Area-Humidity Controlled System	28.9 in^2	Same as Test System
o Cone Area-Temperature Controlled System	To be Calculated	
o Weight-Humidity Controlled System	8.75	Test System Adjusted for Improved Water Delivery System
o Weight-Temperature Controlled System	To be Calculated	

These assumed parameters are applicable to the following design optimization only; any change in values would require that the optimization be repeated.

Integration with Humidity Controlled Systems

In environmental control systems where humidity control is separate from the thermal control subsystem, two regions of water separator performance are of importance. If the separator is less than 100 per cent efficient and the total system air flow is set by humidity control requirements, the air flow will vary inversely as the efficiency. As a result, all components related to the humidity control subsystem are penalized by the increased air flow rate. If, however, the water separator performs at 100 per cent efficiency, as was demonstrated in the test program, the air flow rate through all of the components can be established by the allowable humidity level, available sink temperature, and water generation rate. The water separator operating at 100 per cent efficiency results in the minimum system air flow consistent with humidity control requirements. Thus, each of the components in the system can then be optimized on a component basis relatively independent of the other components. The water separator optimization is then dependent only on its weight and power penalty characteristics.

Performance Evaluation.- As previously mentioned, the reduced data from the test program was used to illustrate the selection of an optimum configuration for a system whose water separator flow is established by humidity control requirements. To determine the optimum water separator design characteristics, the performance of the various configurations was evaluated in the following three steps:

Step 1 - Hydrophobic screen performance independent of spinner performance was evaluated to determine the optimum cone mesh sizes (fig. 25).

Step 2 - Water separator performance with spinner installed was evaluated to determine optimum spinner configuration (fig.26).

Step 3 - Water removal capability over the range of system volumetric flows was evaluated for the optimum water separator configuration, as determined from Steps 1 and 2, to determine the optimum system design flow rate (fig. 27).

The various system configurations were evaluated by comparing total system weight/power penalty as a function of operating performance(expressed as total equivalent weight per pound of water removed or TEW/WH_2O) for each configuration over the range of test flows. The derivation of this term is described in Appendix A.

Hydrophobic Screen Performance.- In fig. 25, the total equivalent weight is plotted as a function of the air flow rate for each of the hydrophobic cones. This figure shows the 230 mesh cone to be the optimum of the three tested as it has the lowest penalty over the operating range. This verified the conclusions from the test program based on its lowest pressure loss and 100 per cent efficiency throughout the tested range. At high flow rates, system pressure loss is the dominant penalty factor while at low flow rates the unit fixed weight represents the major portion of the penalty. In addition, the optimum flow rate of the 230 mesh cone is higher than the 325 mesh screens because of their inherent higher pressure loss characteristics over the test range. This results in a minimum volume for the 230 mesh configuration. It was concluded that the 230 mesh cone configuration was the optimum design. Further system evaluation was based on this configuration.

Spinner Evaluation.- Figure 26 shows the effect of various spinner configurations on the total equivalent weight per pound of water removed over the operating range. In original studies, it was felt that the spinner would improve the water separator efficiency and as a result, the higher pressure loss of the unit could be justified. Figure 26, however, shows

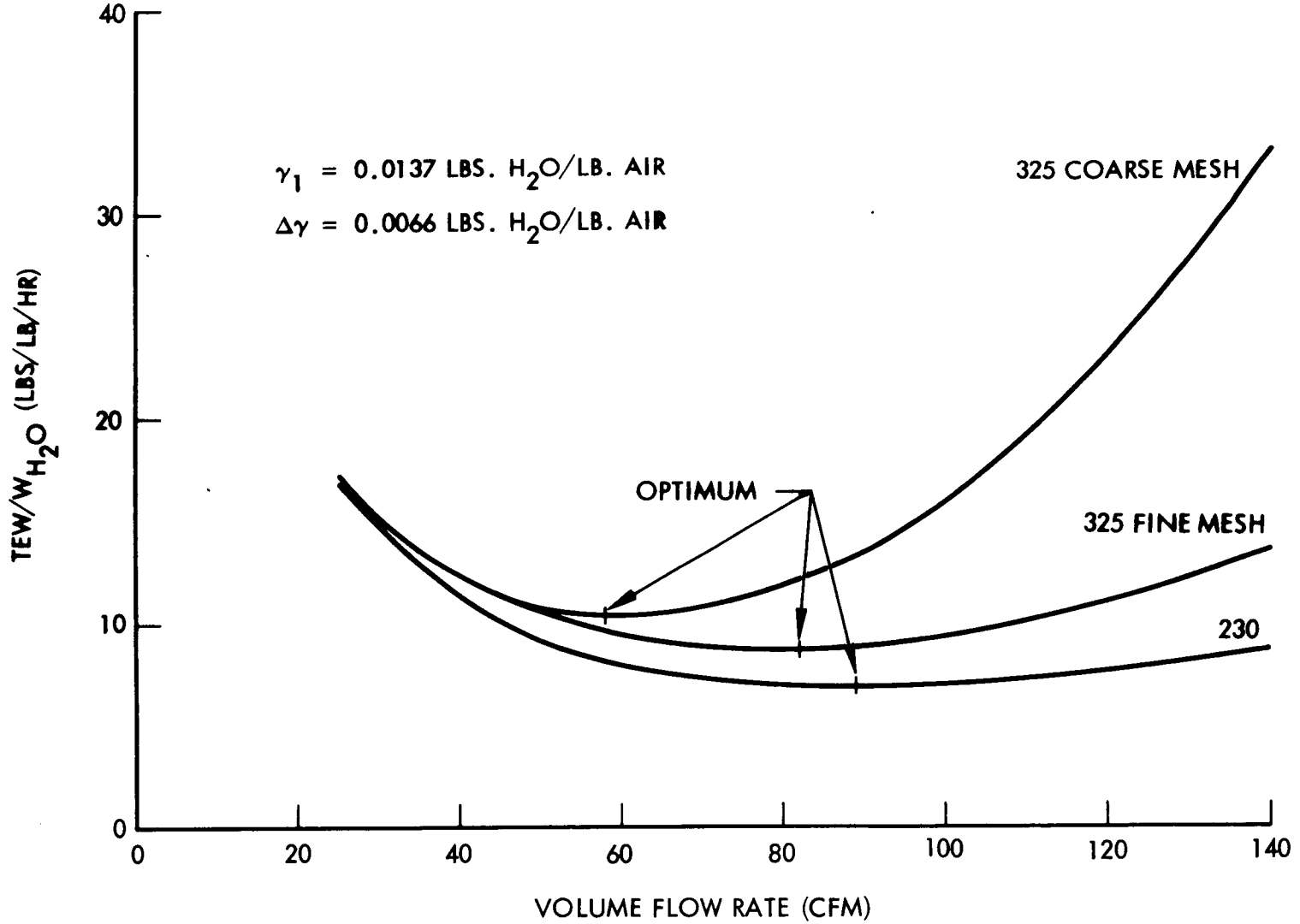

Fig. 25 - Hydrophobic Cone Selection

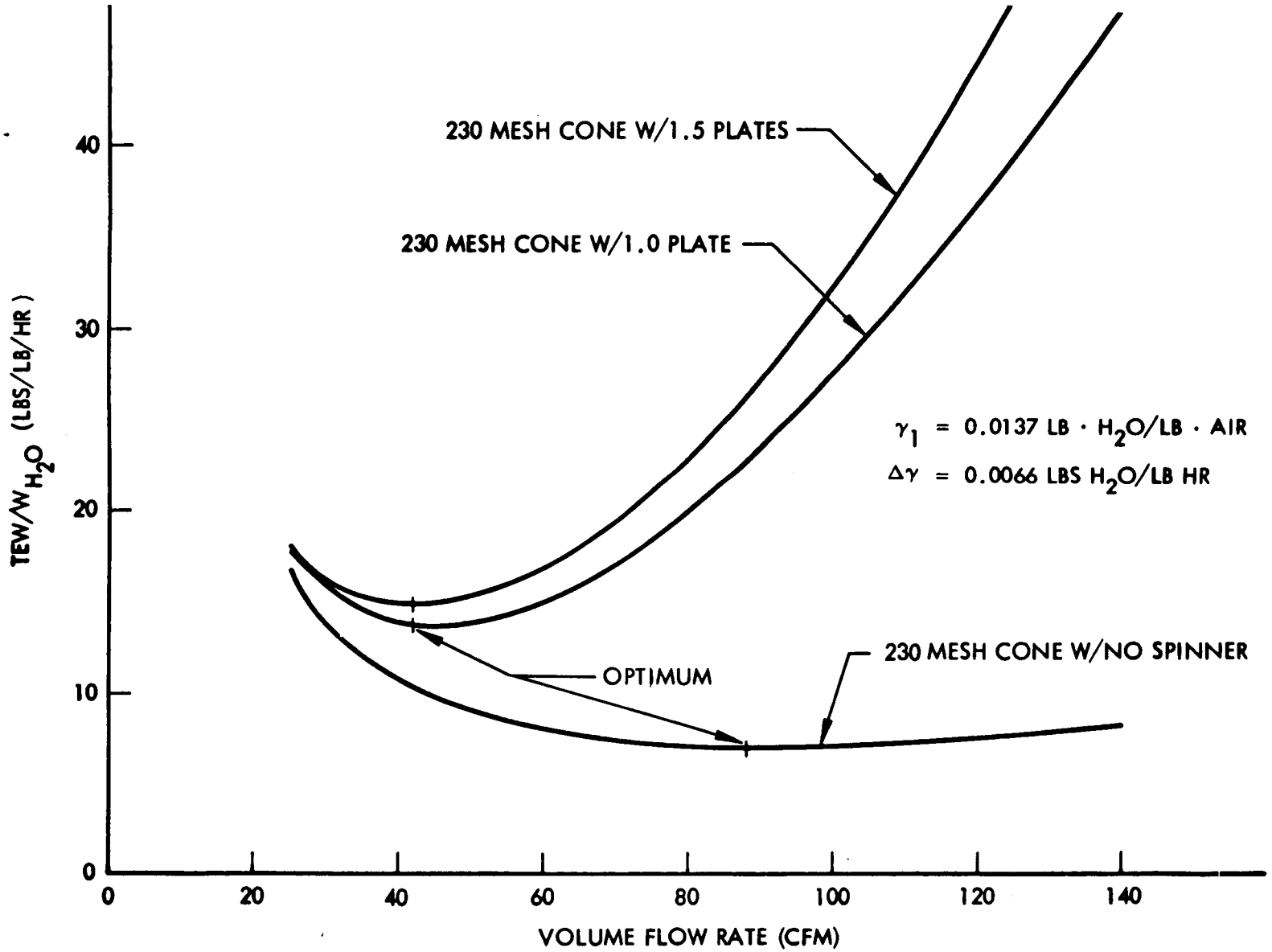

Fig. 26 - Spinner Selection

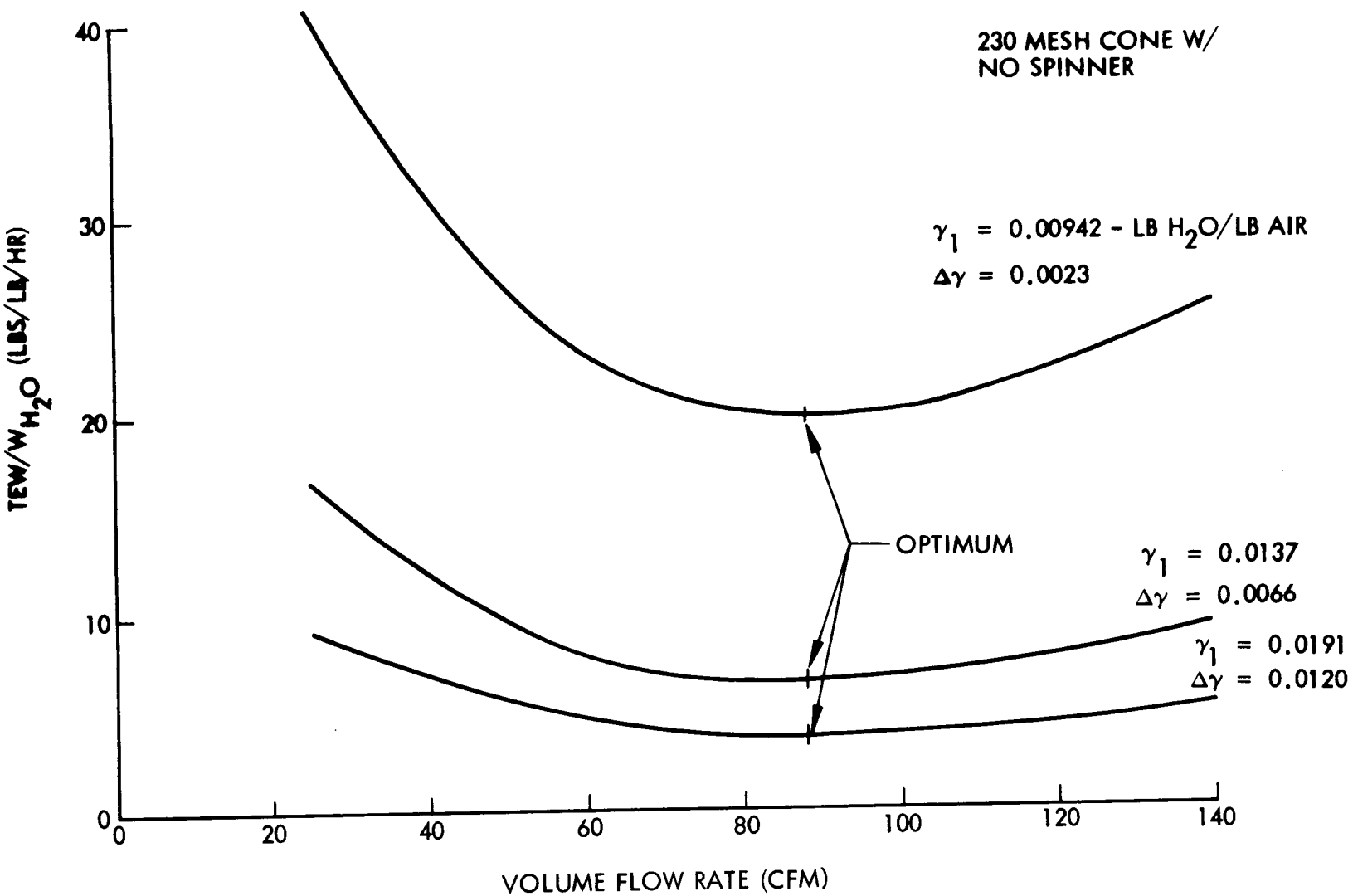

Fig. 27 - Effect of Water Removal

this theory to be in error within the range tested. The performance of the unit with the spinner in the water separator resulted in higher pressure loss, higher weight/performance penalty, and no improvement in performance. It was concluded that the water separator without the spinner was the optimum design configuration.

Optimum Water Removal Capability.- For the optimum configuration of the 230 mesh cone with no spinner, fig. 27 shows the effect of specific water removal rate on performance over the range of system air flows tested. This curve shows that the total equivalent weight per pound of water removed is least (optimum) at the maximum delta humidity (12) at an air flow of 88 cfm. The optimum system design, therefore, occurs at the point of maximum possible humidity difference consistent with system humidity control requirements.

Summary.- In summary, the optimum design characteristics for the tested humidity controlled water separator with a cone area of 28.9 in^2, fixed weight of 8.75 lbs., and a power penalty of 600 lbs/kw is a 230 mesh hydrophobic cone with no spinner configuration with an optimum flow of 88 cfm at the largest specific water removal rate allowed by vehicle design constraints. Based on this analysis, the following criteria apply to the development of an optimum water removal system whose performance is governed by humidity control requirements:

- Select 230 mesh hydrophobic cone with no spinner as optimum configuration.
- Design to maximum allowable cabin humidity and minimum allowable sink temperature.
- Establish vehicle power penalty and fan and motor efficiency for the system ΔP/flow requirements.
- Choose flow which results in minimum weight/power penalty.
- By imperical methods (using fig.24 to determine fixed weight), find optimum cone area at the design flow.

Normal vehicle ECS design specifications define values for minimum available sink temperatures and maximum water production rates and establish requirements for cabin relative humidity. From these values, system flow can be calculated directly with no penalty allowance for water separator efficiency. Water separator efficiency of 100 per cent is within system design capability. System design optimization utilizing the hydrophobic cone for water separation is then primarily one of weight and power of the moving force within the system.

Integration with Temperature Controlled System

In environmental control systems with relative humidity as a byproduct of temperature control requirements or a system with humidity control in combination with temperature control, system flow rates are generally in excess of that required to maintain the desired humidity control. In systems where flow requirements for humidity control are greater than the flow rates for the temperature control requirements, the design optimization is the same as discussed in the previous section. In either case, because the water separator performance efficiency has been demonstrated to be 100 per cent over the range of interest, the water separator penalties in the system design optimization are only those of power consumption, through pressure loss, weight and volume.

The selection of the optimum configuration for the hydrophobic cone and spinner shown in figs. 25 and 26 respectively are also applicable to the integrated temperature controlled system. Assuming a typical fixed thermal control flow requirement of 100 cfm and a vehicle power penalty of 600 lbs/kw, a plot of TEW (lbs) versus cone area (in^2) was made to determine the optimum cone area. This curve was based on the power consumption due to pressure drop, of the 230 mesh cone with no spinner at 100 cfm from fig. 17 and the fixed weight per cone area from fig.24. Figure 28 shows that the optimum TEW of 14.3 lbs, the cone area is 33.6 in^2. Based on this analysis, the following criteria apply to the development of any optimum water removal system whose flow is set by temperature control requirements:

- Select 230 mesh hydrophobic cone with no spinner as the optimum configuration.
- Establish the vehicle power penalty, fan and motor efficiency from the system Δ P/flow requirements.
- For the flow set by the temperature control requirements and the assumed system weight/power penalty (lbs/kw), determine the TEW (lbs) versus cone area relationship from the 230 mesh pressure loss characteristics (fig.17) and the water separator fixed weight per unit cone area (fig.24).
- Select the optimum hydrophobic cone area for the minimum TEW from the curve established in the preceding step.

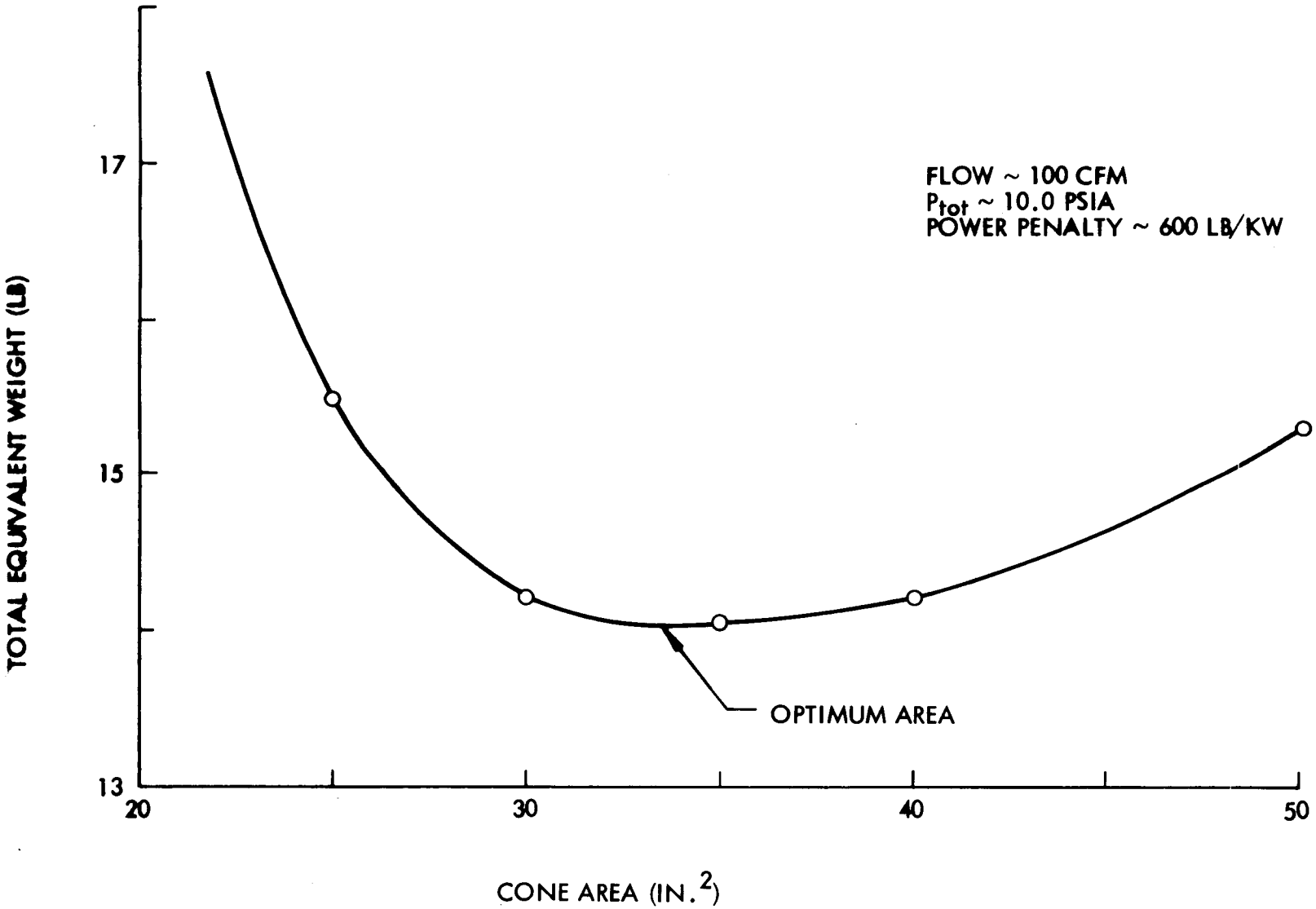

Fig. 28 - Typical Fixed Flow Optimization

CONCLUSIONS AND RECOMMENDATIONS

The following conclusions are based on the test and evaluation program conducted on the Lockheed Humidity Control System:

- The methodology developed in Appendix A and the reduced performance data from the test and evaluation program can be applied to establish optimum design criteria for other zero gravity systems utilizing the hydrophobic/hydrophilic water separator.

- The design concept of a hydrophobic cone with no moving parts as a water separator is valid as demonstrated in the test and evaluation program.

- The optimum configuration for the hydrophobic cone is a Teflon - coated 230 mesh (0.0014" diameter) wire screen, 45° cone angle with no spinner and no coalescer.

- Perform efficiencies of 100%, as demonstrated, are well within system operational and design capabilities.

- Pressure drop penalties across the hydrophobic cone are minimum, compared to other zero gravity water removal systems.

- Testing of the hydrophobic cones in the vertical mode under gravity conditions is valid for zero gravity application as it represents the maximum force of the water/air flow on the cone surface.

- The hydrophilic (sump) system tested was compatible with the water separator tested, however, no attempt was made to optimize the design or performance parameters of this system as gravity has a very beneficial effect on this component.

- The system responded rapidly to transient conditions demonstrating stable performance over a range of operating conditions with a step change input. However, response times are valid only for the volume of the test fixture.

- Based on design simplicity (no moving parts in the water separation mechanism) and performance repeatability, the Lockheed Humidity Control System is highly reliable.

- Maintainability is simple and pending endurance test demonstration and evaluation of mission requirements, maintenance requirements are comparatively low.

- Design and optimization procedures defined in the design criteria section are valid for preliminary design calculations over the range of data presented.

The positive results demonstrated in this program strongly imply that further development of the hydrophobic/hydrophilic humidity control system be undertaken. It is therefore recommended that:

- Endurance testing be conducted on the 230 mesh hydrophobic cone.
- Zero gravity tests be performed on a system to verify operation under zero gravity conditions.
- A man-rated humidity control system of flight configuration be designed, developed and qualified.

APPENDIX A

INITIAL HYDROPHOBIC/HYDROPHILIC HUMIDITY CONTROL SYSTEM

MODEL TRADE-OFF STUDY AND TEST PLAN

INTRODUCTION AND SUMMARY

Lockheed Missiles and Space Company is presently under contract to the NASA Langley Research Center to (1) develop an optimization trade-off methodology to establish requirements for experimental data, (2) develop a test plan directed toward obtaining the data required for the optimization analysis and (3) conduct the experiments defined in the test plan. This report presents the model trade-off study and the test plan.

The data generated during the experimental phase of this program will provide all of the necessary information to allow the optimization to be conducted.

MODEL TRADE-OFF STUDY
HYDROPHOBIC/HYDROPHILIC HUMIDITY CONTROL SYSTEM

The objective of the model trade-off study has been to establish a methodology for optimizing a hydrophobic/hydrophilic type water separator and to thereby identify the test data required to conduct the optimization. The methodology developed during the study is the subject of this report. The proposed three step plan is outlined below and then discussed in detail.

Step I Optimize Design of Present System - The more important physical design parameters (coalescer density and spinner configuration) will be varied and performance noted to support optimization of the laboratory unit under test.

Step II Rate Present System - The optimum flow rate and water removal rate of the present laboratory unit will be established. The methodology developed in accomplishing this task will serve as a basis for optimizing systems larger and smaller than the present unit.

STEP III Sizing of Systems Larger and Smaller Than the Present System - The data obtained in Steps I and II will be extrapolated to support optimization of any sized unit.

Step I Optimize Design of Present System

The basic elements of the humidity control system are the coalescer, spinner, and screen. Several characteristics of each of these elements can be varied with possible changes in system performance resulting. Possible variations in physical design of the unit are listed below.

Coalescer	Spinner	Screen
Type	Pitch	Mesh Size
Density	Number of Plates	Cone Angle
Length	Area	Area

Laboratory investigation of all combinations of these variables would result in a prohibitively large test program. In order to scope the program at a level consistent with the funded effort the two most important variables, coalescer density and spinner configuration were selected for optimization. The area of the unit is considered in Step III and will be discussed later. The wetting and pressure drop characteristics of various coalescer materials present an area of potential trade-off. The ability of a material to catch and hold water droplets will effect the design of the spinner and screen.

Increased coalescer length provides greater opportunity for water droplets to form prior to discharge from the coalescer, but also provides greater pressure drop. The number of spinner plates and spinner pitch affects system pressure drop and establish the amount of water removed from the airstream by centrifugal force which in turn affects screen design. Screen mesh and screen cone angle affect system pressure drop and the water removal efficiency. Increased cone angles will allow shorter unit design but must be offset by smaller screen mesh or increased screen diameter to prevent impact breakthrough. Although the most important variables are coalescer density and spinner configuration, a valuable addition to the current program would be the assessment of the effects of these other variables by test.

The first step in the currently funded effort is then based on optimizing the present design with respect to coalescer density and spinner configuration. The detailed plan for Step 1 is as follows:

1. For a pre-selected airflow (Q), cabin specific humidity (γ_1), and lowest feasible h/x exit specific humidity (γ_2), test the present system using three coalescer densities and with three spinner configurations (0, 1 and $1\frac{1}{2}$ spinner plates. Plot system's pressure drop (Δp) and water removal efficiency (η_R) vs. coalescer density with spinner configuration as a parameter.

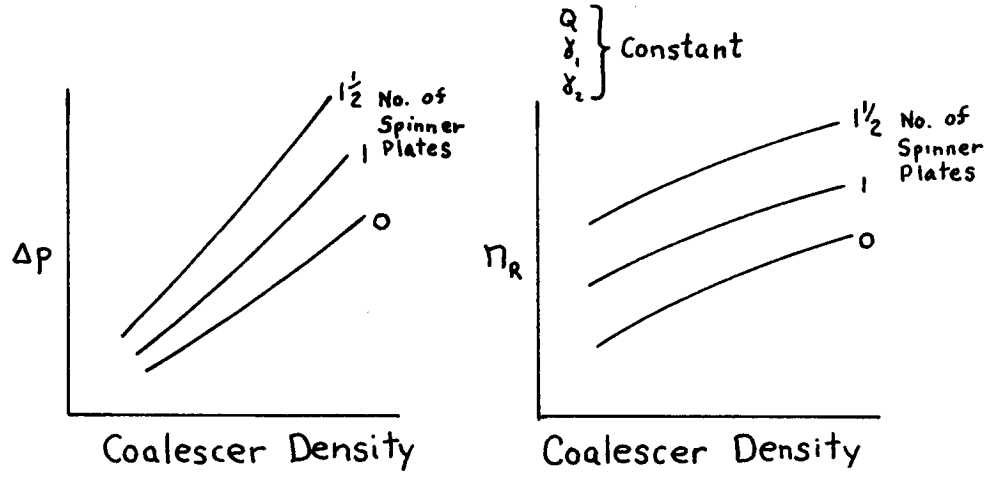

2. For the given Q, γ_1, γ_2 and using Sample 2, calculate the water removal rate ($\dot{\omega}_{H_2O}$)at various coalescer densities for the three spinner configurations.

$$\dot{\omega}_{H_2O} = Q\rho(\gamma_1 - \gamma_2)\eta_R$$

From Sample 1 obtain Δp and calculate the fan power

$$P_{fan} = Q\Delta p / \eta_{fan-motor}$$

3. Calculate the Total Equivalent Weight (TEW) of the system. TEW includes the fixed weight of the water separator and fan, and the power penalty for operation of the fan.

$$TEW = P_{fan}\,(\text{weight/watt}) + W_{system}$$

The system fixed weight will reflect flight weight estimates and not the weight of the present test system.

4. Calculate TEW per pound of water removed and plot it against coalescer density with spinner configuration as a parameter. $TEW/\dot{\omega}_{H_2O}$ is the best measure of overall system optimization.

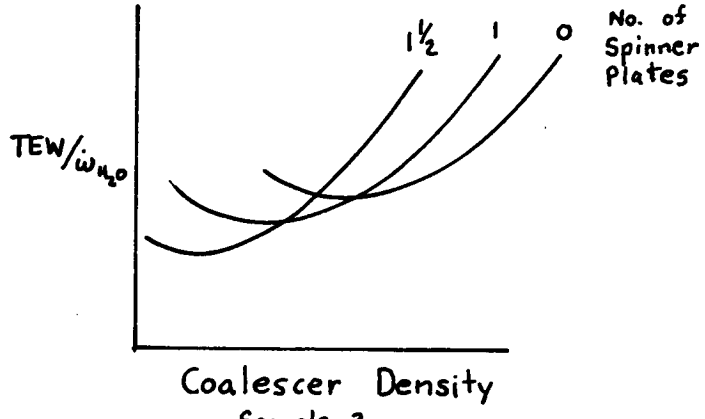

Sample 3

5. From Sample 3 select the coalescer density and spinner configuration that results in minimum $TEW/\dot{\omega}_{H_2O}$.

Coalescer densities to be tested will be selected to cover a wide range of interest. It is possible a minimum will not be identified after completion of Step I and that additional testing will be advisable. In that event LMSC will coordinate revisions in the test plan with LRC.

Step II Rate Present System

Having optimized the laboratory prototype with respect to physical design features, the next step in the program is to optimize it with respect to airflow rate and cabin and heat exchanger specific humidities. The end result of this optimization will be to establish a rating of the present

system (optimum water removal rate) and to thereby establish the basis for optimizing any sized system. The rating of the present system will be accomplished as follows:

1. Using the optimum coalescer density and spinner configuration from Step I, establish by test, system pressure drop and water removal efficiency as a function of Q and γ_1, for a fixed value of γ_2.

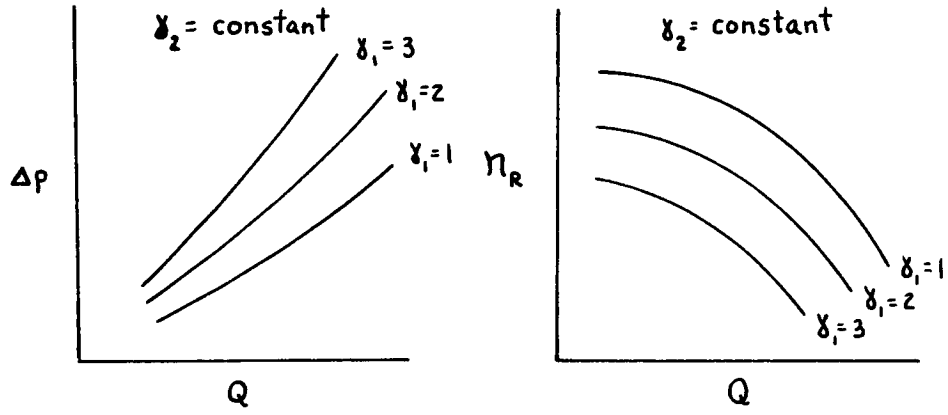

2. For each γ_1, and using at least 3 values of Q, obtain η_R from Sample 5 and calculate water removal rate.

$$\dot{\omega}_{H_2O} = Q\rho(\gamma_1 - \gamma_2)\eta_R$$

3. For each Q and γ_1, obtain Δp from Sample 4 and calculate fan power requirements.

$$P_{fan} = \frac{Q\Delta p}{\eta_{fan\text{-}motor}}$$

4. For each Q and γ_1, calculate $TEW/\dot{\omega}_{H_2O}$ based on the fan power and $\dot{\omega}_{H_2O}$ calculated above and an estimated flight system fixed weight. System weight must now include space radiator and heat exchanger weights which will vary with air flow rate.

5. Plot TEW/$\dot{\omega}_{H_2O}$ as a function of Q for each γ_1.

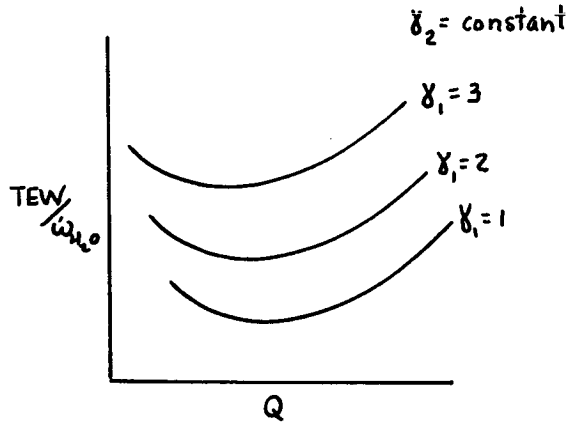

Sample 6

6. For a given γ_1, (Cabin temperature and relative humidity), the optimum flow rate can be obtained. $\dot{\omega}_{H_2O}$ can be calculated and for any given metabolic water production rate a "man-rating" can be established.

Heat exchanger outlet specific humidity has been held constant at the lowest possible value (dew point at approximately 38°F). Use of this value is based on previously conducted trade-off studies that showed the lower the condensing temperature the lower the TEW/$\dot{\omega}_{H_2O}$. In order to check this calculation the effect of varying γ_2 will be determined by test. The testing will consist of three runs at three γ_2's, a preselected γ_1, corresponding to 75°F cabin temperature @ 50% relative humidity and a constant $\dot{\omega}_{H_2O}$ corresponding to the optimum flow rate obtained from Sample 6. Maintaining constant $\dot{\omega}_{H_2O}$ and γ_1, with increasing γ_2 will require airflow to be increased.

7. For the three γ_2's measure and record airflow and Δp (γ_1 and $\dot{\omega}_{H_2O}$ constant)

8. Calculate Fan Power and TEW/$\dot{\omega}_{H_2O}$

   $$TEW = P_{Fan}(Weight/_{Watt}) + W \text{ System}$$

   The system weight includes water separator weight, fan weight and space radiator system weight.

9. Plot TEW/ω_{H_2O} as a function of γ_2.

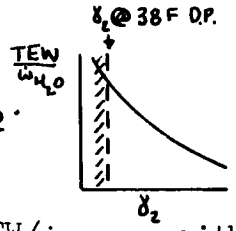

Sample 7

10. Select γ_2 corresponding to minimum TEW/ω_{H_2O} with a 38F cutoff to prevent freezing in the heat exchanger.

Step III - Sizing of Systems Larger or Smaller Than the Present System

The information presented by Samples 4 and 5 can be presented parametrically to facilitate selection of an optimum water separator for any given number of men. Generalized plots of Samples 4 and 5 can be established by dividing Q by the coalescer area. Modifying these plots as such for optimization of all systems assumes that:

a. Coalescer density and spinner configuration established as optimum for the present system are optimum for all sized units.

b. Velocity and γ_1, are the only significant parameters for the determination of η_R and Δp once an optimum physical design (coalescer, spinner and screen) has been established.

These assumptions are considered to be reasonable. In order to verify their validity however, different sized units would have to be built and tested at the constant Q/A.

The following methodology is based on the two assumptions listed above:

1. Divide the airflow (Q) in Samples 4 and 5 by coalescer area (A) in order to generate Samples 10 and 11.

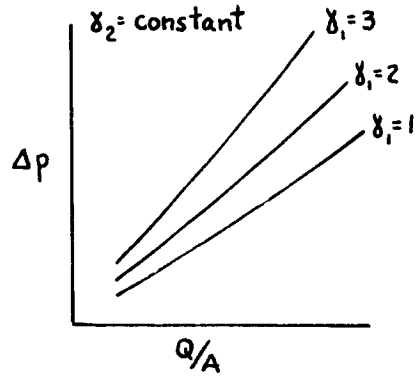

Sample 8

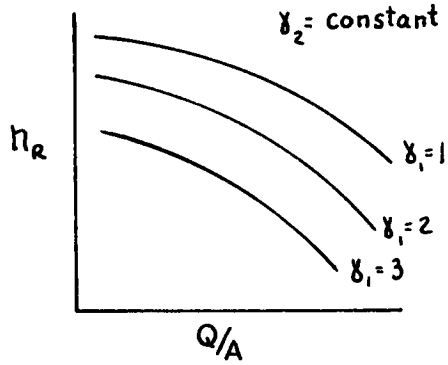

Sample 9

2. Estimate water separator system weight as a function of area (A) and plot as in Sample 10. The system weight will consist of the screen coalescer, spinner and duct.

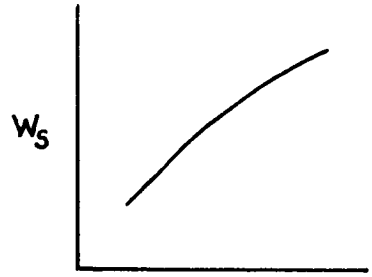

Sample 10

3. Using Sample 9 calculate required airflow for several values of Q/A for each γ_1, for $\dot{\omega}_{H_2O} = 1$. Also calculate (A) and P_{Fan}.

$$Q = \dot{\omega}_{H_2O} / \rho (\gamma_1 - \gamma_2) \eta_R$$

$$A = \frac{Q}{Q/A}$$

$$P_{fan} = \Delta P Q / \eta_{fan\text{-}motor}$$

4. Calculate $TEW/\dot{\omega}_{H_2O}$ from P_{Fan} Sample 10 and an estimate of radiator system weight

$$TEW/\dot{\omega}_{H_2O} = P_{Fan}(\text{Weight/Watt}) + W_{System}$$

System weight includes water separator weight, fan weight, and space radiator system weight.

5. Plot $TEW/\dot{\omega}_{H_2O}$ as a function of Q/A and γ_1 .

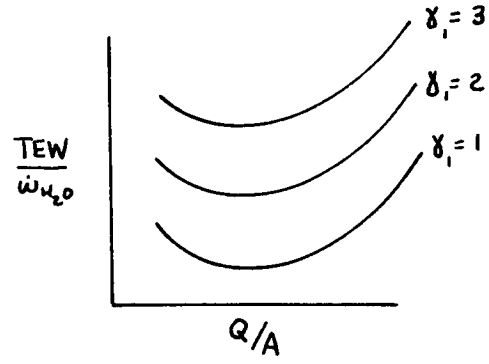

Sample 11

With the information presented by Samples 8, 9 and 11 the following method can be used for establishing the humidity control system design when γ_1, and $\dot{\omega}_{H_2O}$ are known. (γ_1 , and $\dot{\omega}_{H_2O}$ are independent variables generally known to the systems engineer). γ_2 has been established in the optimization of the laboratory system.

- o With γ_1 , and Sample 11 obtain optimum Q/A
- o With known Q/A and Sample 9 obtain η_R
- o Based on required $\dot{\omega}_{H_2O}$ and η_R calculate required Q

$$Q = \dot{\omega}_{H_2O} / \rho (\gamma_1 - \gamma_2) \eta_R$$

- o With known Q/A and Q calculate the area of the system

$$A = \frac{Q}{Q/A}$$

- o From A coalescer, spinner, screen and duct design can be established based on known coalescer type, density and length; spinner pitch and number of plates; and screen mesh size and cone angle.

TEST PLAN
HYDROPHOBIC/HYDROPHILIC HUMIDITY CONTROL SYSTEM

Steady State Test Plan

The steady state tests described herein are based on the model trade-off studies presented in previous section of this Appendix.

The present laboratory system shall be installed in the GFE test stand with the separator axis in a horizontal position. All tests shall be conducted with air at 10 psia utilizing the constant relative humidity controller as furnished to LMSC by LRC.

1. In order to support optimization of the physical design of the water separator system a series of nine test runs shall be made using three coalescer densities equal to 24.1, 48.4, and 72.5 pounds per cubic foot and three spinner configurations consisting of zero, one and one and one-half plates. Air flow rate (Q), cabin specific humidity γ_1, and water separator inlet specific humidity γ_2 shall be held constant at approximately the following values:

$Q = 70$ CFM

$\gamma_1 = 0.0137$ lb. H_2)/lb air

$\gamma_2 = 0.0071$ lb. H_2O/lb air

During each of the nine test runs the following data shall be recorded:

- o System air flow (Q) CFM
- o Cabin Specific Humidity (γ_1) lb H_2O/lb air
- o Heat Exchanger Condensing Temperature (T_c)$^{\circ}$F
- o Water Separator Outlet Specific Humidity (γ_3) lb H_2O/lb air (γ_3) is measured downstream of the reheat heater where unremoved water droplets are re-evaporated)
- o System Pressure Drop (ΔP) $"H_2O$

NOTE: Separator water removal efficiency is established by γ_1, γ_2 and γ_3.

$$\eta_R = \frac{\gamma_1 - \gamma_3}{\gamma_1 - \gamma_2}$$

2. In order to provide data for rating the present system and optimizing other water separator systems, a series of nine test runs shall be made using the optimum coalescer density and spinner configurations established by the previous series of test runs. The nine test runs shall be conducted at approximately the following conditions: three air flows of 20, 70, and 120 CFM, and three values of γ_1 equal to 0.0191, 0.0137, and 0.0082 lb H_2O/lb air. γ_2 shall be held constant at approximately 0.0071 lb H_2O/lb air. Data taken during the tests shall be as listed for the previous set of runs.

3. In order to establish the affect of varying γ_2, two additional test runs shall be made holding $\dot{\omega}_{H_2O}$ constant at a value corresponding to the optimum air flow rate (Q) established as a result of the second series of tests and a γ_1 of approximately 0.0137 lb air H_2O/lb air. γ_2 values of approximately 0.0092 and 0.0113 lb H_2O/lb air shall be used. Air flow during the runs shall be adjusted to maintain $\dot{\omega}_{H_2O}$ constant and γ_1 at approximately 0.0137 lb H_2O/lb air.

APPENDIX B

HYDROPHOBIC/HYDROPHILIC

HUMIDITY CONTROL SYSTEM

MODIFIED STEADY STATE TEST PLAN

APPENDIX B

HYDROPHOBIC/HYDROPHILIC HUMIDITY CONTROL SYSTEM MODIFIED STEADY STATE TEST PLAN

The steady state tests described herein are based on the model trade-off studies presented in the previous section of this Appendix.

The present laboratory system shall be installed in the GFE test stand with the separator axis in a vertical position. All tests shall be conducted with air at 10 psia utilizing the constant relative humidity controller as furnished to LMSC by LRC.

1. In order to support optimization of the physical design of the water separator system a series of 27 test runs shall be made using three screen apertures equal to .00148, .00178 and .00275 inches, three spinner configurations consisting of zero, one and one and one-half plates, and three air flow rate (Q) of 40, 70 and 100 cfm. The cabin specific humidity γ_1, and water separator outlet specific humidity γ_2 shall be held constant at approximately the following values:

$$\gamma_1 = 0.0137 \text{ lb } H_2O/\text{lb air}$$

$$\gamma_2 = 0.0071 \text{ lb } H_2O/\text{lb air}$$

During each of the twenty-seven test runs the following data shall be recorded:

- o System air flow (Q) cfm
- o Cabin Specific Humidity (γ_1) lb H_2O/lb air
- o Heat Exchanger Condensing Temperature (T_c) ^oF
- o Water Separator Outlet Specific Humidity (γ_3) lb. H_2O/lb air (γ_3 is measured downstream of the reheat heater where unremoved water droplets are re-evaporated)
- o System Pressure Drop (ΔP) "H_2O"

NOTE: Separator water removal efficiency is established by γ_1, γ_2, and γ_3.

$$\eta R = \frac{\gamma_1 - \gamma_3}{\gamma_1 - \gamma_2}$$

2. In order to provide data for rating the present system at off design conditions, a series of four test runs shall be made using the optimum screen aperture, spinner configuration, and flow rate established by the previous series of test runs. These test runs shall be conducted at approximately the following values of γ_1 equal to 0.0191 and 0.0082 lb H_2O/lb air. γ_2 shall be held constant at approximately 0.0071 lb H_2O/lb air. Data taken during the tests shall be as listed for the previous set of runs.

   In order to establish the affect of varying γ_2, test runs shall be made holding γ_1 at approximately 0.0137 lb H_2O/lb air. γ_2 values of approximately 0.0092 and 0.0113 lb H_2O/lb air shall be used.

APPENDIX C

OPERATION OF THE LOCKHEED HUMIDITY CONTROL SYSTEM

APPENDIX C

OPERATION OF THE LOCKHEED HUMIDITY CONTROL SYSTEM

GENERAL DESCRIPTION

The zero gravity humidity control system is designed to condense and remove water from an enclosed environment in order to prevent high humidity build up and to provide water for reuse. The humidity control system is presented schematically in fig. C-1.

Air is circulated through the humidity control system by a fan unit. The excess moisture in the air stream is condensed by the condensing heat exchanger to provide cabin humidity control. The coalescer, inside the water separator, ensures that the condensed moisture becomes droplets before leaving the coalescer. The centrifugal action generated by the static spinner will ensure that the water droplets pass over the hydrophilic sump and will minimize the impact of the water droplets on the hydrophobic surface. The hydrophobic surface allows the cooled air to pass but separates the water droplets.

The atmosphere is routed back to the cabin; the water, diverted to the hydrophilic sump, is withdrawn for storage. The hydrophilic sump allows the water to pass freely, but not the cabin atmosphere.

A bladdered-tank-type water delivery system is employed. A small air pump is controlled by the differential switch to provide the proper suction on the bladder and, thus, on the hydrophilic sump. By proper positioning of the 3-way vacuum and vent valves, the air-pump can withdraw water from the water separator or discharge water from the bladdered tank for use.

Four bosses are provided for pressure, temperature and air velocity monitoring during system operation.

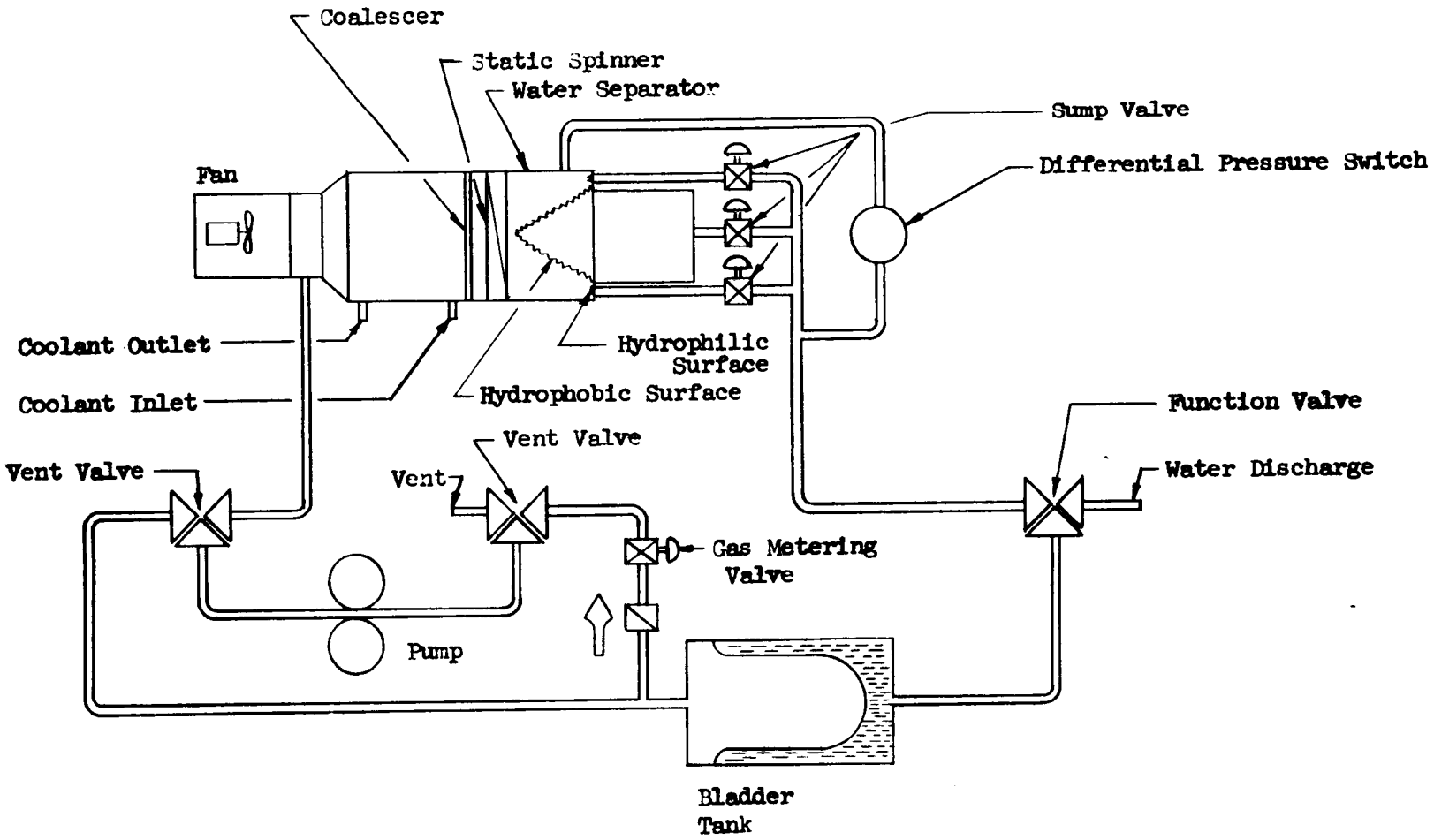

Fig. C-1 Humidity Control System Schematic

PREPARATION FOR USE AND CHECKOUT

Equipment required for operation of the Zero Gravity Humidity Control System

1. 115 VAC 60 cps Power Supply
2. 28 VDC Power Supply (10 AMP capacity)
3. Refrigeration system that will provide a continuous flow of 35°F coolant to the condensing heat exchanger
4. Air flow indicator

Preparation for Use and Checkout

Step	Procedure	Normal Indications	Notes
1	Turn pump and fan switches to off position	Off position indicated on control panel	
2	Connect system to interface equipment		Install system in test fixture
	a. Connect 28 VDC power supply	Meter on power supply to read max 28 V	Terminal board on chassis stand, Fan switch should be in off position
	b. Connect 115 VAC 60 cps power supply		Terminal board on chassis stand. Pump switch should be in off position
	c. Connect coolant lines to heat exchanger		Check for leaks
3.	Check cabling and fuses	Connectors in place and secure	Connector on different pressure switch and connector on sump pump housing fuse for fan

Step	Procedure	Normal Indications	Notes
4	Tighten and leak check all gas and water lines		Pressurize max 5 psi with dry nitrogen and check pressure decay
5	Close all sump valves	Turned clockwise to stop	Valves are metering valves and should be closed finger tight only
6	Close pump valve	Turned clockwise to stop	Valve is a metering valve and should be closed finger tight only
7	Instrumentation ports		If instrumentation is not used all unused ports should be plugged and leak checked.

OPERATION

The Humidity Control System controls for normal operation, are all contained within and on the unit itself. The water recovery system is depicted schematically on the control panel. The function and locations of each control and valve are described below.

Fan Switch

This switch is located on the control panel and indicates the ON or OFF condition of the blower.

Pump Switch

This switch is located on the control panel and has an automatic, OFF and manual position. The three conditions are indicated on the control panel.

Valves for the Water Recovery System

Function valve. - This valve determines the function of the system either to recover and store water or to expel water from the bladder tank to ambient or back through the sumps into the system. Operation and flow paths are depicted on the control panel.

Vent valves. - These valves are located on the control panel and are used to control the flow of air on the gas side of the bladder in bladder tank.

Bladder tank gas metering valve.- This valve is located over the bladder tank and regulates the rate of flow of gas removed by the pump during the water removal cycle.

Sump valves.- These three valves are located in front of the sump plate on the separator unit. There is one valve for each sump. These valves are used during the sump screen wetting procedure and for regulating the liquid flow from the water separator to the bladder tank.

Differential pressure switch.- This switch is located on the side of the separator unit. The switch senses the Δ P across the hydrophilic sump (gas side to liquid side) when there is sufficient Δ P the switch activates the pump which removes the liquid in the sump.

Operating Procedures

Valves on control panel shall always be operated in the following sequence. Close a vent, select a function, open a vent.

Step	Procedure	Normal Indications	Notes
1. Charge bladder tank with water	Open bladder tank metering valve 1/4 turn ccw. Set control panel valves as shown in fig. C-2. Attach function valve outlet to water supply. Close sump valves. Switch pump to ON position and fill bladder tank approx. 3/4 full; when bladder tank is 3/4 full turn pump switch to OFF	Water in bladder tank	Turn valves in right sequence
2. Wet sump screens	Change control panel valves to position shown in fig.C-3, Turn pump switch to ON position. Open one sump valve approx. $\frac{1}{4}$ turn ccw. Let sufficient water flow to wet screen and close valve. Follow the same procedure for all three sumps	Sump outlet tubes are filled with gas-free liquid	Turn control panel valves in right sequence
3. P switch	Set Δ P switch to 4 inches of water. Effective at the sump.	Read directly on switch adjustment screw	
4. HX	Flow coolant thru H-X at desired temp.	H-X body will become cool to the touch	Check inlet and outlet connection are correct for counter flow operation.

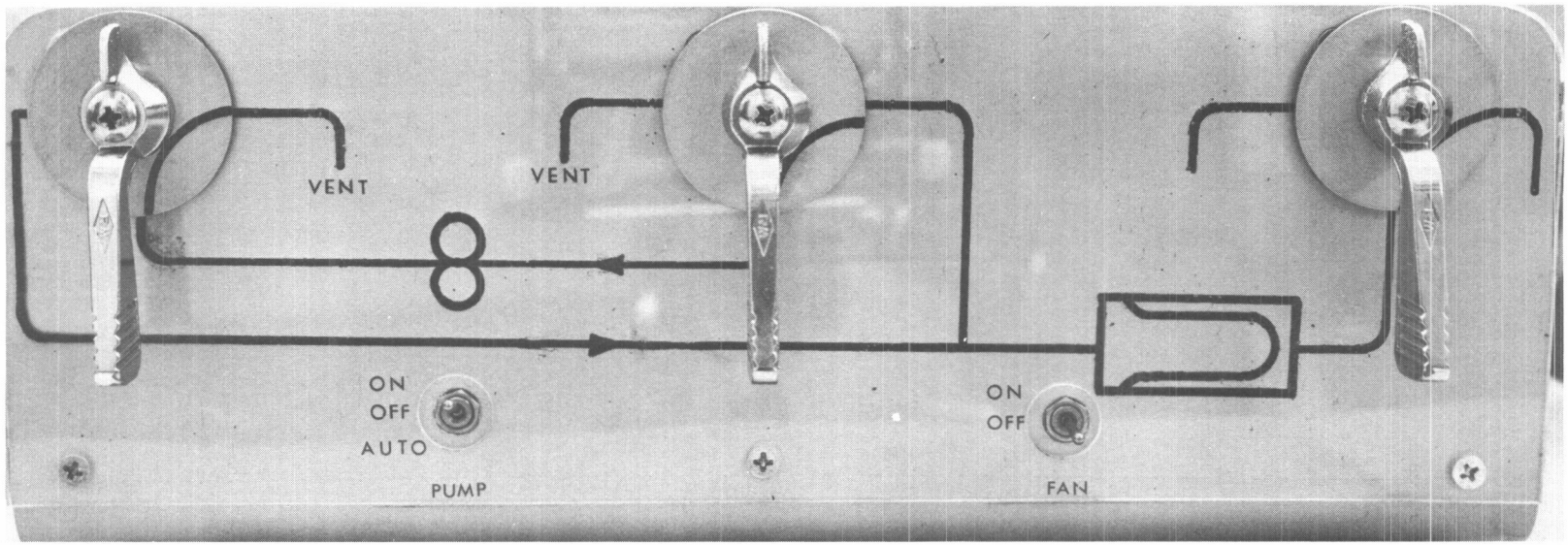

Fig. C-2 Valves Set to Charge Bladder Tank

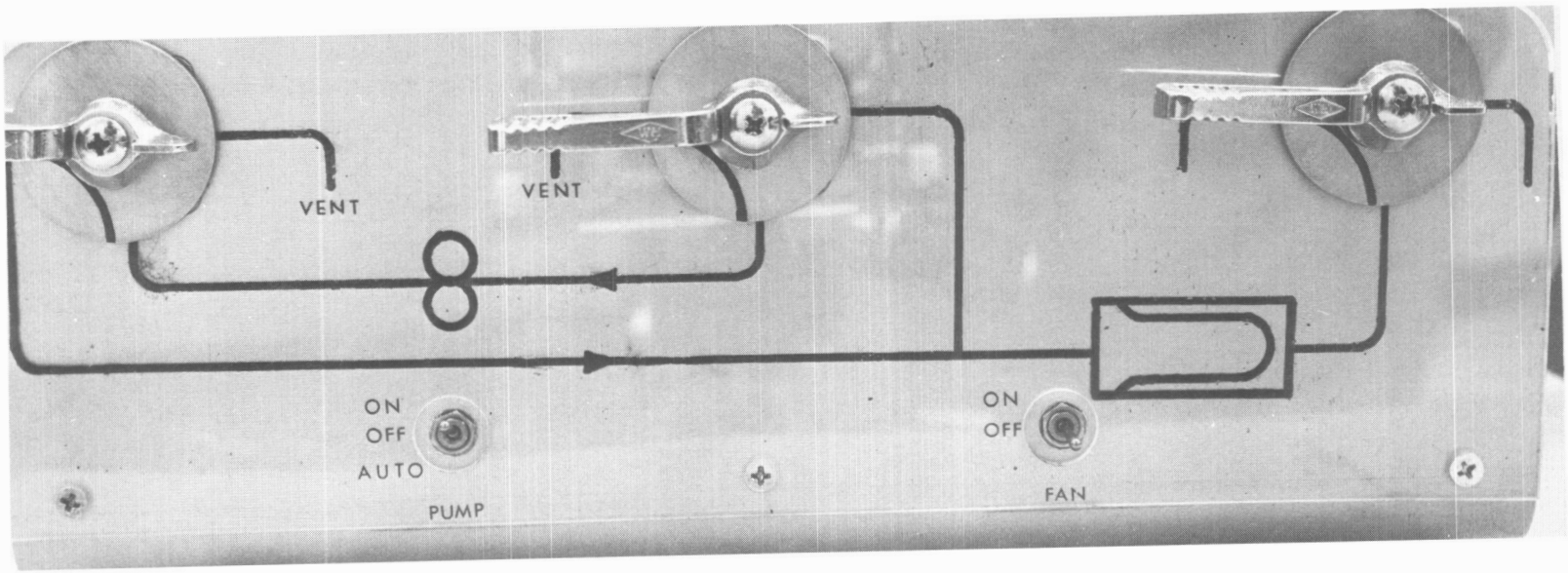

Fig. C-3 Valves Set to Wet Sump Screens

Step	Procedure	Normal Indications	Notes
5. Blower	Activate blower switch to ON position. Vary voltage on 28 VDC power supply to achieve correct air flow.		28 VDC max
6. Water	Set control panel as shown in fig. C-4. Activate pump switch to auto position. When light goes out, open desired sump valves 1/8 turn ccw and observe that water stays in outlet tube for that sump.		Operate control panel valves in proper sequence. If water leaves sump outlet tube, close sump valve and re-do Step 2.
7. Water Withdrawal	Close sump valves. Set control panel valves as shown in fig. C-5.		Operate control panel valves in proper sequence.

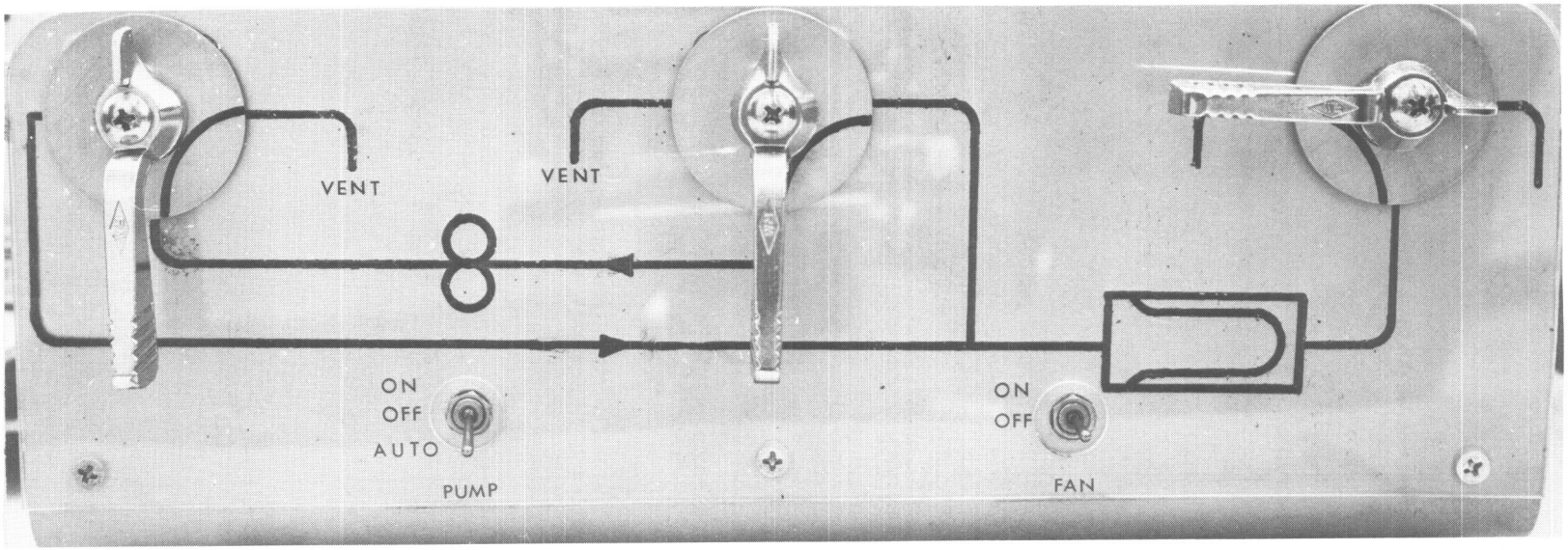

Fig. C-4 Valve Set to Remove Water From Sump and Store

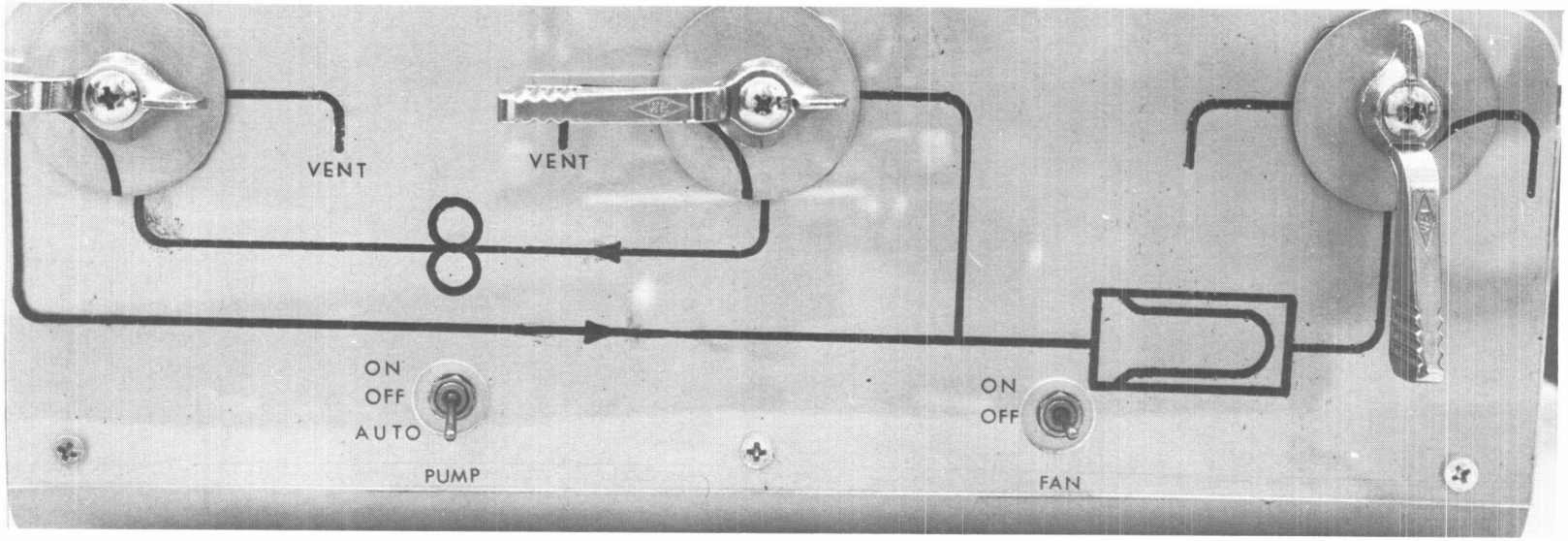

Fig. C-5 Valves Set for Water Withdrawal

APPENDIX D

TEST DATA FOR HYDROPHOBIC/HYDROPHILIC HUMIDITY CONTROL SYSTEM EVALUATION

PERTINENT UNITS FOR DATA IN APPENDIX D

Parameter	Units	Notes
1	millivolts	See fig. D-1 for conversion to ^{o}F dew point
2	millivolts	See fig. D-2 for conversion to ^{o}F dew point
3	millivolts	See fig. D-2 for conversion to ^{o}F dew point includes radiation loss to coolant fins
Thox	^{o}F	Includes radiator loss to coolant fins
Flow	ft/min	See fig. D-3 for conversion to CFM
Psys	in Hg	Represents level of test system pressure below ambient
P	inches water	Pressure loss across water separator

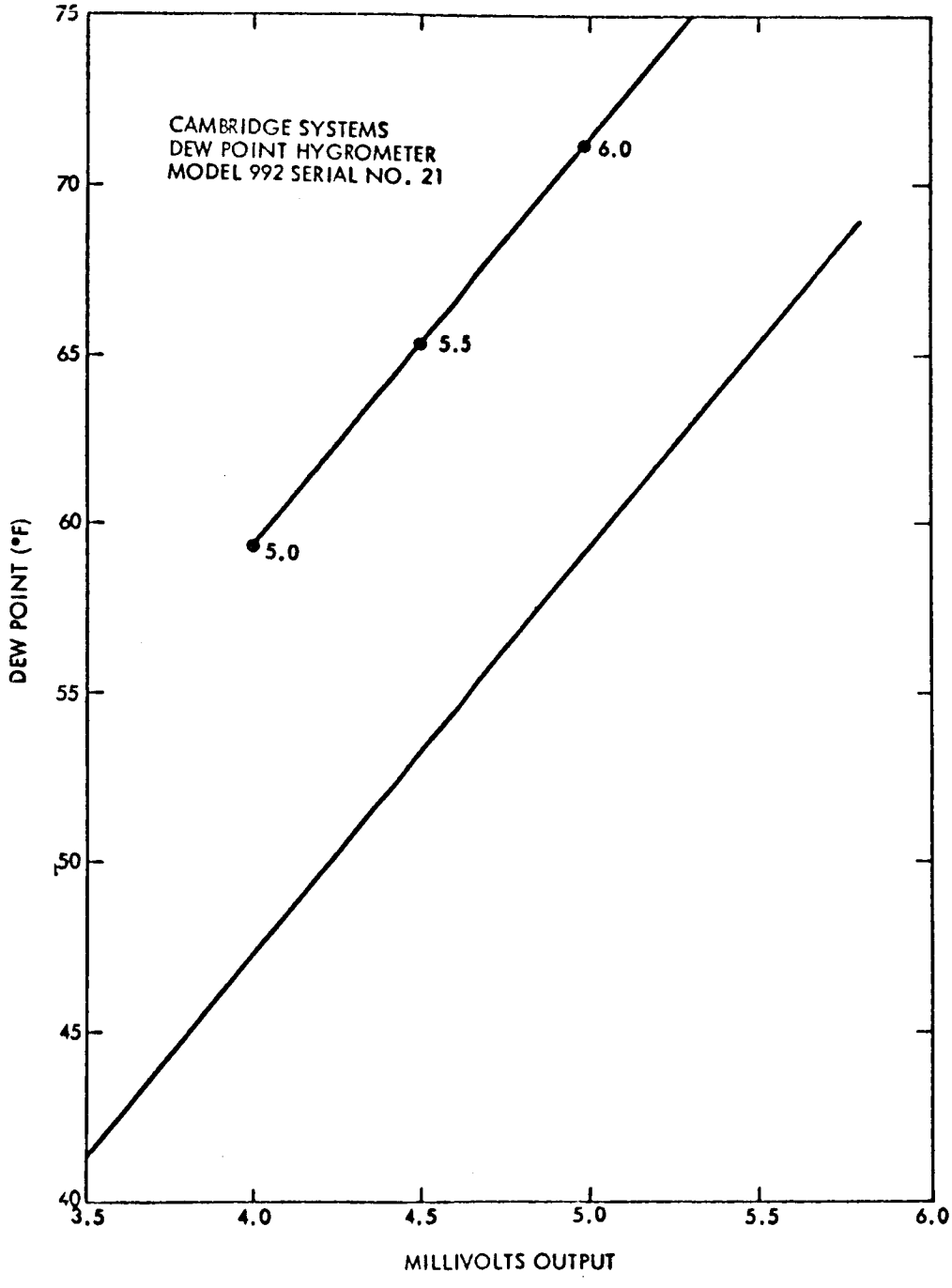

Fig. D-1 Inlet Dewpoint Conversion

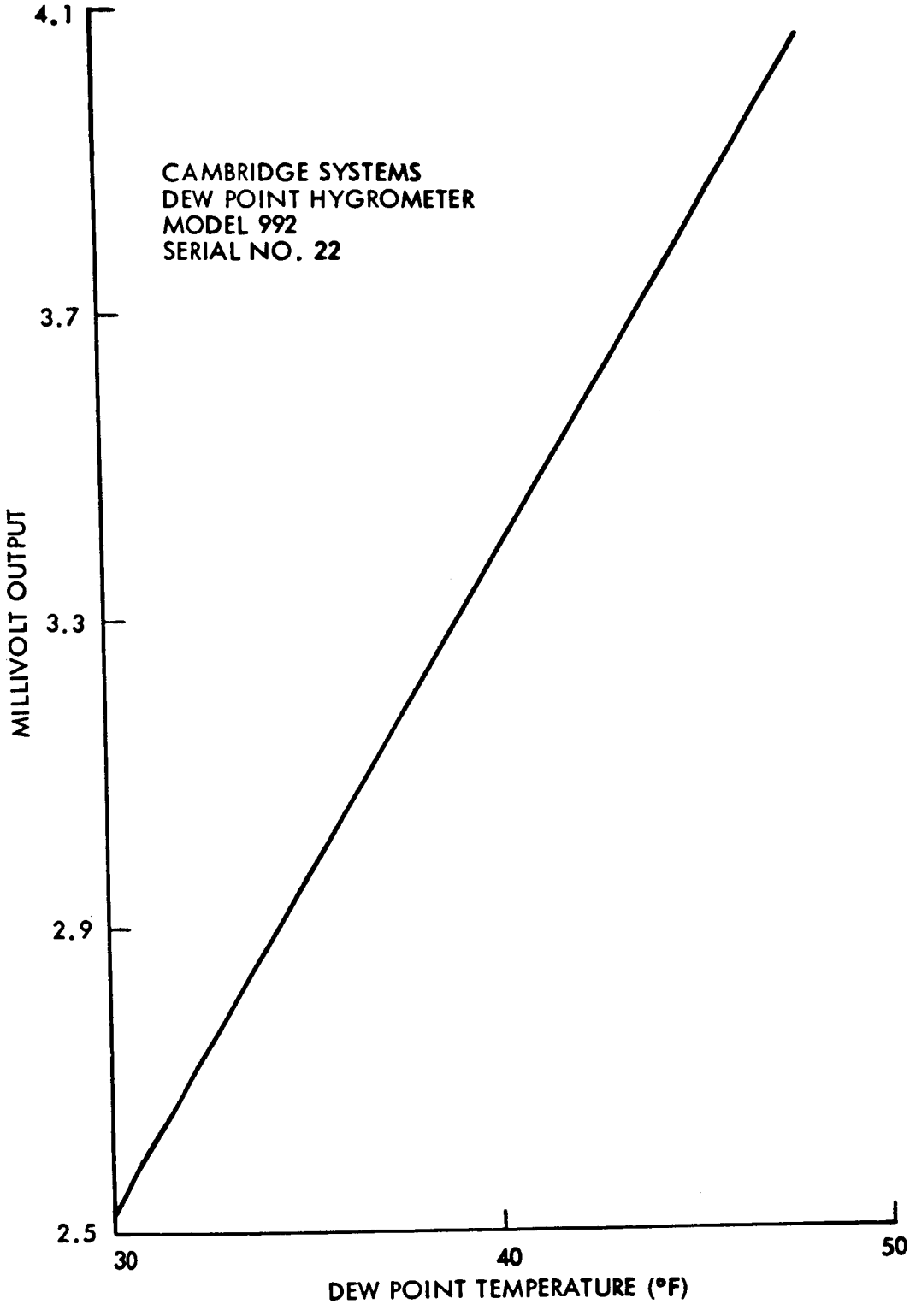

Fig. D-2 Outlet Dewpoint Conversion

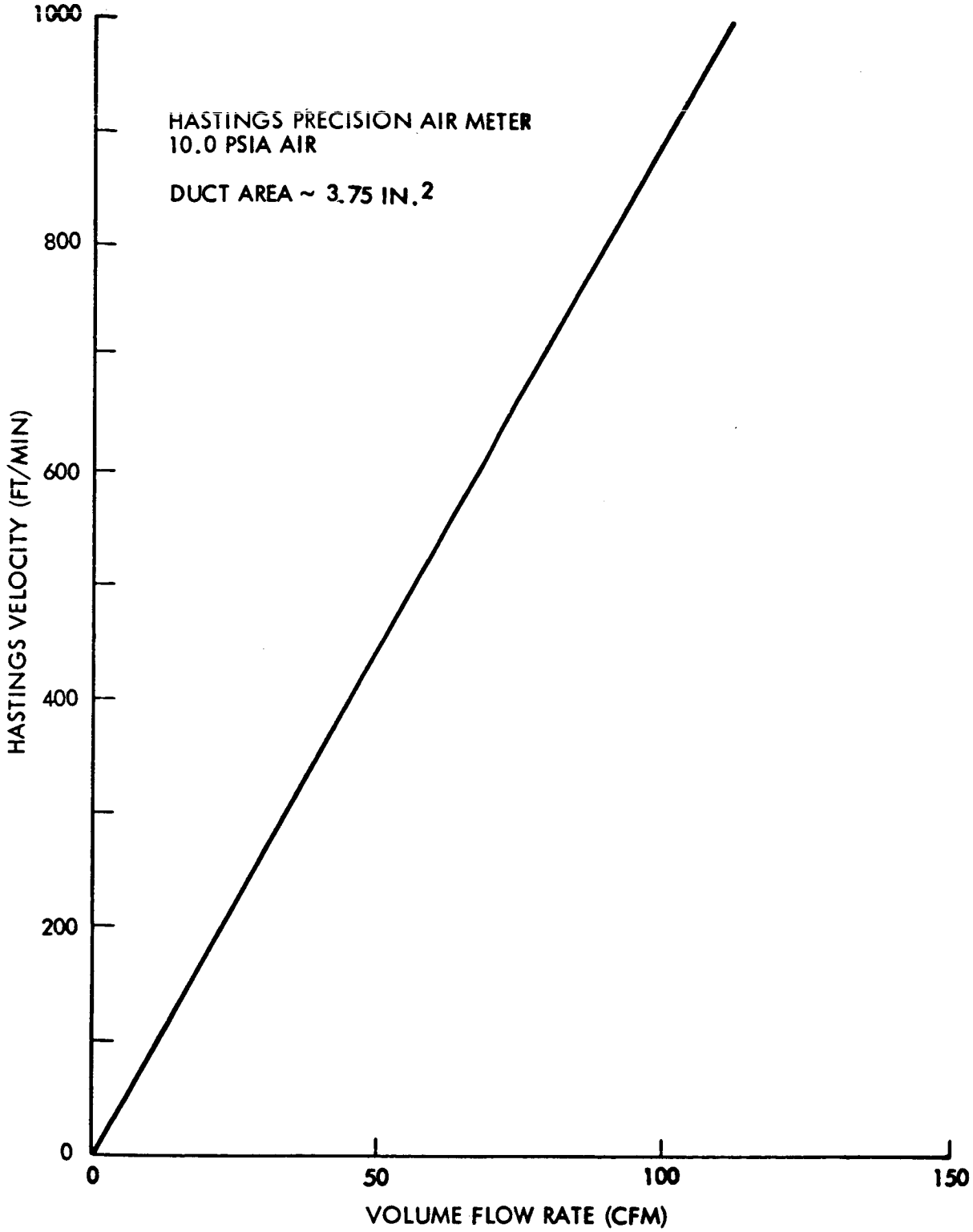

Fig. D-3 Flowrate Conversion

Run No. 1
Date - 9-27-66
Page - 2
Title - Typical Sump Performance Data

P (in H_2O) Switch Settings	Flow (cc/min)
6.5	15
8.0	33
10.0	66
12.0	92
8.0	33
11.0	air breakthrough
10.0	air breakthrough
9.0	air breakthrough
8.0	33 (no air flow)

Run No. - A1
Date - 10-3-66
Page - 5
Screen - 325 Mesh - Coarse Wire
Spinner - 1.5 turns
Coalescer - Low Density
Orientation - Horizontal
Title - Initial Horizontal Run - Low Flow

Time	γ_1	γ_2	γ_3	T_{HXO}	Flow	P_{SYS}	ΔP
4:43	4.55	3.44	3.43	35.3	630	-9.55	1.40

Run No. - A2
Date - 10-4-66
Page - 7
Screen - 325 Mesh - Coarse Wire
Spinner - 1.5
Coalescer - Low Density
Orientation - Horizontal
Title - Horizontal High Flow Run - Spinner Acting as Dam

Time	γ_1	γ_2	γ_3	T_{HXO}	Flow	P_{SYS}	ΔP
11:45	5.14	4.20	-	-	1010	-9.55	5.6

Run No. - A3
Date - 10-10-66
Page - 11
Screen - 325 Mesh - Coarse Wire
Spinner - 0 turns
Coalescer - Low Density
Orientation - Horizontal
Title - Horizontal Run - Postulate Gravity Acting as Separator

Time	γ_1	γ_2	γ_3	T_{HXO}	Flow	P_{SYS}	ΔP
11:04	5.15	4.04	4.05	43.5	1020	-9.5	.74
3:00	4.56	3.30	3.31	-	590	-9.55	.32

Run No. - A4
Date - 10-12-66
Page - 13 and 15
Screen - 325 Mesh - Coarse Wire
Spinner - 0 turns
Coalescer - Low Density
Orientation - Vertical
Title - Vertical Run - Postulate Heat Exchange as Coalescer

Time	ϕ 1	ϕ 2	ϕ 3	T_{HXO}	Flow	P_{SYS}	Δ P
10:52	2.10	4.35	4.33	46	1020	-9.5	1.66
2:50	55°	3.60	3.60	35.5	620	-9.5	.45

Run No. - A5
Date - 10-14-66
Page - 17
Screen - 325 Mesh - Coarse Wire
Spinner - 0 turns
Coalescer - None
Orientation - Vertical
Title - High Flow Run

Time	ϕ 1	ϕ 2	ϕ 3	T_{HXO}	Flow	P_{SYS}	Δ P
3:17	5.15	4.39	4.38	46.5	1020	-9.5	1.55
4:51	4.54	3.67	3.67	37	640	-9.5	.4

Run No. - A6
Date - 10-17-66
Page - 19
Screen - 325 Mesh - Coarse Wire
Spinner - 0 turns
Coalescer - None
Orientation - Vertical
Title - Full Run with Variable Specific Water Removal

Time	ϕ 1	ϕ 2	ϕ 2	T_{HXO}	Flow	P_{SYS}	Δ P
11:55	5.16	3.38	3.41		580	-9.6	.306
1:07	5.16	3.96	4.13		720	-9.5	.612
2:30	5.10	4.09	4.14		840	-9.55	.810
3:30	5.30	4.39	4.39	47.5	950	-9.5	1.10
4:25	5.50	4.69	4.75	52	1100	-9.5	2.14
5:40	5.15		3.64	-	580	-9.5	.356

Run No. - A7
Date - 10-18-66
Page - 21
Screen - 325 Mesh - Coarse Wire
Spinner - 0 turns
Coalescer - None
Orientation - Vertical
Title - High Flow Run - Effects of Specific Water Removal Rates

Time	γ_1	γ_2	γ_3	T_{HXO}	Flow	P_{SYS}	ΔP
10:55	3.36	3.34	3.35	-	910	-9.6	.608
11:35	3.70	3.54	3.56		900	-9.55	.628
1:05	4.05	3.76	3.73		950	-9.55	.678
1:55	4.7	4.03	4.01		950	-9.55	.750
2:40	5.3	-	4.29		890	-9.55	.928
3:05	5.72	4.48	4.53		910	-9.5	1.21
3:25	6.30	4.85	4.90		900	-9.5	1.63
4:40	5.50	4.81	4.85	53	1200	-9.45	4.2
5:00	4.90	4.14	4.14		890	-9.5	.840

Run No. - A8
Date - 10-19-66
Page - 23
Screen - 325 Mesh - Coarse Wire
Spinner - 0 turns
Coalescer - None
Orientation - Vertical
Title - Medium Flow Run - Effects of Specific Water Removal Rates

Time	γ_1	γ_2	γ_3	T_{HXO}	Flow	P_{SYS}	ΔP
11:15	3.17	3.08	3.10	-	600	-9.6	2.80
11:55	4.00	3.28	3.32	-	600	-9.55	.30
1:50	4.5	3.40	3.42	-	600	-9.55	.344
2:15	4.52	3.50	3.52		600	-9.55	.370
3:15	5.10	3.72	3.72		600	-9.55	.390
3:45	5.70	3.95	-		600	-9.55	.402

Run No. - B1
Date - 7-6-67
Page - 37
Screen - 230 Mesh
Spinner - 0 turns
Title - Standard Pressure Loss Run

Time	γ_1	γ_2	γ_3	T_{HXO}	Flow	P_{SYS}	ΔP
1:35	4.66	3.08	3.04	35	260	-9.5	.052
2:05	4.66	3.30	3.24	35	360	-9.5	.068
3:15	4.66	3.20	3.20	32	650	-9.5	0.146
4:15	4.66	3.23	3.25	32	890	-9.5	0.252
4:35	4.66	3.47	3.49	37	1100	-9.5	0.400
4:55	4.66	3.52	3.53	38	1150	-9.5	0.438

Run. No.- B2
Date - 7-27-67
Page - 51
Screen - 230 Mesh
Spinner - 0 turns
Title - Standard Pressure Loss Run

Time	γ_1	γ_2	γ_3	T_{HXO}	Flow	P_{SYS}	ΔP
2:15	-	3.08	3.05	90	280	-9.5"	0.053
2:50	4.70	3.13	3.11	115	350	-9.5"	0.064
3:00	4.70	3.25	3.20	108	640	-9.5	0.129
3:50	4.70	3.24	3.22	94	750	-9.5	0.197
4:10	4.70	3.23	3.23	87	900	-9.5	0.245
4:35	4.70	3.34	3.28	82	1000	-9.5	0.288

Run No. - B3
Date - 7-28-67
Page - 53
Screen - 230 Mesh
Spinner - 0 turns
Title - Standard Pressure Loss Run

Time	γ_1	γ_2	γ_3	T_{HXO}	Flow	P_{SYS}	ΔP
11:10	4.70	3.41	3.20	98	520	-9.5"	0.101
1:45	4.70	3.10	3.07	67	750	-9.5"	0.189
2:25	4.70	3.46	3.42	94	950	-9.5"	0.270
3:00	4.70	3.46	3.46	88	1100	-9.5	0.360
3:20	4.70	3.56	3.60	81	1180	-9.5"	0.485
4:30	4.70	3.90	3.95	90	1100	-9.5	0.412

Run No. - B4
Date - 7-12-67
Page - 41
Screen - 325 Mesh - Coarse Wire
Spinner - 0 turns
Title - Full Flow - 28 run

Time	γ_1	γ_2	γ_3	T_{HXO}	Flow	P_{SYS}	ΔP
1:40	4.47	3.55	3.58	38	1250	-9.5	2.505

Run No. - B5
Date - 7-13-67
Page - 43
Screen - 325 Mesh - Coarse Wire
Spinner - 0 turns
Title - Standard Pressure Loss Run

Time	γ_1	γ_2	γ_3	T_{HXO}	Flow	P_{SYS}	ΔP
11:00	4.70	3.23	3.26	32	470	-9.5	0.270
11:30	4.70	3.20	3.21	32	450	-9.5	0.262
2:15	4.70	3.19	3.19	32	660	-9.5	0.452
3:15	4.70	3.30	3.30	32	900	-9.5	0.930
4:40	4.70	3.37	3.40	32	1000	-9.5	1.260

Run No. - B6
Date - 7-14-67
Page - 45
Screen - 325 Mesh - Coarse Wire
Spinner - 0 turns
Title - Pressure Loss High Flow Runs

Time	γ_1	γ_2	γ_3	T_{HXO}	Flow	P_{SYS}	ΔP
10:30	4.70	3.45	3.47	38	1125	-9.5	1.550
4:00	4.70	3.47	3.53	37	1100	-9.5	1.619

Run No. - B7
Date - 10-17-66
Page - 19
Screen - 325 Mesh - Coarse Wire
Spinner - 0 turns
Title - Series I Standard Pressure Loss Run

Time	γ_1	γ_2	γ_3	T_{HXO}	Flow	P_{SYS}	ΔP
11:55	5.16	3.38	3.41	-	580	-9.6"	0.306
1:07	5.16	3.96	4.13	-	720	-9.6"	0.612
2:30	5.10	4.09	4.14	-	840	-9.55"	0.810
3:30	5.30	4.39	4.39	47.5	950	-9.5	1.10
4:25	5.50	4.69	4.75	52	1100	-9.5	2.14

Run No. - B8
Date - 7-18-67
Page - 47
Screen - 325 Mesh - Fine Wire
Spinner - 0 turns
Title - Standard Pressure Loss Run

Time	γ_1	γ_2	γ_3	T_{HXO}	Flow	P_{SYS}	Δ P
10:00	4.70	3.19	3.10	32	460	-9.5"	0.205
11:00	4.70	3.16	3.12	32	660	-9.5	0.287
11:14	4.70	3.19	3.15	32	680	-9.5	0.300
2:15	4.70	3.19	3.18	32	880	-9.5	0.432
3:25	4.70	3.24	3.27	35	1000	-9.5	0.560

Run No. - B9
Date - 7-19-67
Page - 49
Screen - 325 Mesh - Fine Wire
Spinner - 0 turns
Title - Pressure Loss High Flow Runs

Time	γ_1	γ_2	γ_3	T_{HXO}	Flow	P_{SYS}	Δ P
10:00	4.70	3.40	3.40	37	1100	-9.5	0.633
10:10	4.70	3.46	3.47	38	1200	-9.5	0.706

Run No. - B10
Date - 7-31-67
Page - 55
Screen - 230 Mesh
Spinner - 0 turns
Title - Pressure Loss Run High Inlet Humidity

Time	γ_1	γ_2	γ_3	T_{HXO}	Flow	P_{SYS}	Δ P
1:50	5.50	3.12	3.10	108	520	-9.5"	0.101
2:30	5.50	3.48	3.50	96	980	-9.5"	0.270
3:10	5.50	3.74	3.78	90	1090	-9.5"	0.370
3:50	5.50	3.47	3.41	106	750	-9.5"	0.201
4:30	5.50	3.96	4.00	88	1180	-9.5"	0.469

Run No. - B11
Date - 8-1-67
Page - 57
Screen - 230 Mesh
Spinner - 0 turns
Title - Pressure Loss Run High Inlet Humidity

Time	γ_1	γ_2	γ_3	T_{HXO}	Flow	P_{SYS}	ΔP
2:30	5.50	3.24	3.20	96	520	-9.5	0.106
3:00	5.50	3.21	3.18	92	750	-9.5	0.194
3:50	5.50	3.40	3.38	93	990	-9.5	0.310
4:20	5.50	3.58	3.59	88	1100	-9.5	0.380
4:50	5.50	3.44	3.45	84	1180	-9.5	0.445

Run No. - B12
Date - 8-8-67
Page - 65
Screen - 230 Mesh
Spinner - 0 turns
Title - Pressure Loss Run Low Inlet Humidity

Time	γ_1	γ_2	γ_3	T_{HXO}	Flow	P_{SYS}	ΔP
11:15	3.50	3.04	3.02	94	520	-9.5	0.102
11:30	3.50	3.06	3.05	86	750	-9.5	0.180
1:15	3.50	3.12	3.12	80	980	-9.5	0.300
2:00	3.50	3.27	3.29	80	1100	-9.5	0.401
2:10	3.50	3.27	3.30	79	1180	-9.5	0.485

Run No. - B13
Date - 8-9-67
Page - 63
Screen - 230 Mesh
Spinner - 0 turns
Title - Pressure Loss at Fixed Flow Variable Outlet Humidity

Time	γ_1	γ_2	γ_3	T_{HXO}	Flow	P_{SYS}	ΔP
11:30	4.70	4.22	4.21	96	950	-9.5	.286
1:00	4.70	4.22	4.23	95	950	-9.5	.288
1:10	4.70	4.07	4.08	94	950	-9.5	.288
1:20	4.70	3.96	3.96	88	950	-9.5	.290
1:30	4.70	3.86	3.89	83	950	-9.5	.289
1:50	4.70	3.76	3.76	82	950	-9.5	.288
2:05	4.70	3.70	3.70	76	950	-9.5	.288
2:10	4.70	3.56	3.57	75	950	-9.5	.288
2:20	4.70	3.42	3.41	69	950	-9.5	.288
2:40	4.70	3.27	3.29	69	950	-9.5	.298
2:50	4.70	3.25	3.27	70	950	-9.5	.295

Run No. - B14
Date - 8-10-67
Page - 69
Screen - --
Spinner - 1.5 turns
Title - Pressure Loss 1.5 Turn Spinner

Δ P	Flow	P_{SYS}
0.560	460	-9.5"
1.181	660	-9.5"
1.778	880	-9.5"
2.700	1000	-9.5"

Run No. - B15
Date - 8-10-67
Page - 69
Screen - --
Spinner - 1.0 turns
Title - Pressure Loss 1.0 Turn Spinner

Δ P	Flow	P_{SYS}
0.420	460	-9.5"
0.940	660	-9.5"
1.750	880	-9.5"
2.444	1000	-9.5"

LIBRARY CARD ABSTRACT

This report describes a test and evaluation program to demonstrate the feasibility and establish optimum design criteria for a Humidity Control System with a Hydrophobic/Hydrophilic cone zero gravity water separator. The test program demonstrated water separator performance at 40, 70 and 100 CFM at inlet humidities up to 0.191 lbs. H_2O/lb.air and a water removal rates up to 0.012 lbs. H_2O/lb.air. The report defines the methodology and provides the reduced test program data to establish optimum design/performance criteria for zero gravity Humidity Control Systems utilizing a Hydrophobic/Hydrophilic cone water separator.

NASA CR-66543

EVALUATION TESTING OF ZERO GRAVITY HUMIDITY CONTROL SYSTEM

Prepared Under Contract No. NAS 1-5622

by

Biotechnology Organization
Lockheed Missiles & Space Company
Sunnyvale, California

NATIONAL AERONAUTICS AND SPACE ADMINISTRATION
LANGLEY RESEARCH CENTER
LANGLEY STATION
HAMPTON, VIRGINIA

NASA CR-66543

EVALUATION TESTING OF ZERO GRAVITY HUMIDITY CONTROL SYSTEM

Prepared Under Contract No. NAS 1-5622
by
Biotechnology Organization
Lockheed Missiles & Space Company
Sunnyvale, California

NATIONAL AERONAUTICS AND SPACE ADMINISTRATION
LANGLEY RESEARCH CENTER
LANGLEY STATION
HAMPTON, VIRGINIA

NASA CR-66543

EVALUATION TESTING OF ZERO GRAVITY HUMIDITY CONTROL SYSTEM

Prepared Under Contract No. NAS 1-5622
by
Biotechnology Organization
Lockheed Missiles & Space Company
Sunnyvale, California

Thomas M. Olcott
and
Richard A. Lamparter
25 October 1967

NATIONAL AERONAUTICS AND SPACE ADMINISTRATION
LANGLEY RESEARCH CENTER
LANGLEY STATION
HAMPTON, VIRGINIA

LIST OF CONTRIBUTORS

Name	Area of Contribution
T. M. Olcott	Project Leader
R. B. Jagow	Model Trade-Off Studies
R. A. Lamparter	Experimental Evaluation
J. W. Brunner	Report Preparation

NASA Technical Monitor

C. Saunders

Life Support Section
Flight Instrumentation Division
NASA Langley Research Center

CONTENTS

ILLUSTRATIONS

EVALUATION TESTING OF ZERO GRAVITY HUMIDITY CONTROL SYSTEM

Prepared by

Thomas M. Olcott
and
Richard A. Lamparter
Biotechnology Organization
Lockheed Missiles & Space Company

SUMMARY

A test and evaluation program was conducted on a Zero Gravity Humidity Control System to establish data for the development of optimum design criteria for the hydrophobic/hydrophilic type humidity control system. The system tested was built by Lockheed and delivered to NASA/LRC under contract NAS 1-5622. The humidity control system was subsequently returned to Lockheed along with associated test equipment for a test and evaluation program. The program was conducted in four separate phases, as follows:

- o Phase One - Development of evaluation criteria and test plan.
- o Phase Two - System integration and checkout, initial steady state tests, and test plan modification.
- o Phase Three - Final steady state and performance evaluation testing and test data analysis.
- o Phase Four - Development of optimum design criteria.

These are described below.

Development of Evaluation Criteria and Test Plan

An optimization trade-off methodology was developed in Phase One to evaluate the various configurations of the humidity control system by developing total equivalent weights, considering weight/power penalties, as a function of performance. These values of total equivalent weight as a function of performance (determined by water removal capability and efficiency) can then be compared for each condition of test of configuration to assess the optimum design and performance parameters.

The procedure for evaluating the humidity control system performance is presented in Appendix A and was used as a basis for developing the test plan also shown in Appendix A. The objective of the test program is to develop data for a trade-off analysis to show the optimum configuration

of the spinner and coalescer in the water separator. Because of test program limitations, no test evaluation of hydrophobic cone mesh sizes or cone geometries was planned.

System Integration and Checkout, Initial Steady State Test, and Test Plan Modification

During system integration and checkout, in the horizontal mode, it was observed that the moisture was coalescing on the plate fin surface of the condensing heat exchanger and gravitating to the lower portions of the heat exchanger/water separator and not reaching the hydrophobic cone. From this observation it was determined that the optimum attitude for simulating zero gravity test conditions was the vertical mode. The test apparatus was reoriented to the vertical mode where initial tests verified that the coalescing function was being performed by the condensing heat exchanger and that the water separator performed at 100 percent efficiency without the coalescer in place.

In addition, it was observed that the hydrophobic cone performance was sensitive to varying water removal rates particularly at high flow rates. Based on these observations, testing was stopped and the test program re-evaluated. It was concluded that the optimum water separator configuration was with no coalescer in place. The coalescer evaluation testing was eliminated from the program and additional cone mesh sizes evaluated. The test plan was modified in accordance with Appendix B and additional hydrophobic cones of 325 mesh screen with finer wire and a 230 mesh screen were selected for fabrication and test evaluation. These cone materials were chosen as optimum based on commercial availability thereby avoiding high cost and schedule delay of special weaves.

Final Steady State and Performance Evaluation Testing and Test Data Analysis

Performance evaluation testing was conducted on three hydrophobic cone materials and three spinner configurations in this phase of the program. The test data, reduced to parametric form, was then plotted in curve form to evaluate the comparative unit performance and select the optimum configuration for additional evaluation testing to determine the effects of varying humidity loads and response to transient conditions. The results showed that the 230 mesh screen hydrophobic cone with no spinner performed with 100 percent water removal efficiency over the entire test range at the lowest power penalty. Additional testing resulted in no performance efficiency change at varying inlet and outlet humidity loads and fast response to transient conditions. The performance data was then normalized to define the pressure/density relationship versus mass flow per unit area for use at all cabin pressures and hydrophobic cone areas.

Development of Optimum Design Criteria

As demonstrated in the sample systems parameters below, the objective of the test and evaluation program to develop optimum design criteria for the zero gravity humidity control system was accomplished. By applying the optimization methodology developed in Phase One (Reference Appendix A), and the reduced data from the test and evaluation program (Reference Design Criteria Section), optimum design criteria can be developed for other systems with water removal requirements up to 0.012 lbs. H_2O/lb. air at flows up to 140 CFM (maximum tested values). Given system flow requirements as in the case in the temperature controlled ECS, optimum cone area and weight can be determined. Given outlet humidity requirements as in the case in the humidity controlled ECS, optimum air flow corresponding to cone areas and weights can be determined.

By assuming values for critical system parameters, optimum design criteria were established for a humidity control system regulated by humidity requirements and for one regulated by temperature control requirements.

Test program results showing the 230 mesh hydrophobic cone with no spinner as the optimum configuration for both the humidity controlled and temperature controlled systems were confirmed in the analysis using normalized data.

The following is a summary of the optimum design criteria established for two sample humidity control systems:

PARAMETER	SAMPLE SYSTEM		REMARKS
	Humidity Controlled	Temperature Controlled	
1. System Power Penalty (lb/kw)	600	600	Assumed
2. System Flow (CFM)	88 (Calculated)	100 (Assumed)	
3. Cone Area (in^3)	28.9 (Assumed)	33.6 (Calculated)	
4. Weight (lbs.)	8.75 (Assumed)	9.8 (Calculated)	
5. System Pressure (psia)	10	10	Assumed
6. Water Removal Rate (-lbs. H_2O/lb.air)	0.012 (Optimum)	Variable up to 0.012 maximum	Maximum measured value from test data. Temperature controlled ECS varies with temperature requirements.

INTRODUCTION

The NASA-Langley Research Center, recognizing future manned space program requirements, directed the Lockheed Missiles & Space Company to conduct a test program on a hydrophobic/hydrophilic type humidity control system to evaluate system performance and establish optimum design criteria. A number of zero gravity water separator concepts are currently under evaluation including rotating units, integrated wick heat exchangers, elbow-wick units, and the Lockheed hydrophobic/hydrophilic design. The Lockheed separator has the advantage of no moving parts, outside of the water pumping system, low pressure loss, ease of maintenance, and large surface areas to prevent clogging. These features have made it a desirable unit for developmental studies. Recognizing these features NASA directed Lockheed to produce a four-man humidity control system of the hydrophobic/hydrophilic type. This unit included a fan and aluminum plate-fin condensing heat exchanger. The system was produced and delivered to NASA as part of contract NAS 1-5622.

In an attempt to evaluate the Lockheed Humidity Control System and gain design data on this type of unit, NASA designed and built a test stand for the gathering of data on the system. The specific purpose of this program is to evaluate the hydrophobic/hydrophilic water separator system in the NASA test stand.

The tasks involved in the program are to:

- o Perform a model trade-off study to establish test parameters and optimization methodology for the experiment.
- o Conduct steady state tests for the purpose of evaluating the unit.
- o Conduct dynamic tests to determine the recovery rate from an upset condition.
- o Conduct tests on the humidity control system at various attitudes.
- o Reduct test data and provide an optimum design criteria for generalized application to future spacecraft.

The program was modified after preliminary testing in the following manner:

- o Modify initial test plan.
- o Fabricate additional hydrophobic cones of different mesh for testing.
- o Delete attitude tests.

This report describes in detail the results of the evaluation testing of the Lockheed Humidity Control System

APPARATUS

The test apparatus consisted of the hydrophobic/hydrophilic humidity control system designed and fabricated by Lockheed for the NASA/LRC, the closed circuit test stand designed and built by the LRC and furnished to Lockheed, and the supporting instrumentation and controls required to run the test. The test set-up, including instrumentation is shown in fig. 1. A schematic of this test system is shown in fig. 2. This schematic includes location of the sensing points for the instrumentation.

Description

The test apparatus is designed to evaluate the operation and performance of the Lockheed humidity control system. The system is a closed air circulating loop with the hydrophobic/hydrophilic humidity control system, reheat chamber, steam feed, and mixing chamber. The hydrophobic/hydrophilic humidity control system components are a fan, condensing heat exchanger, and a water separator. The water separator components are a hydrophobic cone, a coalescer, a spinner, and a hydrophilic sump system consisting of a pump, valves, bladder tank, and a control sensing system. The system is described in Appendix C of this report.

Equipment

The major pieces of supporting equipment consisted of:

- γ_1 measurement - Cambridge Systems Model 992 Dew Point Hygrometer
- γ_1 recorder - Honeywell Electronic 18
- γ_2 and γ_3 measurement Cambridge Systems Model 992 Dew Point Hygrometer
- γ_2 and γ_3 recorder - Leeds and Northrup Speedomax-H
- Flow measurement - Hastings Precision Air Meter
- Pressure measurement - Wallace and Tiernan Gauge
- Pressure loss measurement - Dwyer No. 1425 Hook Gauge
- Steam supply - Hotshot Electric Steam Boiler
- Steam feed control - Honeywell Electr-O-Volt Controller and Control Valve
- Coolant supply - Acme Chiller
- Power supply -0 -28 volt for fan

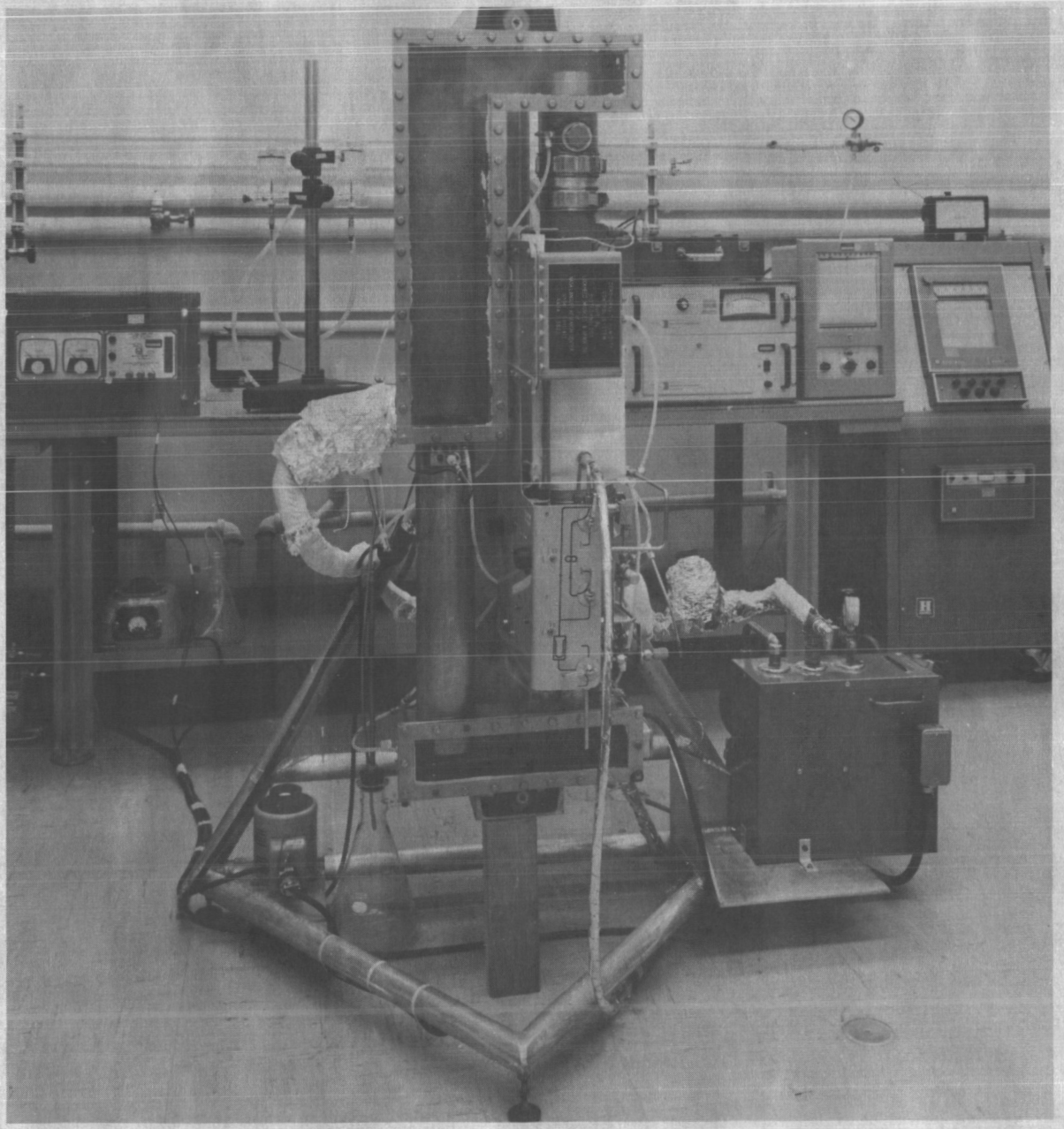

Fig. 1 - Water Separator Test Apparatus

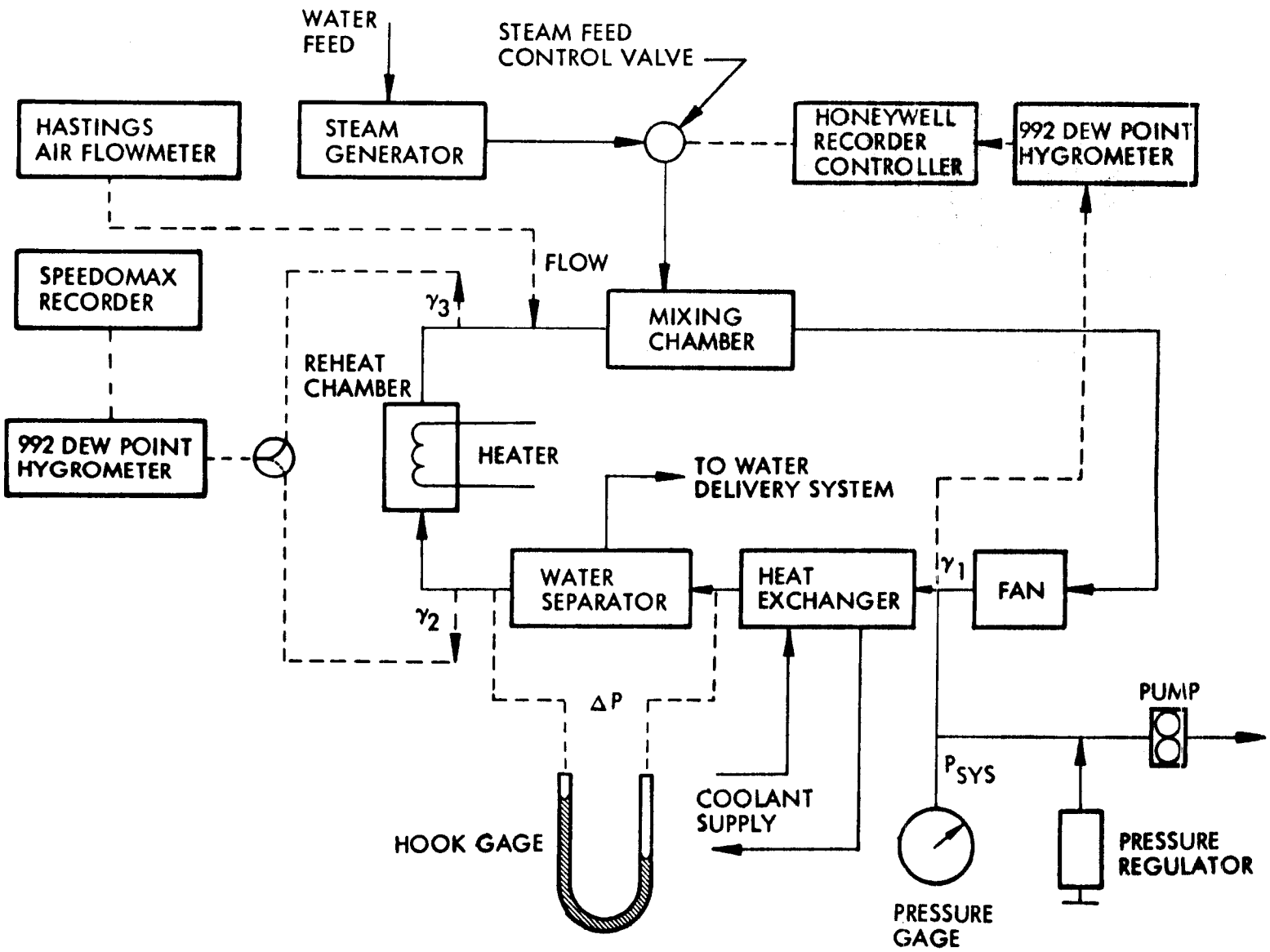

Fig. 2 - Schematic - Water Separator Test System

- Pressure regulator - Fairchild Hiller Strators Vacuum Regulator
- Air pump - Air Control Inc., Dia-Pump

Procedures

Humid air first enters the fan of the humidity control system from the mixing chamber. This component provides the impetus required to circulate the air stream in the closed system. A portion of the air leaving the fan is then sampled to determine the humidity control system inlet dew point (γ_1). The pump which maintains the system at the desired pressure is also connected to the system downstream of the fan. The major portion of the air leaving the fan then passes through the condensing heat exchanger which removes a portion of the inlet water content by condensation. The heat exchanger uses a cold glycol-water solution as a heat sink. Free water and chilled saturated air leaving the heat exchanger then enter the hydrophobic/hydrophilic water separator. The air is free to pass through the hydrophobic cone while the free water is deflected to the hydrophilic sumps where it is pumped from the system. Air will not pass through the sumps when they are wet. The water separator also includes a coalescer material and a spinner which provides a rotational velocity to the air stream to improve the capability of free water removal. A small portion of the air stream leaving the water separator is sampled to determine the air outlet dew point (γ_2). The water separator outlet stream then passes through a reheat chamber where any free moisture in the air stream can be re-evaporated. A small portion of the air leaving the reheat chamber is sampled to determine the outlet dew point (γ_3).

This measurement also provides the total water passing through the water separator. A Hastings flow meter in the duct downstream of the reheat chamber measures the circulating velocity of the air stream. Steam is fed into the circulating air stream at this point through the test apparatus humidity control system to make up for the free water condensed in the heat exchanger and removed by the water separator. The steam and air mixture then pass through a mixing chamber back to the humidity control system fan inlet.

The humidity sensed by the humidity control system is sampled downstream of the fan. The signal from the dew point sensor is recorded on a Honeywell recorder and used by the Honeywell Electr-O-Volt Controller to maintain the inlet humidity (γ_1) at the proper level. Steam for the unit is generated in a Hotshot Electric Boiler. The samples for recording the water separator outlet and reheat chamber outlet humidity are selected by a 2-way valve. These samples are measured by a second 992 Dew Point Hygrometer and recorded on a Leeds & Northrup Speedomax-H recorder.

The air flow, in feet per minute, is measured by a Hastings Precision Air Meter. This probe is located just upstream of the steam feed and mixing chamber. The measurements of this probe are converted from flow velocity in feet per minute to CFM using the known duct area (3.75 in^2).

The water separator pressure loss which varies from .1 to 3.0 inches of water is measured within an accuracy of 0.01 in. H_2O with a Hook Gauge.

A system tap at the fan outlet is used to maintain the system pressure at the proper level. A Fairchild Hiller Stratos Pressure Regulator is used to control to the proper level and an Air-Control Inc. Dia-Pump is used to maintain pressure. A pressure gauge is used to monitor system pressure at this point.

An Acme Chiller provided the cold water/glycol mixture used as a coolant in the heat exchanger.

During operation of the test apparatus, a number of system characteristics were observed. These characteristics resulted in the following rules of operation to acquire reliable data.

- o During massive water break through of the hydrophobic cone, total re-evaporation did not take place in the reheat chamber. As a result, Y_3 was only an indication of break through, not a measure of it.

- o In order to get good humidity control at the low steam feed levels for this test, boiler pressure was maintained below 5.0 psig.

- o Condensation takes place in the steam feed lines. To prevent injection of free water into the test set-up, a heated steam trap was inserted at the test apparatus inlet.

- o To assure complete water removal by the hydrophilic sumps the delta pressure switch setting was maintained between 7 and 8 inches of water.

- o Operation of the water collection system air pump caused a step in the pressure differential measurement. As a result, measurements were taken only after the system had settled out after a pulse.

- o The unit has a capacity for considerable amounts of free water. This must be removed from the sumps at the start of each run.

- o The Honeywell Electr-O-Volt control is difficult to adjust. Recommended settings are:

Reset	.1
Rate	.1
Prop Band	8.5

TEST PROGRAM

A Hydrophobic/Hydrophilic Humidity Control System Model Trade-Off Study and Test Plan (Appendix A) was developed by Lockheed and approved by NASA/LRC for system test and evaluation to establish optimum design criteria.

The primary humidity control system component is the water separator. The test program was designed to evaluate the effects on system performance of the coalescer (3 densities), the spinner (3 vane configurations), and the 325 Mesh Coarse Wire hydrophobic cone.

Initial testing was devoted to familiarization with the humidity control system, test apparatus, and associated instrumentation, and to the development of data acquisition requirements in accordance with the plan of test. Following system checkout, initial steady state testing was performed at varying conditions, configurations, and orientations to determine the optimum test configuration, and to define the scope of the important test parameters. The initial steady state tests showed a need for significant modification of the plan of test including the added scope to evaluate various hydrophobic cone configurations. The testing was stopped, test plans were modified, and two new cone configurations were selected and fabricated. Upon delivery of the two new hydrophobic cones, the test program was conducted in accordance with the modified test plan (Appendix B). In the final phase of the program, the test data was reduced and analyzed to evaluate the humidity control system performance and establish optimum design criteria. The following paragraphs provide a detailed technical discussion and evaluation of the test program. The tabulated data points, taken from the test data log books, which were used to generate the figures in the report are presented in Appendix D. A summary of the significant conclusions from the test program is as follows:

1. The optimum attitude to simulate "zero g" conditions for the water separator is the vertical mode.

2. The optimum configuration of water separator is the 230 Mesh hydrophobic cone with no spinner and no coalescer.

Initial Steady State Tests

System Integration and Checkout.- Upon completion of the test apparatus/instrumentation integration and system checkout, tests were run on the water separator to evaluate separator performance in the horizontal mode.

Initial testing at high air flow rates and low ΔP switch settings showed that an intermittent massive water breakthrough occurred indicating inadequate water removal capacity by the sumps. System testing was then stopped and testing was conducted on sump water flow rate as a function of differential pressure switch setting to determine the optimum water separator/sump ΔP switch settings within the range of test parameters (Appendix D- Run No. 1). The curve showing the relationship of these parameters

is presented in fig.3. The conclusions from this testing are as follows:

- o At low ΔP switch settings, flow falls off rapidly approaching zero at switch settings of 5 inches H_2O ΔP. (Region of inadequate sump water removal capacity resulting in water breakthrough at the separator cone.)

- o At a switch setting of 8 inches H_2O ΔP the sump breaks through and passes air.

As a result, the ΔP switch was set at just below 8 inches H_2O to cover the full test range of water flows with no air flow breakthrough at the sump.

Horizontal Runs.-Continued runs in the horizontal mode (Appendix D Run No. A1 and A2) showed unpredictable performance of the water removal system. Further investigation revealed that the spinner acted as a dam in the horizontal mode, causing water to build up upstream of the spinner resulting in major water pulses when the overflow point was reached. To prevent this condition from occurring, the spinner was removed. This change in configuration resulted in a 100 percent water separator efficiency at conditions up to 115 cfm (Appendix D Run No. A3), which represents a flow well beyond the test design flow of 70 cfm. (The 115 cfm flow was the maximum test apparatus output with the 28 VDC supply.) Heat exchanger studies show that it is characteristic of condensing heat exchangers for water to leave the core in the form of large drops. In the horizontal mode these drops under the influence of the air stream, gravitate from the downstream face of the plate fin core and collect at the bottom of the heat exchanger. Any remaining free water that was carried over by the air stream was trapped by the coalescer where it in turn gravitated to the low spot of the water separator casing. It was felt that the objective of the experiment was not being accomplished in the horizontal mode because water separation was performed primarily by the heat exchanger and coalescer and not by the hydrophobic cone.

To eliminate this test deficiency, the vertical mode was selected for future testing to most closely assimulate "zero g" conditions. In the vertical mode with flow in the direction of gravity, the total free moisture flow is delivered to the hydrophobic cone, thereby placing more than maximum load on the cone because of the added one "g" velocity increment. In addition, the vertical mode causes no effective disturbances to the radial flow distribution. At this point the test apparatus was rotated and set up for operation in the vertical mode.

Vertical Runs.- Initial tests in the vertical mode resulted in 100 percent water separation efficiency within the range of the moisture and velocity load requirements of the plan of test. At conditions above 100 CFM air flow, massive water breakthrough occurred. During breakthrough conditions, the reheat chamber was not able to totally re-evaporate the

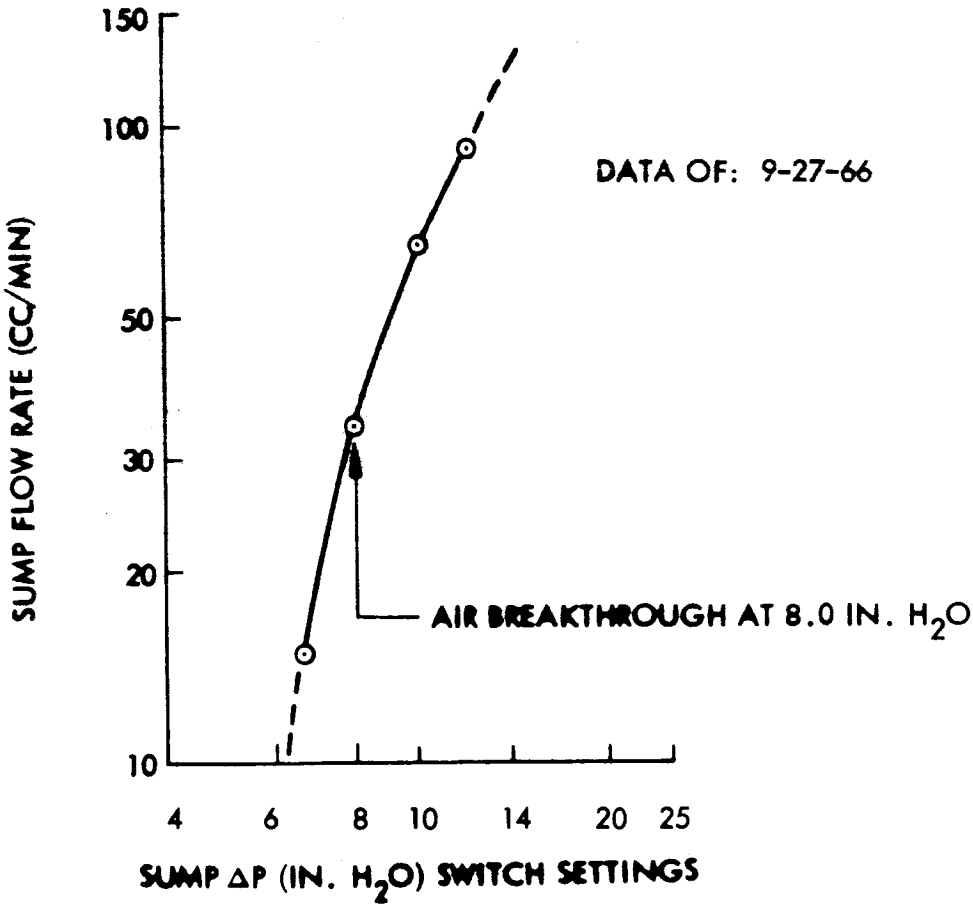

Fig. 3- Typical Hydrophilic Sump Characteristics

free moisture and therefore no measure of water separator efficiency was possible. Based on the fact that water condensation occurs on the metal surface of the heat exchanger and leaves in the form of droplets under the combined influence of gravity and the air stream (thereby performing the function of the coalescer), the coalescer was removed from the water separator. Tests were then run to evaluate the humidity control system performance with the coalescer removed. Comparative data, from both the test with the low density coalescer in place (Appendix D Run A4), and with no coalescer in the water separator (Appendix D Run A5), showing pressure loss as a function flow at a fixed moisture removal rate is presented in fig.4 for reference. Although the additional pressure drop caused by the coalescer represented less than 10 percent of the total system pressure loss, the significant result was that no difference in separator efficiency was observed when the coalescer was removed. The unit functioned at 100 percent water separation efficiency to above the test requirement condition of 100 CFM (duct velocity 880 ft/min on fig. 4) before breakthrough occurred. In the test, with the water separator in the vertical mode and the spinner and coalescer removed, the chiller used was not capable of maintaining the required dew points at high flow rates.

Therefore the inlet humidity was increased with flow to maintain a nearly constant specific water removal rate. Figure 4 shows that the sharp increase in the rate of pressure rise occurs in the region (above velocity of 900 ft/min) that water breakthrough was initially observed. It was then postulated that at some high pressure difference across the screen, water is forced into the mesh and held causing increased pressure loss as area is blocked and ultimately resulting in breakthrough. This theory is fortified by observations of pressure loss data taken as the flow rate was reduced from high flow rates. The data shows that the higher than expected pressure loss which is attributed to screen blockage by water accumulated at the higher flow, purges itself from the screen with time and the pressure loss is restored to the data level recorded at increasing flow rates. As a result of these observations, a new set of tests was developed which would show the effect of water flow on pressure at some fixed value of flow.

Water Removal Effects.- The final tests in the initial series consisted of testing to determine pressure loss for fixed values of flow with variable water removal rates (Appendix D Runs No. A6, A7 & B7). This data is presented in fig. 5. At each of the test points several readings were obtained to assure that the pressure loss had achieved a stable steady state value. The data shows a marked increase in pressure loss with water removal at 101 CFM. At low air flow rates water removal efficiency was 100 percent. However, as water flow was increased beyond .042 pounds per minute, breakthrough occurred. This curve clearly shows the effect of increasing water flow rate on water separator pressure drop, and indicates that the important parameters (lbs.H_2O/lb. air flow), is missing from fig.4.

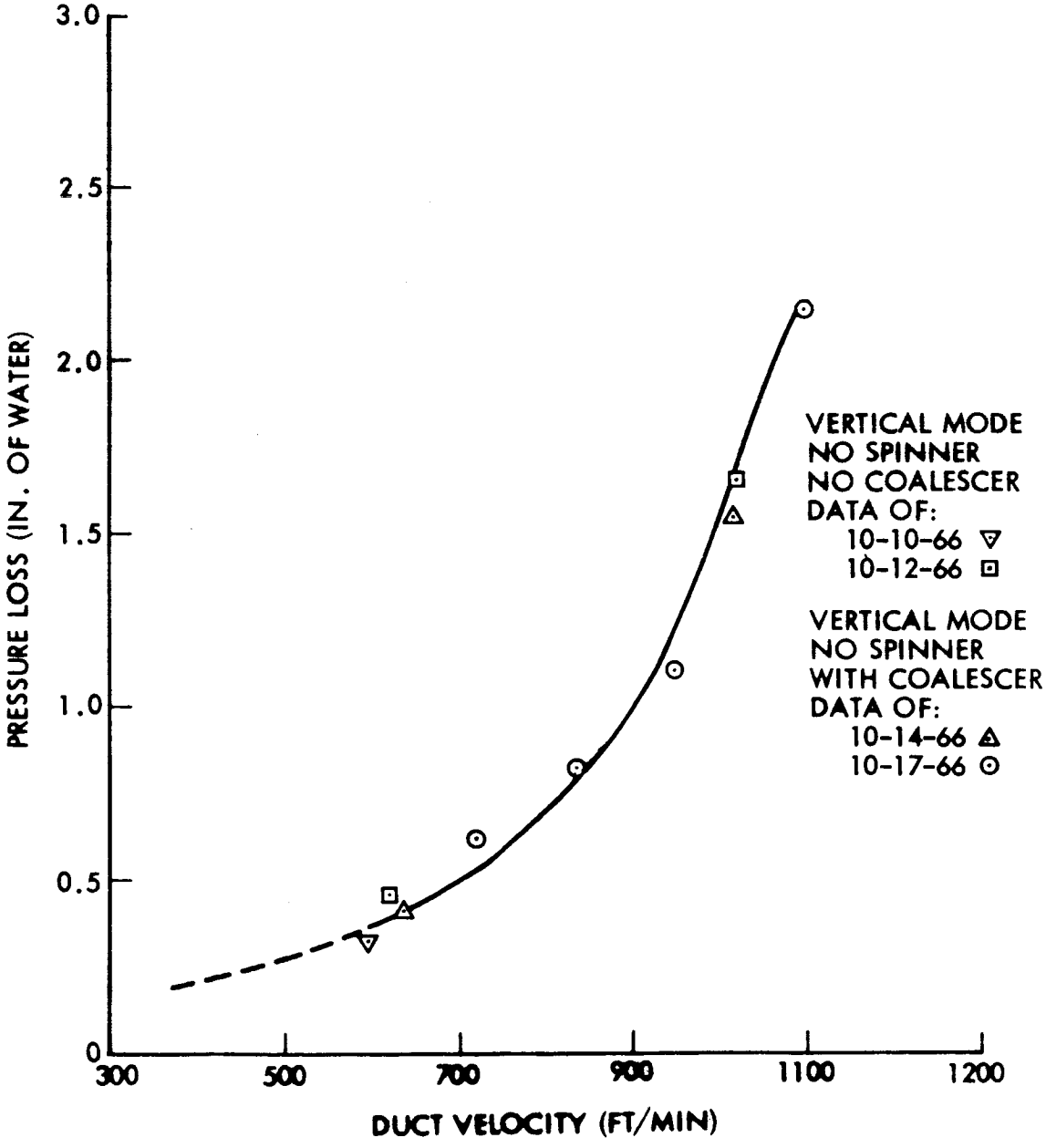

Fig. 4 - Mesh Coares Wire Pressure Loss

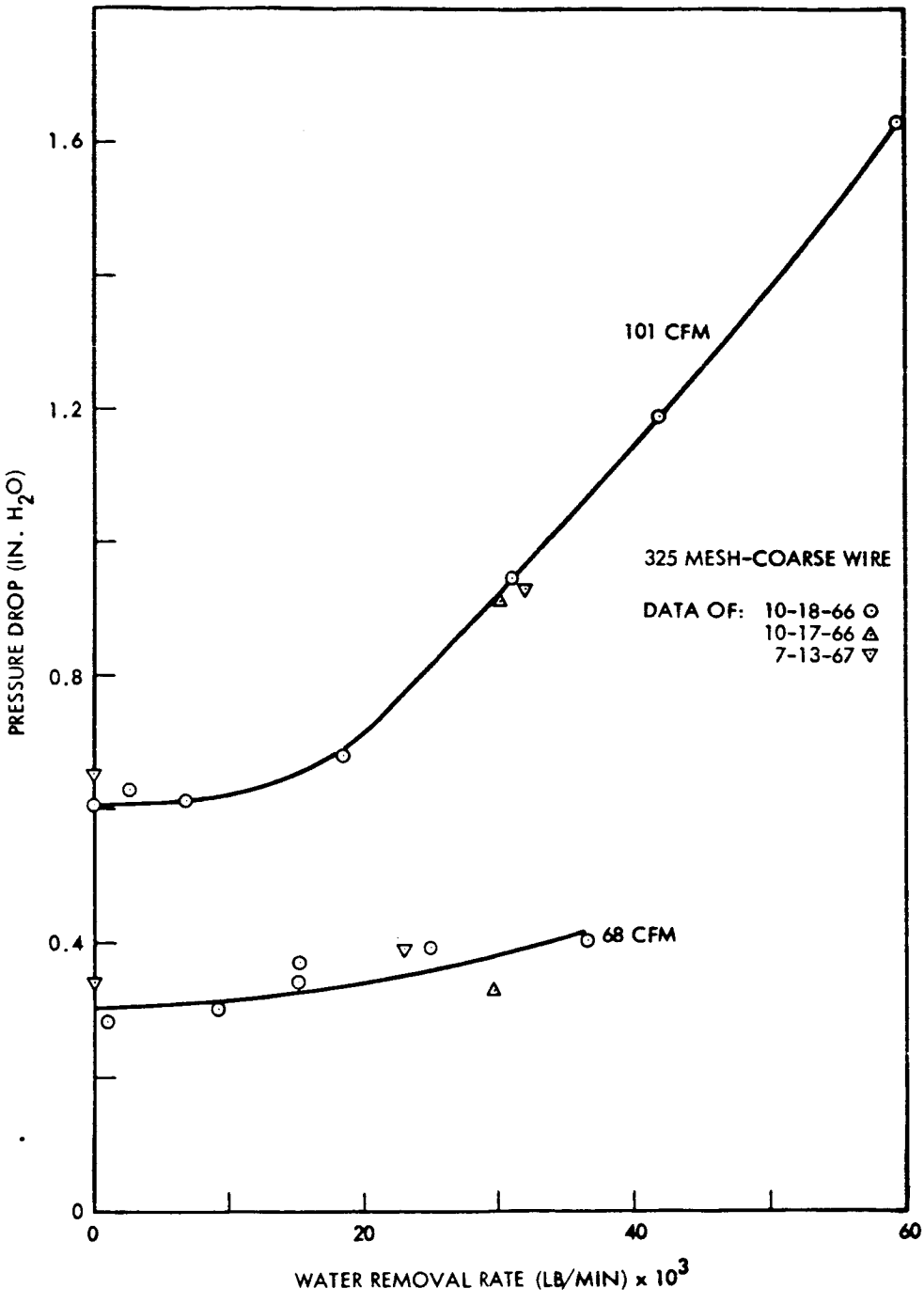

Fig. 5 - Effects of Specific Water Removal Rate

A repeat of this test procedure at 68 CFM shows only a slight increase in pressure drop with water flow (Reference Appendix D Run No. A8). A possible explanation of this effect is that the lower pressure difference across the cone at the lower flow rate was not enough to cause water on the surface to be held.

Test Plan Modification

The results of the initial steady state tests indicated a need for revising the plan of test. The following conclusions were made from analysis of the initial steady state test data:

1. The objective of the first phase of the steady state tests was to determine the performance of the water separator in a series of nine test runs with three different coalescer densities and three spinner configurations. An optimum configuration for the spinner and coalescer then was to be established for further test and evaluation. The initial steady state tests indicated that the water separator performed at 100% separation efficiency for the test conditions with no spinner and no coalescer. This accomplished the objective for determining the optimum configuration for the coalescer and spinner configurations within the water separator. The test plan was then modified to establish the optimum configuration for the hydrophobic cone screen size and to further evaluate spinner configurations. It was thought that configurations which encompass larger screen apertures would tend to reduce water separator efficiency and pressure drop.

2. Evaluation of the data from the initial steady state tests indicates that the heat exchanger upstream of the water separator serves as a coalescer and thus the coalescer is redundant. Therefore, variation in coalescer density was deleted from the test plan.

3. Operation of the system in a vertical downward rather than a horizontal attitude during the steady state test runs was most representative of a zero gravity situation. The performance of the separator was affected in the horizontal mode by the tendency for water to drop to the bottom of the separator. Testing in a vertical mode eliminated this affect and produced a more rigorous and realistic operational test of the hydrophobic cone.

4. In step 1 of the initial steady state test plan, the configuration trade-off studies were performed at a single air flow rate. Based on observed test data it was considered desirable to include the parametric variation of air flow with the configuration variations. This increases the number of data points to be taken in the steady state tests and improves the probability of defining the true optimum configurations.

Based upon these observations, the test plan was modified for the final phase testing. The revised test plan is presented in Appendix B.

Screen Selection

In the selection of new hydrophobic screens to be tested, three major areas of importance were considered. These were mesh, wire diameter, and finally open area which is a result of the first two. The remaining parameter, cone angle, was held constant. These parameters are related as discussed below.

Theory of Operation.- Theoretical consideration of two capillary phenomena are important to the design of a hydrophobic/hydrophilic phase-separation humidity control system. These are: (1) the pressure differential existing across a stable liquid-gas interface in a porous material, and (2) the velocity which will cause a liquid droplet, striking a porous hydrophobic surface, to penetrate that surface.

The porous material used in the humidity control system is a fine-mesh stainless steel screen. This material is used in the uncoated form on the hydrophilic sumps. Coated with Teflon, it behaves as a hydrophobic material and is used on the hydrophobic cone.

Analytical models available for prediction of the low-gravity phase separation capabilities of woven screens are far from exact. For this reason a fairly simple model was used, recognizing that inaccuracies in performance predictions would result. The variance between predicted and actual performance shows that an analytical model chosen can be used at least to estimate the order of magnitude of performance.

Stability of the Liquid-Gas Interface.- The conditions for stability of a liquid-gas interface in a porous material are shown in fig. 6. For example, if liquid droplets on the gas side of the porous plate shown in the illustration reach the stable liquid-gas interface, they will enter the liquid phase. In this way liquid is extracted selectively from a two-phase medium with a hydrophilic screen mesh surface.

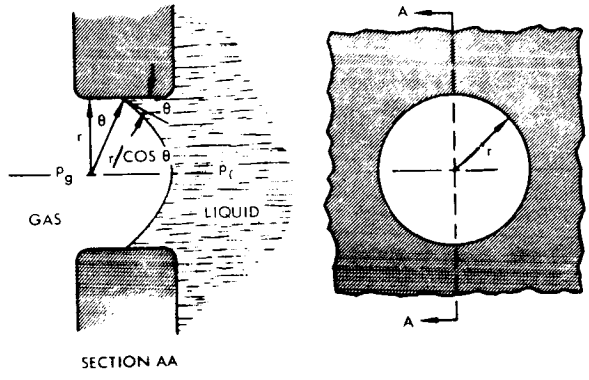

Fig.6- Stability of Liquid Gas Interface in a Cylindrical Hole

The model used for predicting the pressure differential existing across a stable gas-liquid interface is shown in fig.6. The analytical expression for the pressure differential across the interface is given by the capillary pressure rise equation attributed to Laplace:

$$P_g - P_l = \sigma\left(\frac{1}{r_1} + \frac{1}{r_2}\right) \qquad (1)$$

where

P_g = pressure on gas side

P_l = pressure on liquid side

σ = surface tension

r_1 and r_2 = principal radii of curvature of the liquid-gas interface.

For a cylindrical hole as shown in the model, the principal radii of curvature are identical and equal to

$$\frac{r}{\cos\theta}$$

where

r = radius of cylindrical hole

θ = contact angle

Substituting $r_1 = r_2 = r/\cos\theta$ in Eq. (1) gives

$$P_g - P_l = \frac{2\sigma\cos\theta}{r} \qquad (2)$$

The geometry of interest, a woven screen however, is roughly approximated by the square opening shown in fig.7; for the lack of a better model, this approximation was used.

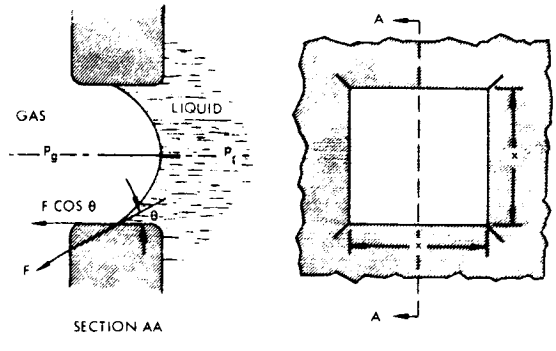

Fig. 7- Stability of Liquid-Gas Interface in a Square Hole

To apply the solution for the round opening to the square configuration the hydraulic radius, r_h, was substituted for the term r/2 in Eq. (2), giving

$$p_g - p_l = \frac{\sigma \cos \theta}{r_h} \qquad (3)$$

where r_h = area/wetted perimeter. This approach appears to be justified on the basis of a force balance on the liquid surface as depicted in fig. 7. The sum of the forces acting parallel to the axis of the opening contributes to the pressure difference:

$$(p_g - p_l) = \frac{\Sigma F}{A} = \frac{4\sigma x \cos 0}{x^2} = \frac{4\sigma \cos \theta}{x} \qquad (4)$$

The hydraulic radius of the square opening is:

$$r_h = \frac{x^2}{4x} = \frac{x}{4}$$

Substituting in Eq. (4) gives an expression identical to Eq. (3)

Using Eq. (3), pressure differential calculations were made for the hydrophilic (uncoated stainless steel) screen with θ = 45 deg, and for the hydrophobic (Teflon-coated) screen with θ = 105 deg.

Droplet Penetration Velocity.- For a hydrophobic screen it is interesting to note that if gas with entrained liquid droplets were to flow to the screen, it would be possible to stop the liquid droplets from passing the screen mesh while the air was allowed to continue through. One requirement for this type of separation is that the droplet must be larger than the screen porosities. Additionally, when the liquid droplet contacts the hydrophobic screen, a liquid stagnation will develop at the region of impact. As long as the pressure difference developed across the screen results in a stable interface the liquid droplet will not pass through the screen.

To estimate the maximum velocity that a droplet may have and still be stopped by a hydrophobic screen, consider the schematic diagram of fig.8. With the liquid droplets approaching the hydrophobic screen at a velocity V, the difference between the stagnation and static pressures of the liquid drop is:

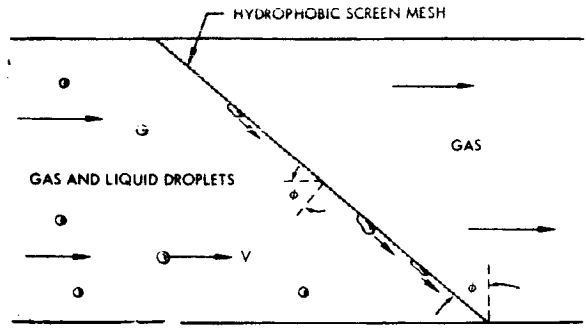

Fig.8-Separation of Liquid Droplets from a Gaseous Stream by a Hydrophobic Surface

$$p_{stab.} - p_{static} = \frac{\rho V^2}{2g_c}$$

where

ρ = liquid density

V = approach velocity

g_c = gravitational constant

If the radii of the droplets are large compared with the screen opening, then the static pressure of liquid in a drop will be equal to the pressure of the gas surrounding it; that is $p_{stat} = p_g$. Hence the difference between the stagnation pressure of the moving liquid droplets and the gas-stream pressure may be expressed by:

$$p_{stag} - p_g = \frac{\rho V^2}{2g_c}$$

If, as shown in fig. 8, the angle between the normal to the screen surface and the direction of the gas-liquid droplet flow steam is ϕ, then only a fraction of the stagnation pressure will be developed on the hydrophobic screen as a liquid droplet impinges. The difference between liquid and gas pressures at the point of impact may be expressed by

$$p_l - p_g = \frac{\rho V^2}{2g_c} \cos \phi$$

The maximum stable pressure difference $(p_l - p_g)$ that can be supported across a hydrophobic screen can be estimated from Eq. (3), thereby allowing calculation of the impingement velocity below which penetration should not occur.

In evaluating the driving force for passing water through a hydrophobic screen material, the pressure difference across the screen must also be considered. Water on the surface of the screen will be subjected to the full pressure loss across the screen. In the case of the 325 mesh screen tested in the initial steady state tests, this pressure difference, at high air flow rates, constitutes a large part of the pressure difference indicated by equation (3). Thus, lowering unit pressure loss may, even if the effective hydraulic radius is increased, reduce the possibility of water breakthrough.

Final Hydrophobic Screen Selection.- Examination of the 325 mesh coarse wire hydrophobic cone tested showed that the initial uncoated free area of 30 percent is reduced significantly by coating. However, the reduced free area increases the air pressure loss across the cone significantly. As water is held upon the surface of the cone, free area decreases and consequently the air pressure loss increases still further.

In an attempt to reduce the humidity control system pressure loss penalty, a search was made for screens which would have a lower pressure loss and at the same time provide high unit performance. Standard screen material available on the market have open areas, generally less than 50 percent. This results from using larger diameter wire as mesh is reduced. A 230 mesh (with .0014 m diameter wire) stainless steel screen represented the optimum size screen within the commercially available screen sizes providing the minimum hydraulic radius and the maximum free area. This had an uncoated area of 46 percent. The 325 mesh screen (with .0011 m diameter fine wire) selected also had a smaller hydraulic radius but had an uncoated area of only slightly less than 42 percent because of the closer weave. Other special screens may be more desirable but were ruled out because of the high cost and schedule penalty of special mill runs. A summary of the three screens chosen for the final tests is shown below:

Screen	Mesh	Wire Diameter (M)	Relative Rh	Uncoated Open Area (%)	Referred To As
1	325	.0014	min.	30	325 mesh coarse wire
2	325	.0011	--	42	325 mesh fine wire
3	230	.0014	max.	46	230 mesh

Hydrophobic cones were manufactured to the original 325 mesh specification dimensional configuration for screens 2 and 3 and used in the final steady state test plan presented in Appendix B.

Final Steady State Tests

Upon receiving the new hydrophobic cones from manufacturing, the test apparatus was again checked out and a new chiller, which would provide a more stable outlet humidity at all flows, was integrated into the system. The final steady tests consisted of the following:

- Performance on each of the three hydrophobic cones - 325 mesh coarse wire, 325 mesh fine wire, and 230 mesh.
- Performance on each of the spinner configurations - 0, 1.0, and 1.5 plates.
- Effects of variable inlet and outlet humidity levels for the optimum configuration.
- Dynamic tests

A summary of this data appears in tabular form in Appendix D Runs No. B1 - B15 and is presented in the figures that follow in this section.

Test Data Runs.- Final steady state testing was started on the 325 mesh with coarse wire, no spinner and no coalescer. These tests showed a much higher pressure loss and earlier water breakthrough than the previous tests conducted during the initial steady state test phase. The unit was disassembled and examination of the 325 mesh showed a large buildup of oil and dirt which had accumulated from the initial runs and storage. The screen was cleaned in Freon and prepared for future runs. In cleaning, dirt collected appeared to be carbon dust as might originate from the fan motor brushes.

Hydrophobic Cone Ratings.- The first acceptable complete run was conducted on the 230 mesh hydrophobic cone. The data is presented in Appendix D Run B1, and is plotted in fig. 9. Data taken on the test runs (Reference Appendix D Runs No. B2 and B3) at later dates are also shown on this curve. This is significant as it shows reproducibility after the unit had been disassembled for testing of other configurations. Additional performance on this screen was taken at the maximum test apparatus air velocity at a fan voltage of 28 volts to evaluate the 230 mesh configuration at the maximum stress condition. Flow measurements were off scale, preventing an accurate determination of flow; however, estimates based on pressure loss show the flow to be above 140 CFM with efficiency remaining at 100 percent and no breakthrough. This is better performance than was achieved with the original 325 mesh coarse wire screen. The lower air pressure loss across the screen, as discussed in the screen selection section, provided less potential for driving water through the hydrophobic cone material. The 325 mesh coarse wire unit showed a pressure loss in excess of 1.0 inch of water at breakthrough while the 230 mesh cone never showed a loss greater than .5

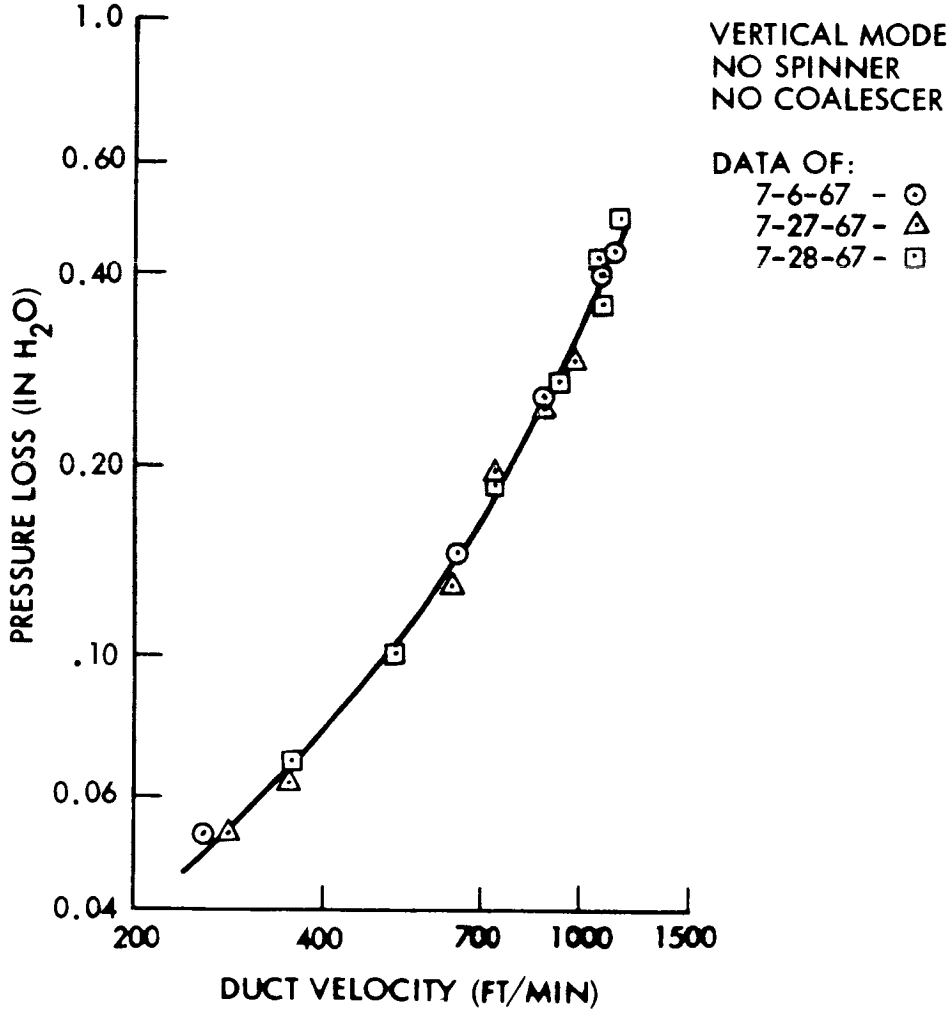

Fig. 9 - 230 Mesh Pressure Loss Data

inches of water even at the maximum test system flow condition. After the initial run on the 230 mesh cone configuration, the new 325 mesh cone with the fine wire weave was installed in the unit for testing.

The performance data for the 325 mesh fine wire weave is shown in fig. 10 (Appendix D Runs No. B8 & B9). This configuration showed a 100 percent removal efficiency up to the maximum test capacity air flow at 28 volts fan motor supply. The pressure loss over the flow range was higher than the 230 mesh unit. The higher pressure loss is attributed to the decrease in free area. This unit does, however, have improved performance over the original 325 mesh design in both pressure loss and water removal efficiency. The final test on the hydrophobic cone configurations was with the original 325 mesh coarse wire cone, which had been cleaned after initial high pressure loss characteristics.

Data on the 325 mesh coarse wire cone is shown on fig. 11 (Appendix D Runs No. B4, B5 & B6). As was the case during the original steady state test, breakthrough was found at high flow conditions over 900 ft/min. It is important to note that data taken after the screen was cleaned, closely reproduces the original data. This can be seen from fig. 11 where both sets of data are plotted. The effect of water removal rate on pressure loss for this cone is evident from the steeper slope of the pressure loss versus flow relationship.

Summary.- Once data on the three hydrophobic cones were gathered, it was analyzed to determine the optimum screen configuration. The 230 mesh was determined to be optimum as it had the lowest pressure loss and maintained a 100 percent removal efficiency throughout its operating range. A brief comparison of pressure loss data at the original design point of 70 CFM (velocity 620 ft/min) is shown below for the three screens tested:

Hydrophobic Cone	Pressure Loss
230 mesh	.135 inches water
235 mesh fine wire	.265 inches water
325 mesh coarse wire	.41 inches water

As a result this screen was chosen for testing of inlet and outlet humidity effects, and for the dynamic test runs.

Effects of Inlet Humidity.- The first test condition on the 230 mesh screen was run with the steady state test inlet and outlet humidities to confirm the data (Appendix D Runs No. B2 and B3). The data is plotted on fig. 9 and shows that the performance is reproducible. Tests were then conducted to determine the effects of high and low humidity level on water separator performance.

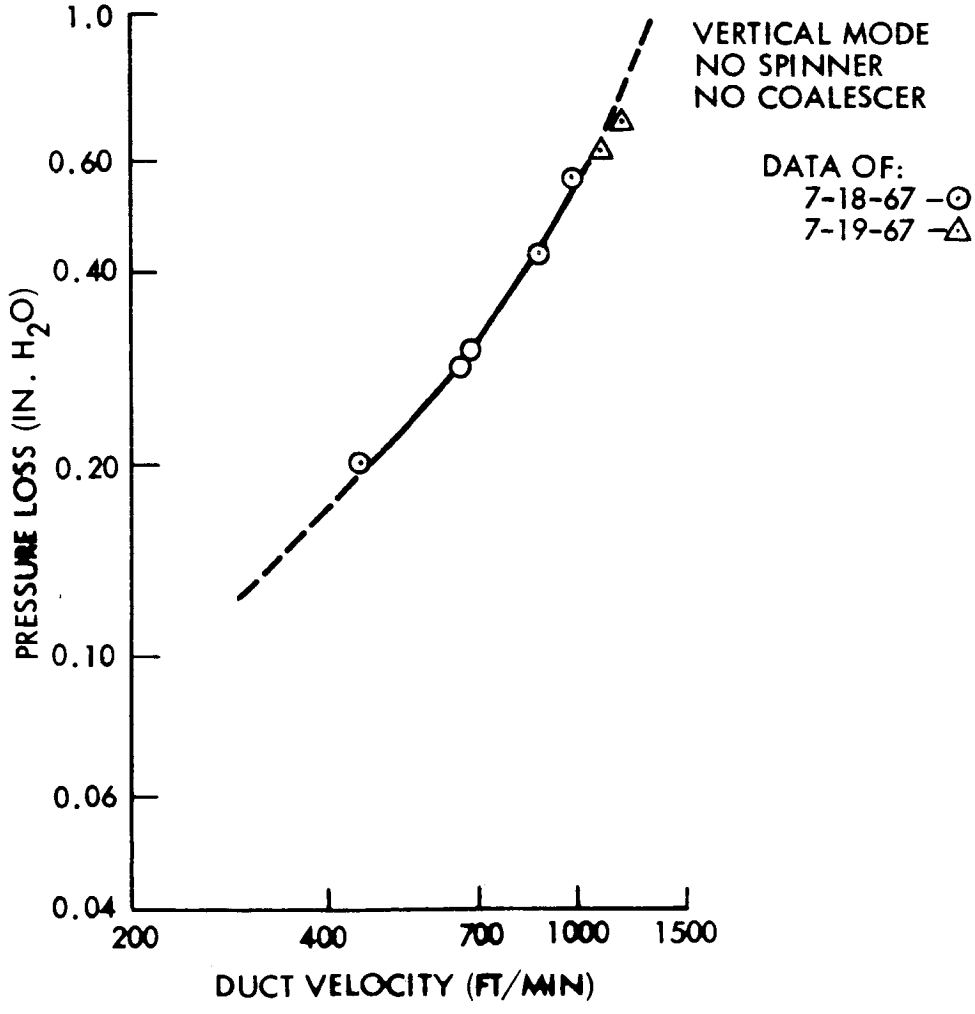

Fig. 10 - Mesh Fine Wire Pressure Loss Data

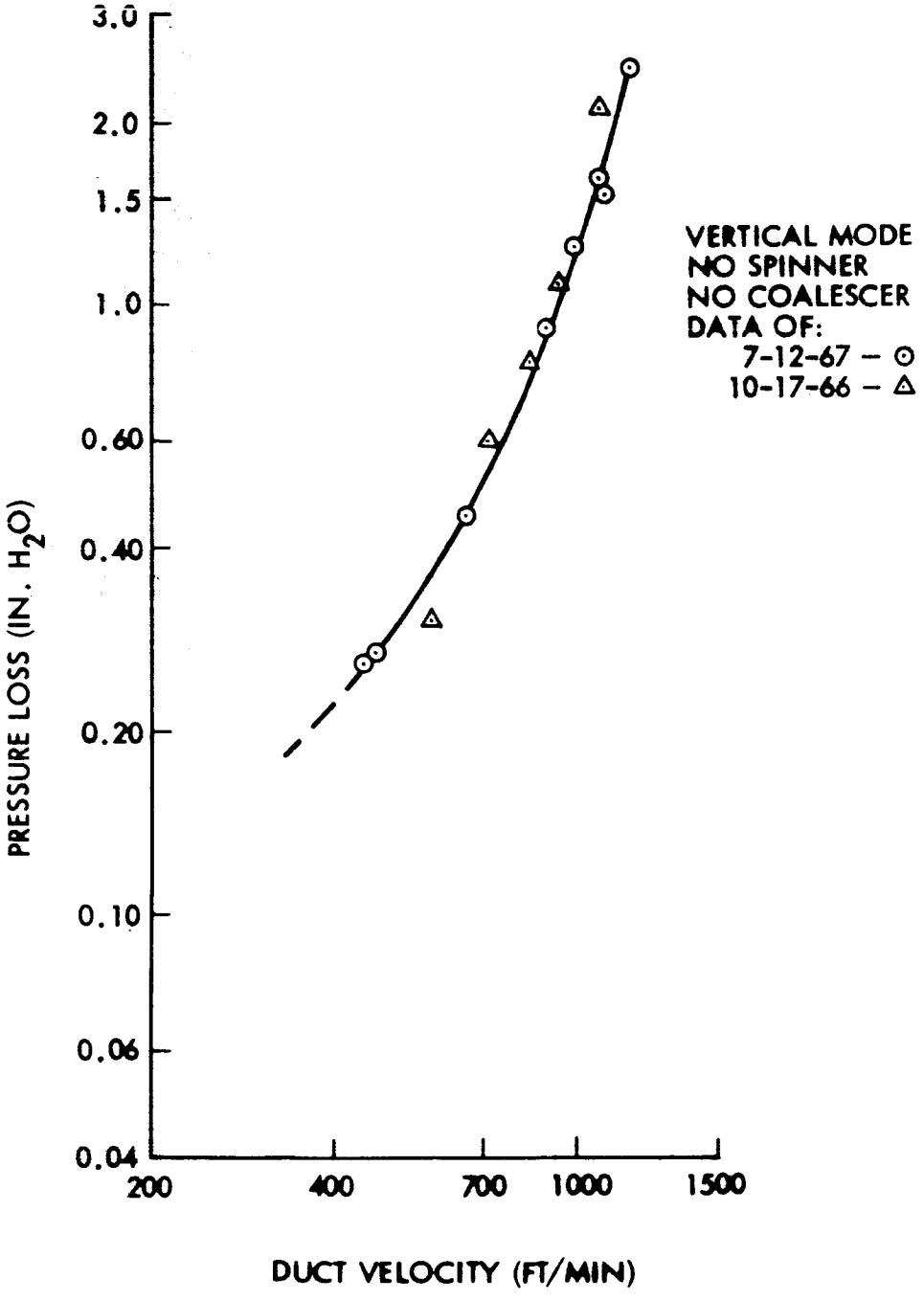

Fig. 11 - 325 Mesh Coarse Wire Pressure Loss Data

The steady state tests were run with an inlet humidity of .0137 lb H_2O/lb air and an outlet humidity of .0071 lb. H_2O/lb air. In order to assess the importance of both inlet and outlet humidity levels, the plan of test required runs with other values of inlet and outlet humidity. The initial series of steady state tests demonstrated the possible importance of water removal rate as shown in fig. 5. This effect would be of great importance to a designer as latent heat loads (which vary over a wide range of work conditions) and available heat sink temperature are important design considerations for relative humidity control. These two parameters have a direct effect on the humidity levels of the humidity control system. Data was taken on the 230 mesh hydrophobic cone without spinner or coalescer for two additional values of inlet humidity. These were .0191 lb. H_2O/lb.air (Appendix D Runs No. B 10 & B11), and .0082 lb. H_2O/lb. air (Appendix D Run No. B12). This data is presented in figs. 12 and 13. Comparison of figs. 12 and 13 with fig. 9 at .0137 lb. H_2O/lb. air shows that for the 230 mesh hydrophobic cone, there is no variation of pressure loss with changes in inlet humidity level, and water removal efficiency was 100 percent within the range of the experiment.

Effects of Outlet Humidity.-Following the test to determine the effects of inlet humidity on pressure loss and water separator performance, tests were run (Appendix D Run B13) to determine the effect of outlet humidity on performance. The outlet humidity rates were changed by varying heat exchanger coolant inlet temperatures. Figure 14 shows no variation in pressure loss with changing outlet humidity for the 230 mesh cone at an inlet humidity of .0137 lb.H_2O/lb.air, and a flow of 107 CFM. As might be expected from the study on effect of inlet humidity, there is no effect on pressure loss due to changing outlet humidity level. These tests showed no effect on the 230 mesh cone water separator performance efficiency either in humidity level or pressure loss. This is contrary to the original steady state tests on the 325 mesh coarse wire cone where increase in outlet humidity level caused a significant increase in ΔP and breakthrough. In this test program it was not possible to define the reasons for the difference. However, it is felt that the lower pressure loss in the 230 mesh unit is the reason. This is justified on the basis of the 68 CFM data shown on fig. 5 which shows minimal effect of water removal rate on the 325 mesh unit where the pressure loss is low.

Spinner Losses.- In order to evaluate the effect of the spinner on the water separator pressure loss, flow tests were run to determine spinner loss data with the hydrophobic cone removed. The initial test was run with no spinner which confirmed that system losses were negligible and the base was considered as zero loss. A pressure loss versus flow test was then conducted on the spinner with 1.5 plates (Appendix D Run No. B14). This unit was then cut down to 1.0 plates and rerun (Appendix D Run No. B15). Figure 15 shows the results of these tests. The small difference between these two

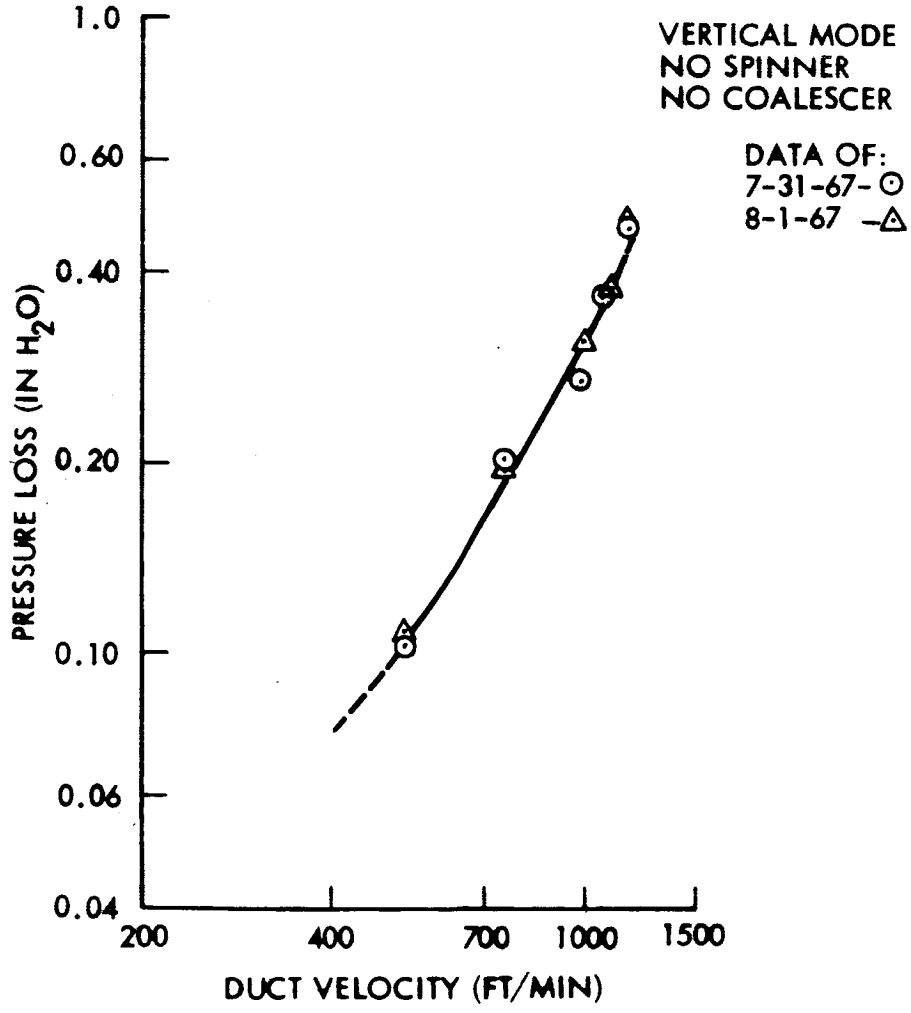

Fig. 12- 230 Mesh High Inlet Humidity Data

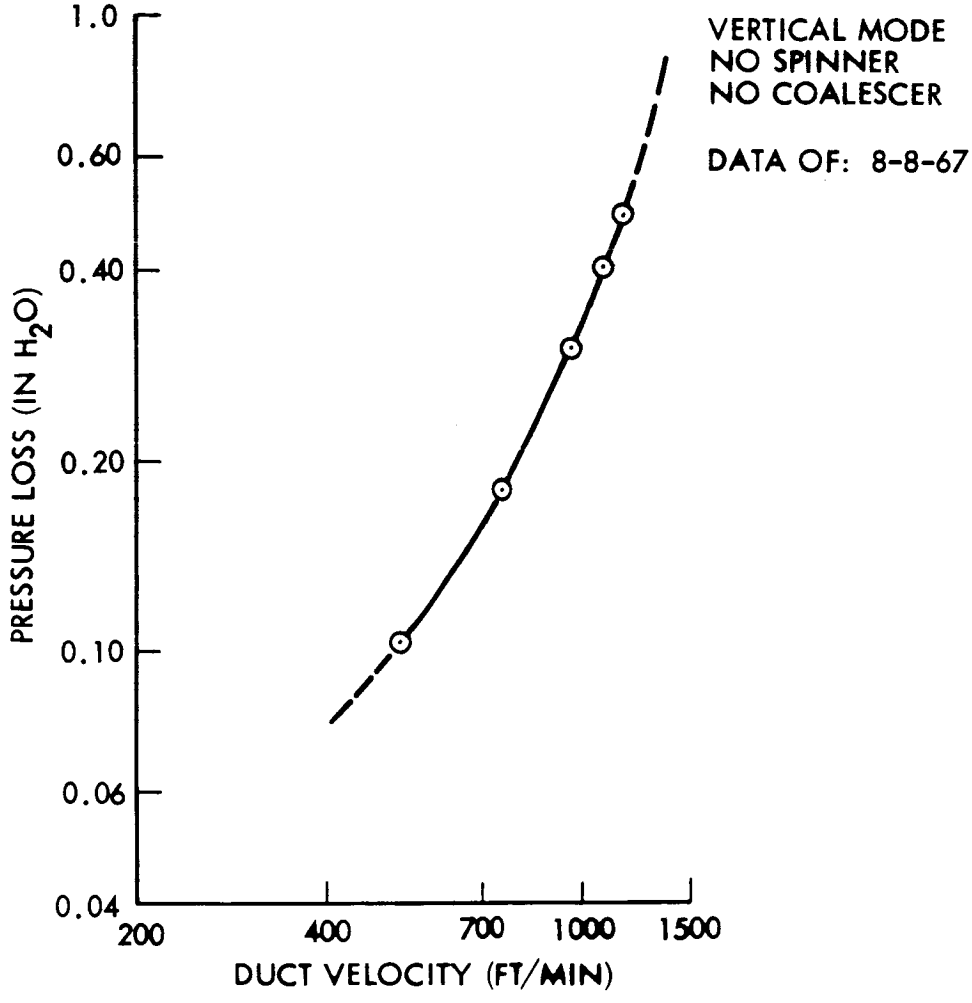

Fig. 13 - 230 Mesh Low Inlet Humidity Data

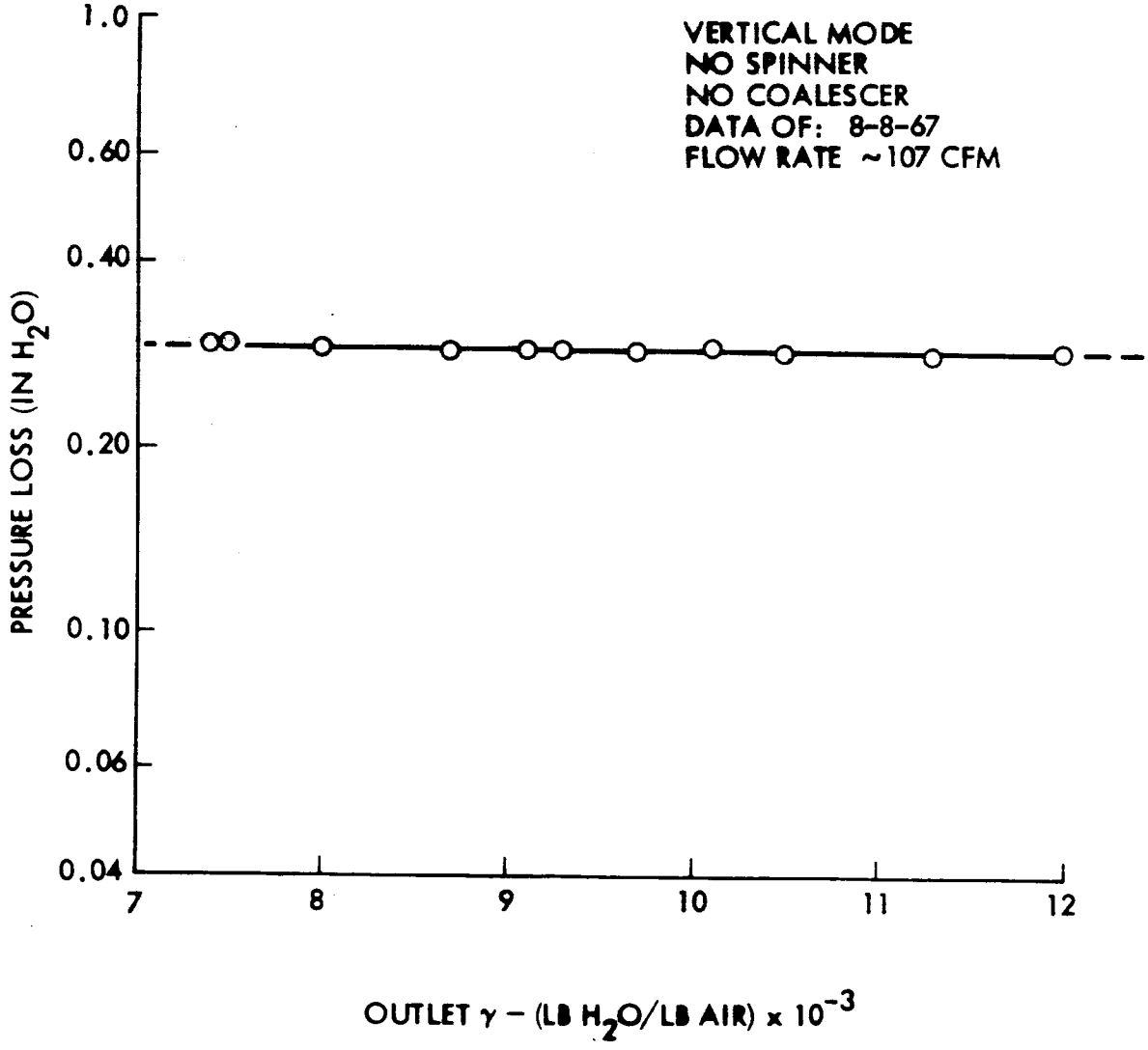

Fig. 14 - 230 Mesh Variable Outlet Humidity Data

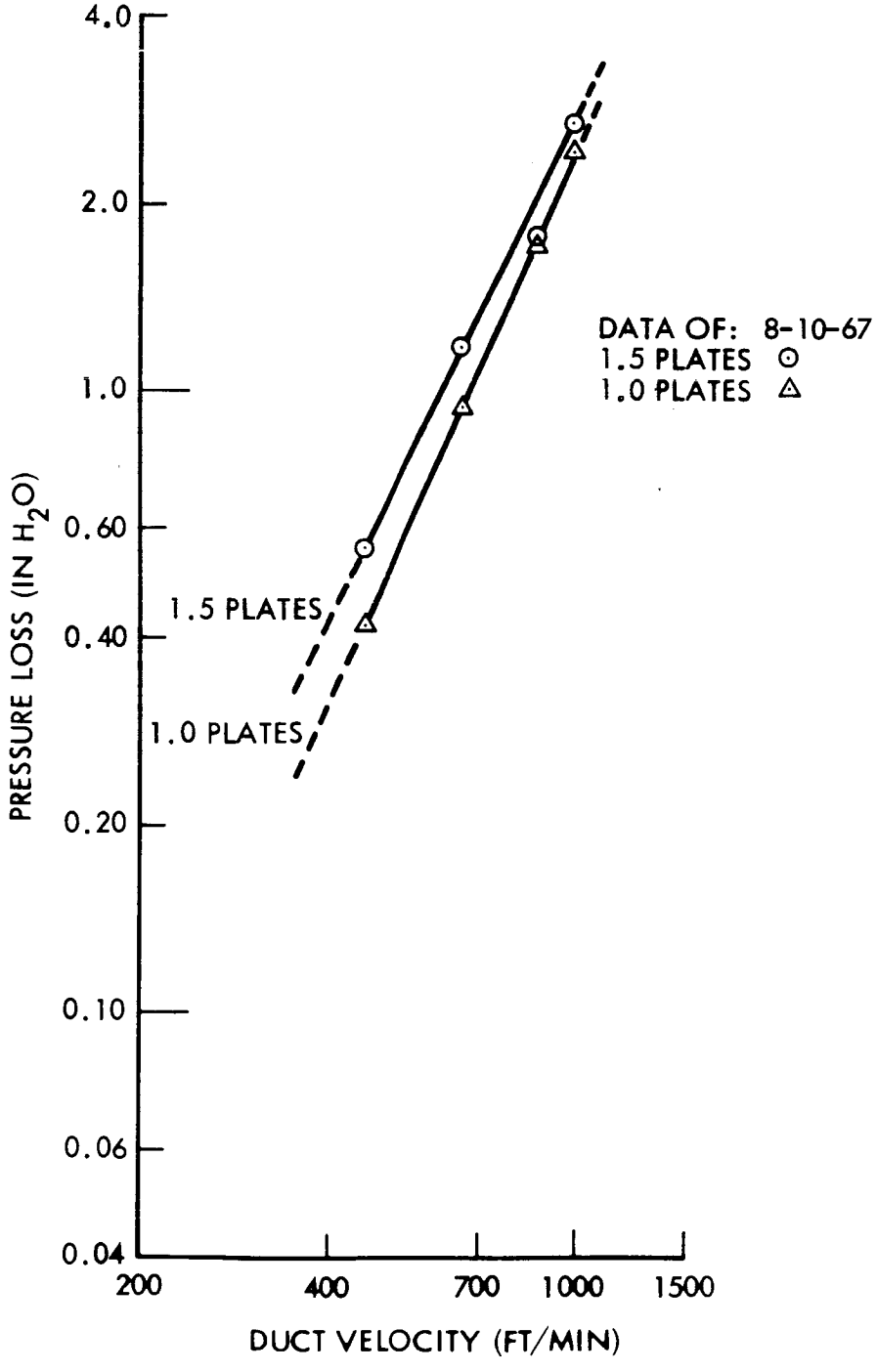

Fig. 15 - Pressure Loss Data - Water Separator Spinner

configurations is explained by the fact that the cross section area for flow was large and had little loss while the entrance and exit losses constituted the major loss.

Test Data Reduction

The test data presented in figs. 9 through 15, was then reduced to determine water separator design criteria. The data as plotted in figs. 9 through 15 is valid only for the pressure, temperature and cone tested. Pressure loss data may be presented in the form of $\sigma \Delta P$ where σ is the ratio of density to standard density of .0765 lb/cubic foot. The duct velocity measurements were converted to true velocity by a pressure conversion then reduced to $lb/min/ft^2$. Although characteristics of pressure loss may vary with cone geometry, it appears from this testing that cone area is the best possible parameter in the absence of more complete data. Spinner losses are additive to screen losses in the evaluation of total system performance data for screen configurations with spinner. Data showing the cumulative system pressure loss versus mass velocity flow per unit area for each of the hydrophobic cones is presented in figs. 16 through 19. These data can then be used in any combination of pressure/density relationships for evaluating system design parameters for each screen mesh configuration shown in figs. 16 through 19.

Dynamic Performance Tests

Dynamic tests were performed on the humidity control system to determine the recovery rate of an upset condition produced from a sudden increase in inlet humidity level caused by some emergency. The test was accomplished by establishing a high humidity level, in excess of a 70°F. dew point, by controlling the level with the automatic steam controller. At a period in time a manual step change was made to the steam feed valve which resulted in dew point of about 58° F. The rate of system recovery from the elevated dew point to the lower was recorded on the Honeywell recorder for inlet humidity δ 1. This procedure was repeated three times to assure consistency at each flow of 40, 70 and 100 CFM. The initial rate of recovery indicated a problem of instrument response time. Thus, an attempt was made to measure this response. Saturated air was fed to the dew point sampling system. At a point in time a step was made to lower dew point air and the response recorded. The results of the instrument check are shown in fig. 20, and the data taken at each of the flows in figs. 21 through 23. The data from the chart has been reduced to show the dew point temperature as a function of time.

As might be expected with systems of small volume and high flow rate, the figures show a rapid recovery rate. The small difference in time between the instrument and system response is most likely due to an unmeasureable characteristic of the steam feed system.

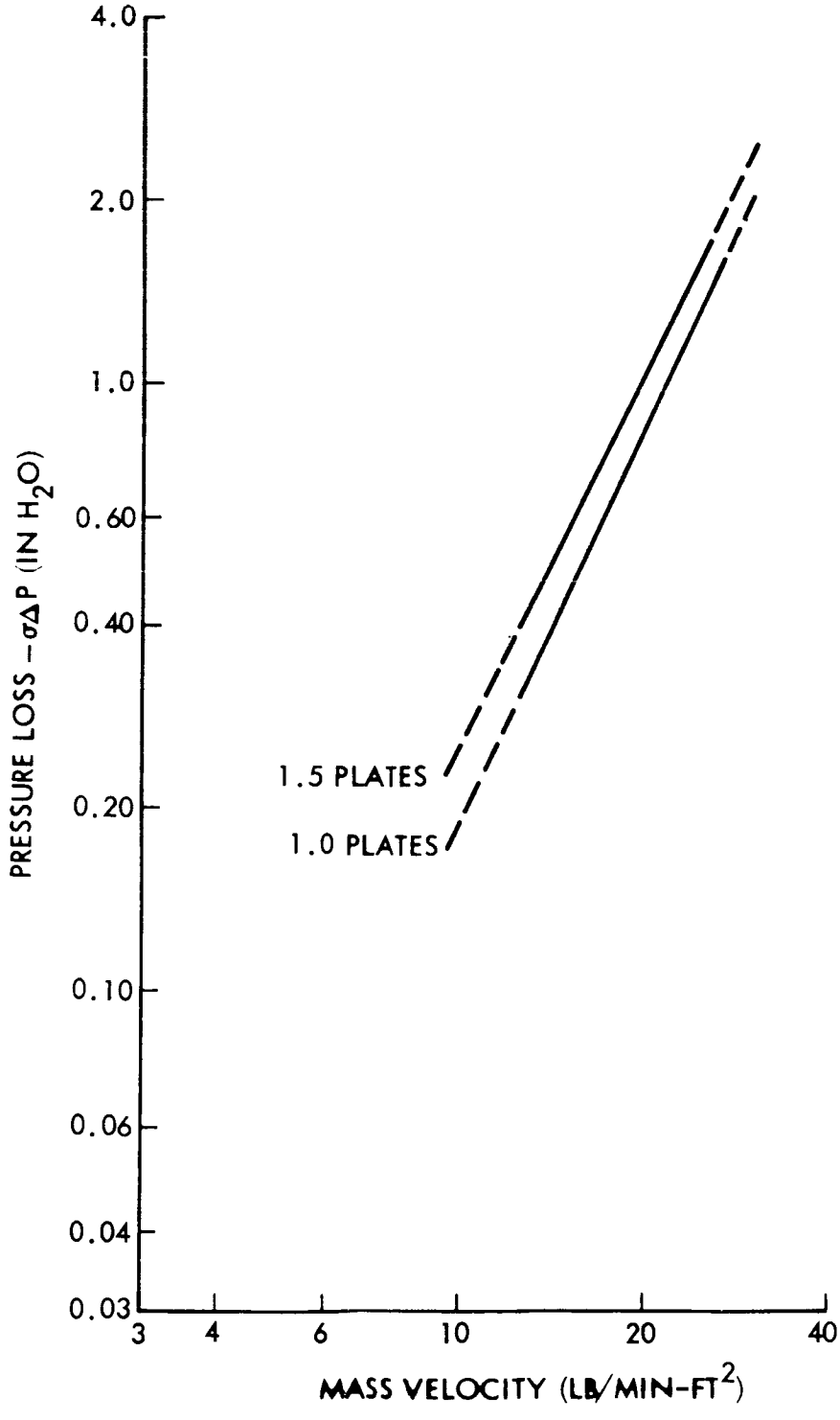

Fig. 16 - Water Separator Spinner Pressure Loss Characteristics

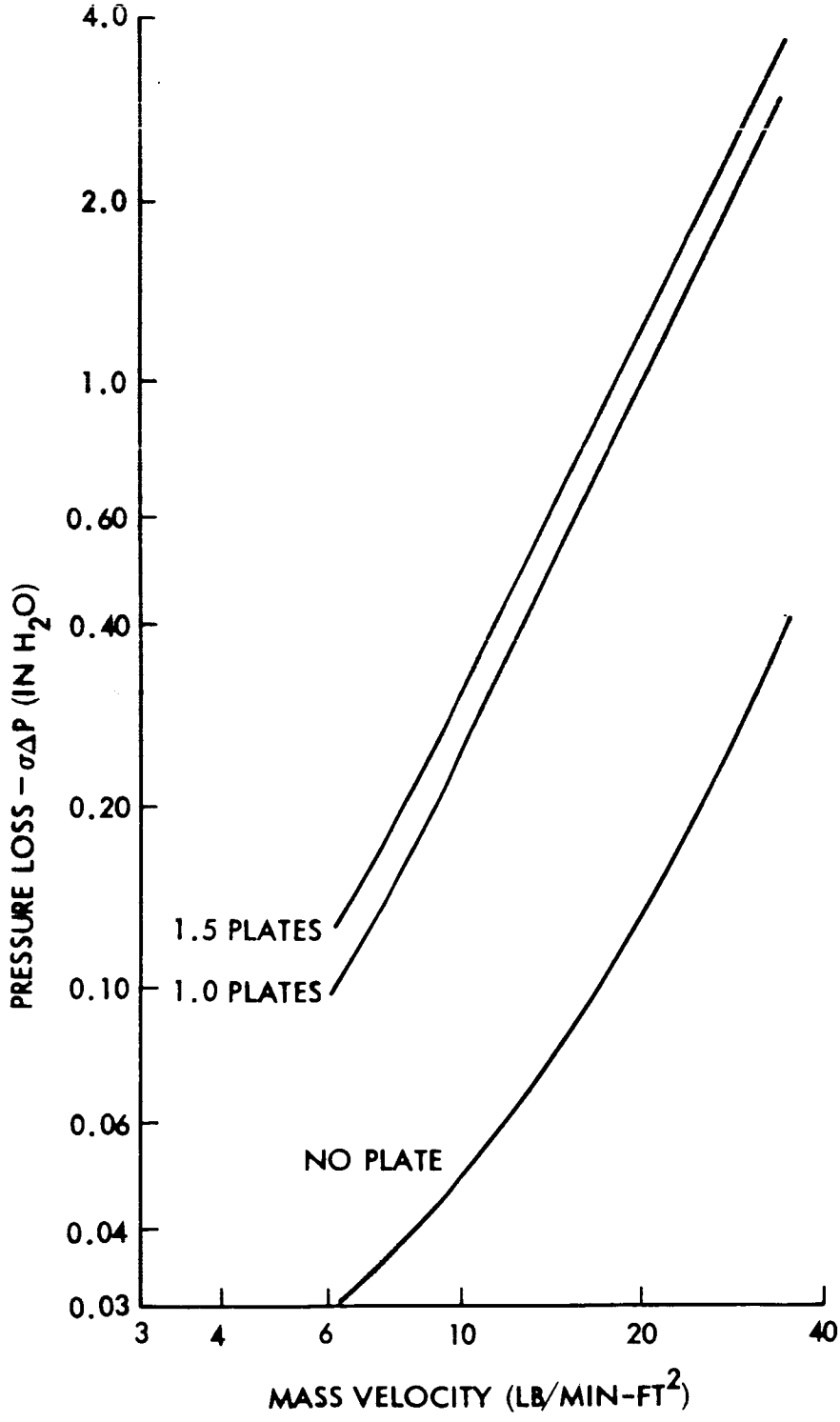

Fig. 17 - 230 Mesh Pressure Loss Characteristics

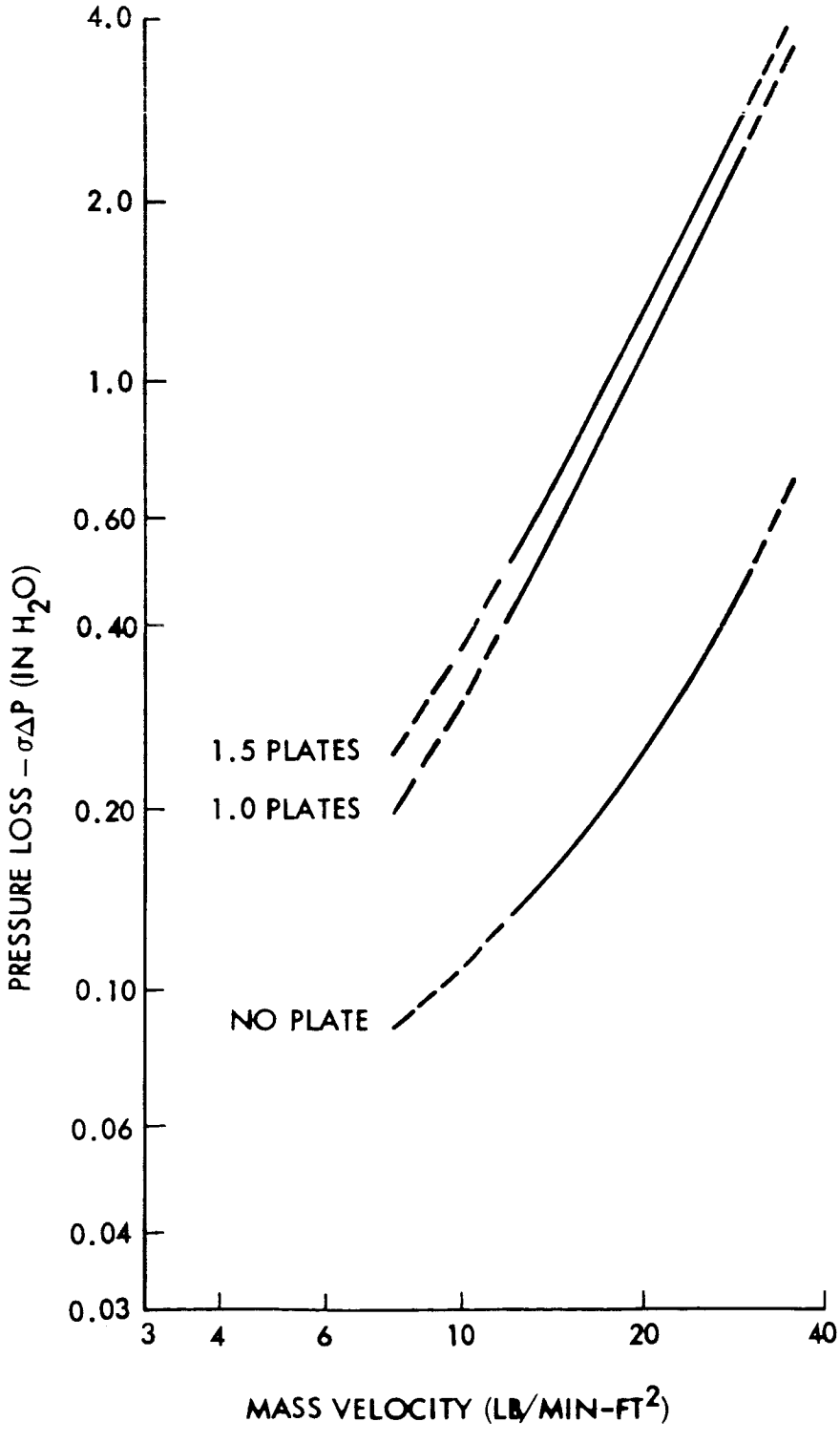

Fig. 18 - Mesh Fine Wire Pressure Loss Characteristics

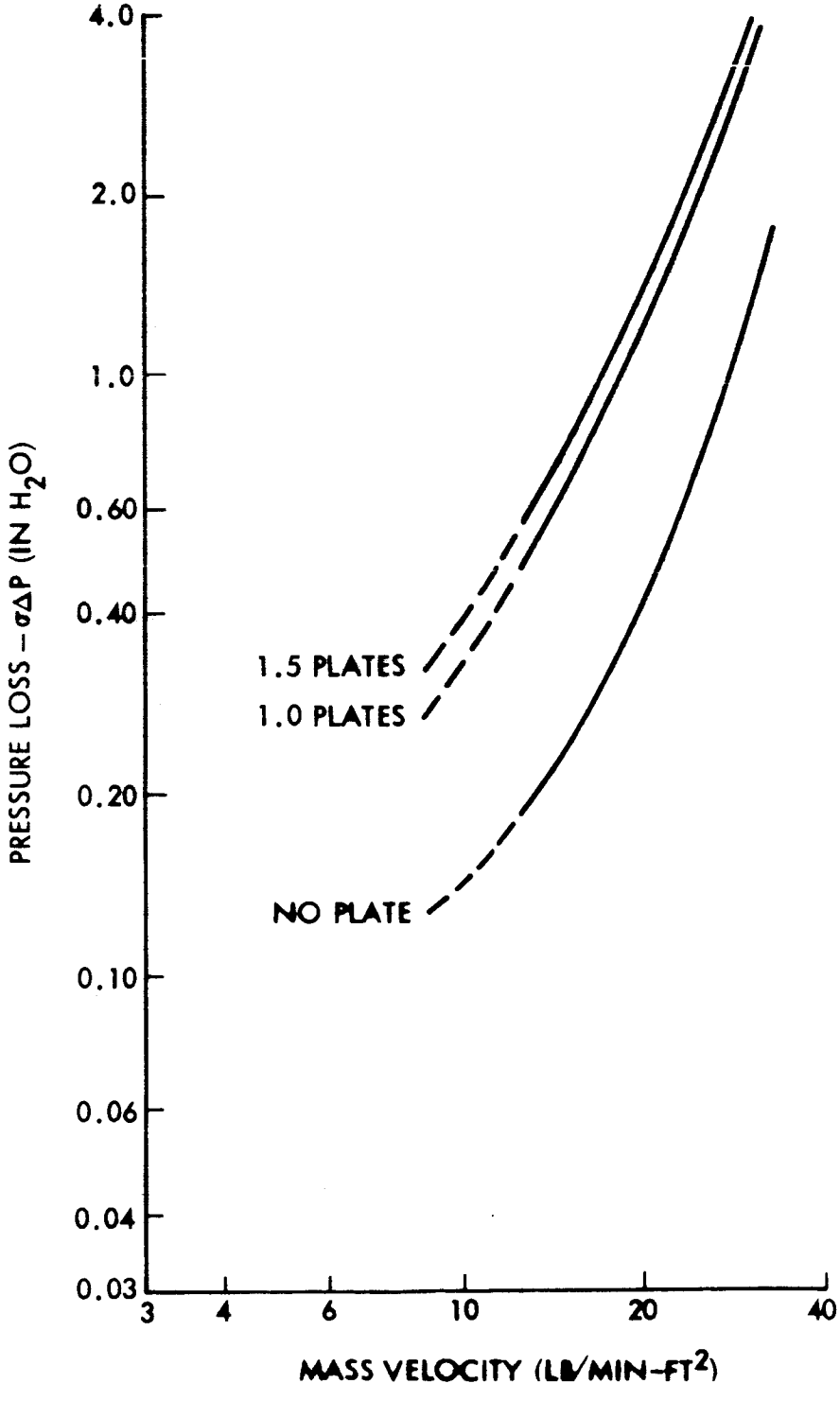

Fig. 20 - Response of Humidity Control System Instrumentation

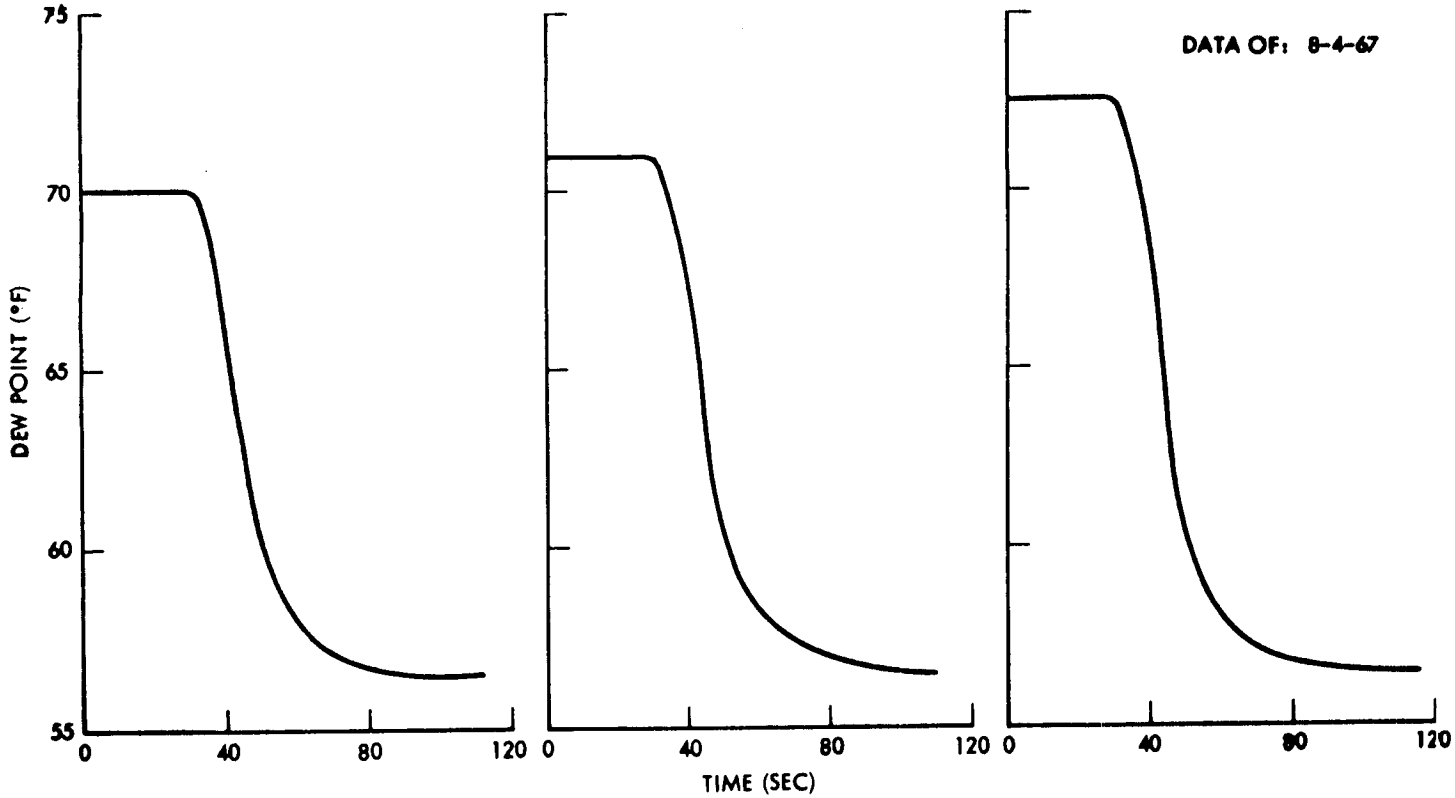

Fig. 20 - Response of Humidity Control System Instrumentation

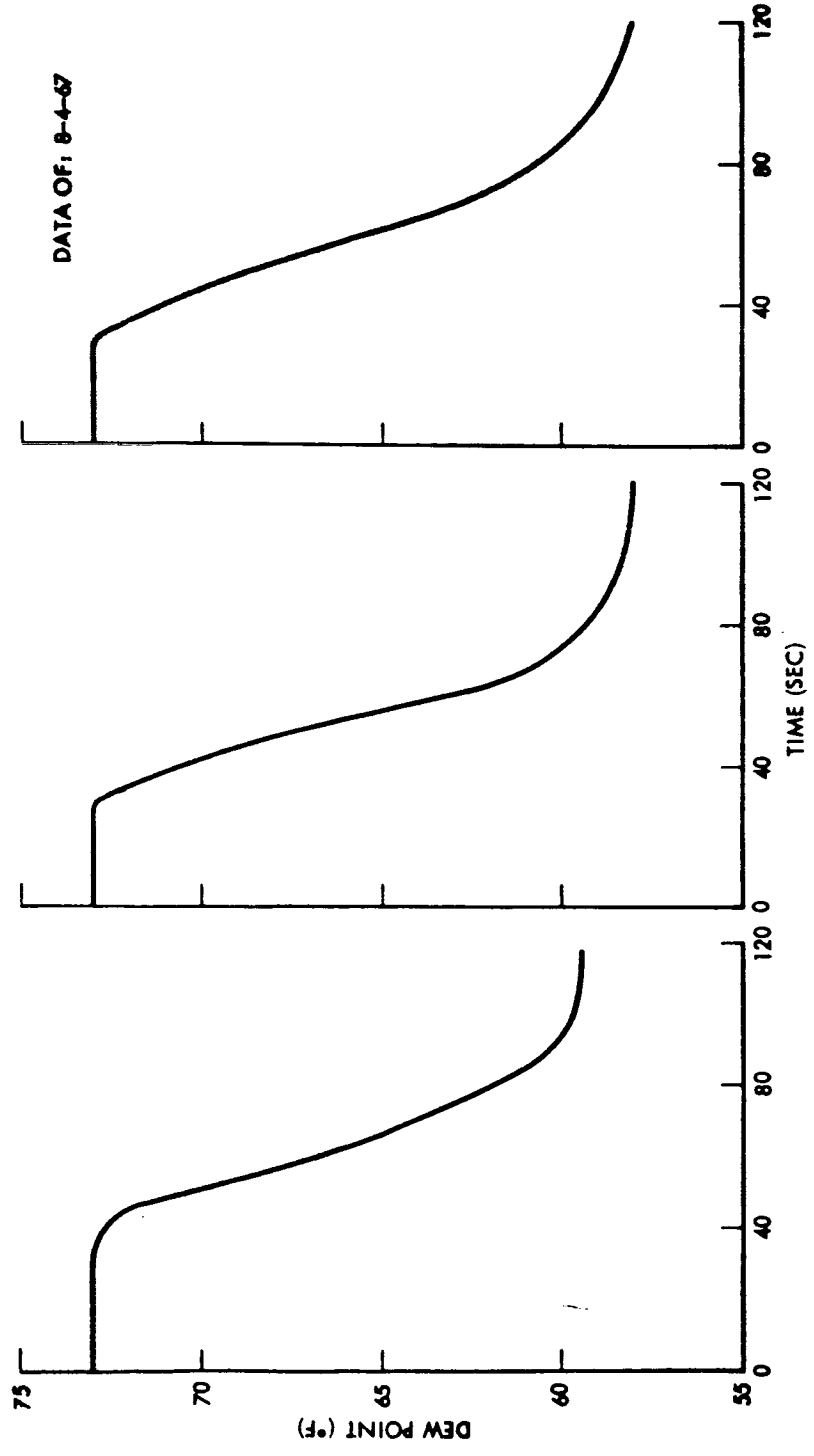

Fig. 21 - Dynamic System Response at 40 CFM

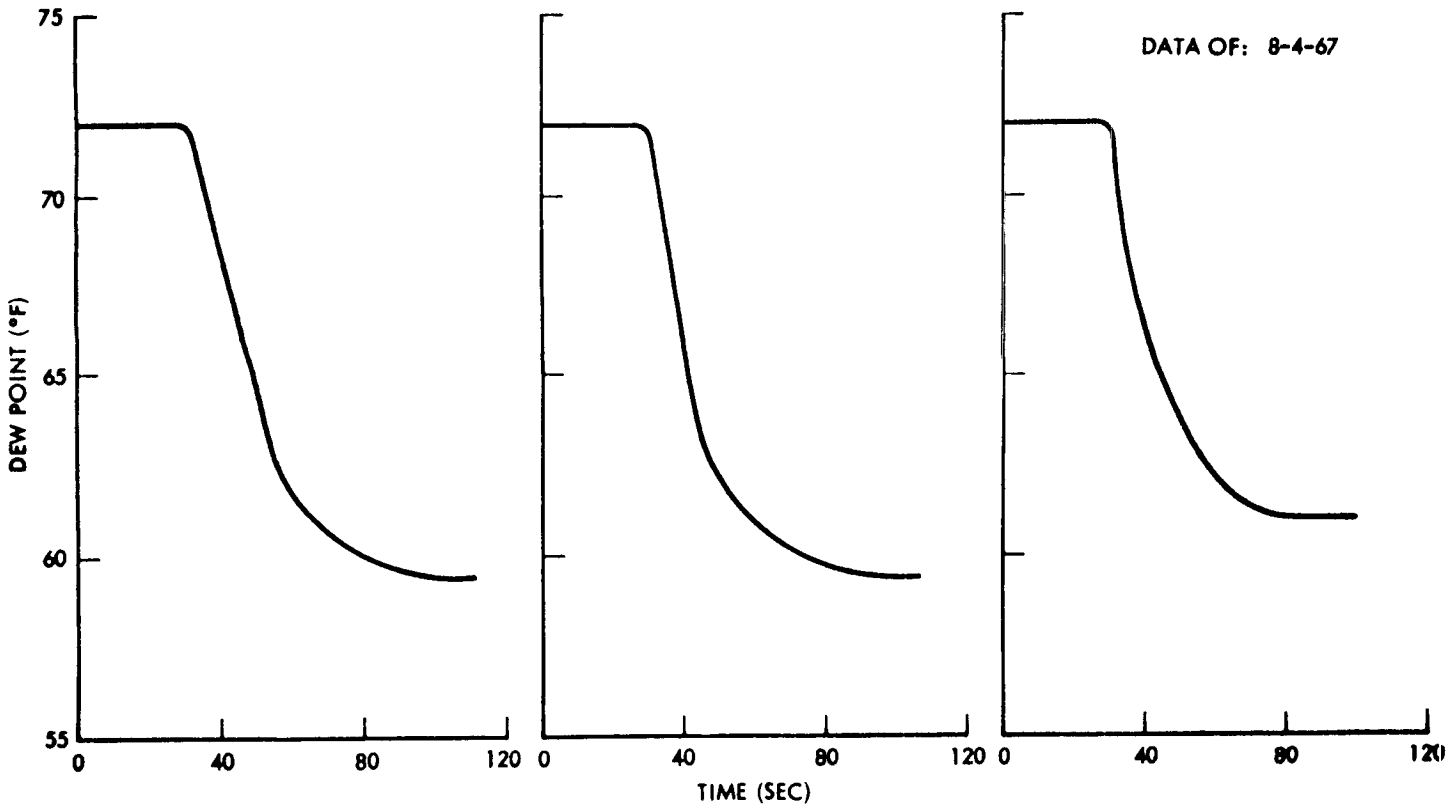

Fig. 22 - Dynamic System Response at 70 CFM

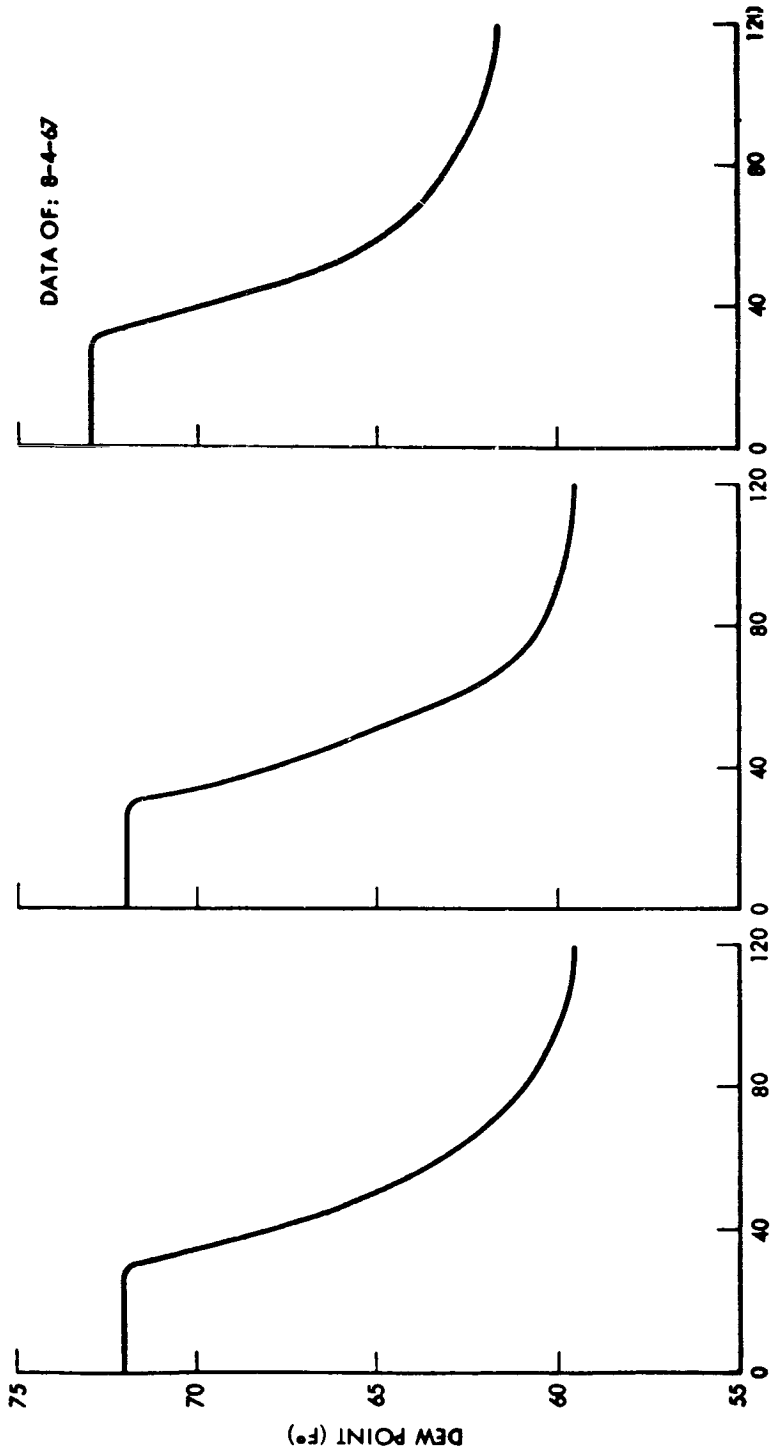

Fig. 23 - Dynamic System Response at 100 CFM

DESIGN CRITERIA

The optimization of the humidity control subsystem for a space vehicle depends upon a number of vehicle parameters and a definition of complete environmental system requirements. The following major parameters were considered for this optimization analysis:

- Subsystem reliability requirements
- Subsystem maintainability requirements
- Vehicle power penalty
- Available sink temperature
- Water generation rate
- Allowable humidity level
- System pressure
- System integration concept

The task of generating a concise optimization of the water separator subsystem design criteria, including the consideration of the total variables in the above list, is not practical at this point in system evaluation testing without defined system parameters and performance requirements. However, by assigning values to certain variables, a system approach can be established for evaluating an optimum humidity control subsystem design. Two major environmental control system integration arrangements were examined for the design optimization analysis; one, utilizing the basic assumption that water separator flow is established by humidity control requirements; and the other, that water separator flow is fixed as established by thermal control requirements.

The humidity control system used in the test program was evaluated as a basis to illustrate selection of an optimum configuration for a system whose water separator flow is established by humidity control requirements. The second system optimization consisted of a fixed flow system as established by thermal control requirements and is presented as a sample system. Other systems with different requirements may be evaluated in the same manner as these two illustrations.

Figure 24 was developed for environmental control systems which may require a water separator of different size from the test unit. This figure presents water separator weight for the optimum configuration showing weight as a function of cone area. The curve is based on the 230 mesh test unit

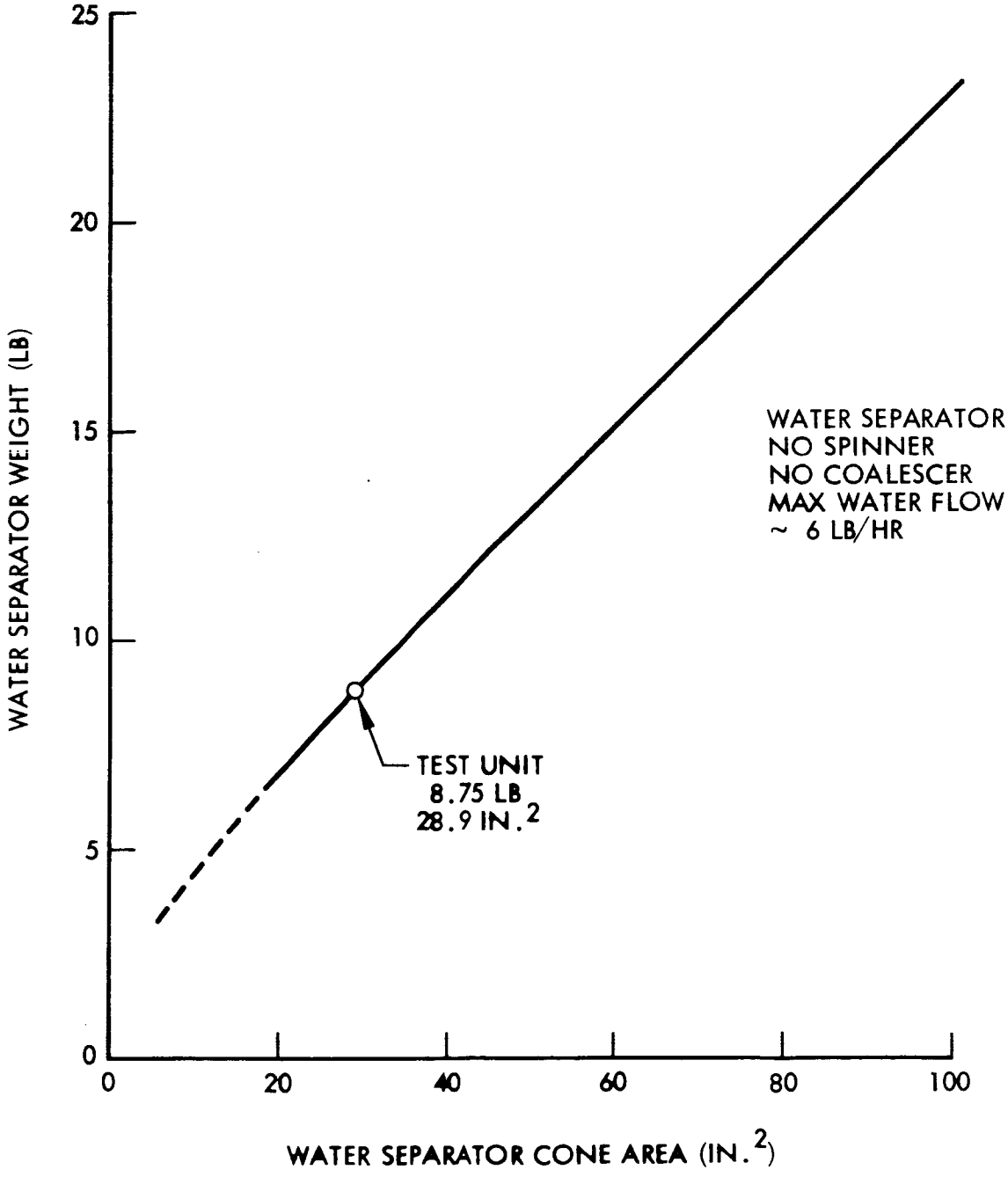

Fig. 24 - Water Separator Fixed Weight

with individual components and is scaled proportionately for other sizes. For reference, the cone area of the test unit water separator is 28.9 square inches and the unit weighs 8.75 lbs.

The performance data from the water separator test program shown in fig. 17-19 was reduced to the common system denominators of pressure/density/flow per unit area relationship. The reduced performance data together with the weight/area relationship shown in fig. 24 for the water separator configuration, serve as a basis for establishing design criteria in this report.

Reliability and Maintainability

The Lockheed hydrophobic/hydrophilic water separator contains no moving parts and is, therefore, completely passive in nature except for a water delivery system which is common to all water separator concepts. The test program, though limited in duration, showed no loss of unit performance with time. Further, the hydrophobic cone which became contaminated during storage was easily restored to its original performance when cleaned. The hydrophilic sumps are also easily removed and cleaned. It was concluded from this test program, that the high inherent reliability and the demonstrated characteristics of total recovery after simple cleaning procedures compares favorably with all other water separator concepts. These parameters of reliability and maintainability are applicable to both the humidity control and the thermal control systems and were not considered further in the establishment of design criteria.

System Integration

In addition to assuming the environmental control system integration concepts of either humidity or temperature control, the following values were assumed for the vehicle parameters considered in the design optimization of the two humidity control subsystem concepts:

VEHICLE PARAMETER	VALUE	REMARKS
o Power Penalty	600 lb/kw	Typical of Advanced Solar Cell Technology
o Sink Temperature-Humidity Controlled System	38°F	Practical Minimum to Avoid Freezing in Heat Exchanger
o Sink Temperature-Temperature Controlled System	Variable	Function of Temperature Control
o Operating Pressure	10 psia	Assumed to Correlate Test Data

VEHICLE PARAMETER	VALUE	REMARKS
o Humidity Level	50% at 70° F	Typical Design Criteria for Cabin
o Volume	Not Considered	Function of Cone Area and System Flow
o Flow-Humidity Controlled System	To be Calculated	
o Flow-Temperature Controlled System	100 cfm	Typical System Value
o Cone Area-Humidity Controlled System	28.9 in^2	Same as Test System
o Cone Area-Temperature Controlled System	To be Calculated	
o Weight-Humidity Controlled System	8.75	Test System Adjusted for Improved Water Delivery System
o Weight-Temperature Controlled System	To be Calculated	

These assumed parameters are applicable to the following design optimization only; any change in values would require that the optimization be repeated.

Integration with Humidity Controlled Systems

In environmental control systems where humidity control is separate from the thermal control subsystem, two regions of water separator performance are of importance. If the separator is less than 100 per cent efficient and the total system air flow is set by humidity control requirements, the air flow will vary inversely as the efficiency. As a result, all components related to the humidity control subsystem are penalized by the increased air flow rate. If, however, the water separator performs at 100 per cent efficiency, as was demonstrated in the test program, the air flow rate through all of the components can be established by the allowable humidity level, available sink temperature, and water generation rate. The water separator operating at 100 per cent efficiency results in the minimum system air flow consistent with humidity control requirements. Thus, each of the components in the system can then be optimized on a component basis relatively independent of the other components. The water separator optimization is then dependent only on its weight and power penalty characteristics.

Performance Evaluation.- As previously mentioned, the reduced data from the test program was used to illustrate the selection of an optimum configuration for a system whose water separator flow is established by humidity control requirements. To determine the optimum water separator design characteristics, the performance of the various configurations was evaluated in the following three steps:

Step 1 - Hydrophobic screen performance independent of spinner performance was evaluated to determine the optimum cone mesh sizes (fig. 25).

Step 2 - Water separator performance with spinner installed was evaluated to determine optimum spinner configuration (fig.26).

Step 3 - Water removal capability over the range of system volumetric flows was evaluated for the optimum water separator configuration, as determined from Steps 1 and 2, to determine the optimum system design flow rate (fig. 27).

The various system configurations were evaluated by comparing total system weight/power penalty as a function of operating performance(expressed as total equivalent weight per pound of water removed or TEW/WH_2O) for each configuration over the range of test flows. The derivation of this term is described in Appendix A.

Hydrophobic Screen Performance.- In fig. 25, the total equivalent weight is plotted as a function of the air flow rate for each of the hydrophobic cones. This figure shows the 230 mesh cone to be the optimum of the three tested as it has the lowest penalty over the operating range. This verified the conclusions from the test program based on its lowest pressure loss and 100 per cent efficiency throughout the tested range. At high flow rates, system pressure loss is the dominant penalty factor while at low flow rates the unit fixed weight represents the major portion of the penalty. In addition, the optimum flow rate of the 230 mesh cone is higher than the 325 mesh screens because of their inherent higher pressure loss characteristics over the test range. This results in a minimum volume for the 230 mesh configuration. It was concluded that the 230 mesh cone configuration was the optimum design. Further system evaluation was based on this configuration.

Spinner Evaluation.- Figure 26 shows the effect of various spinner configurations on the total equivalent weight per pound of water removed over the operating range. In original studies, it was felt that the spinner would improve the water separator efficiency and as a result, the higher pressure loss of the unit could be justified. Figure 26, however, shows

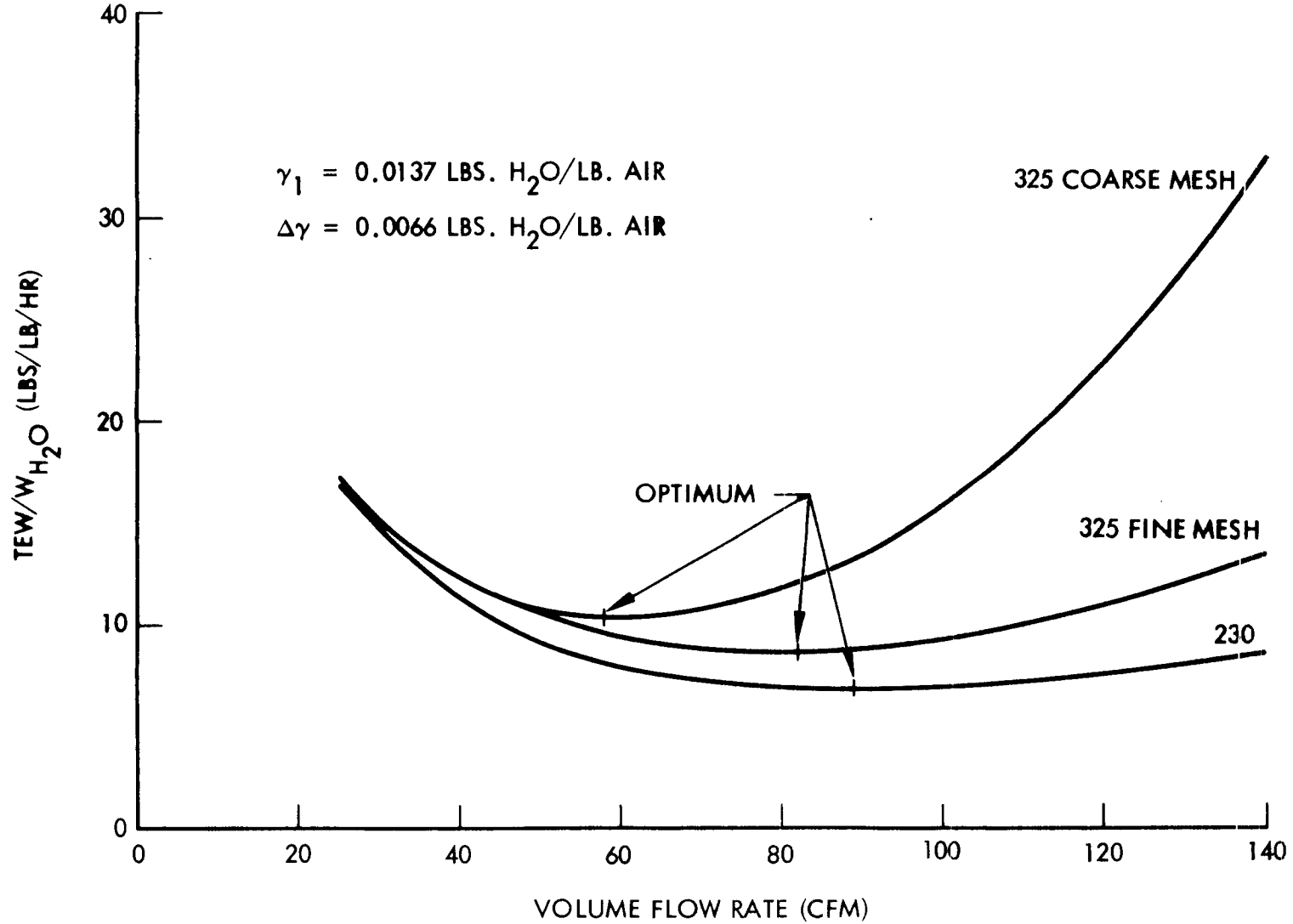

Fig. 25 - Hydrophobic Cone Selection

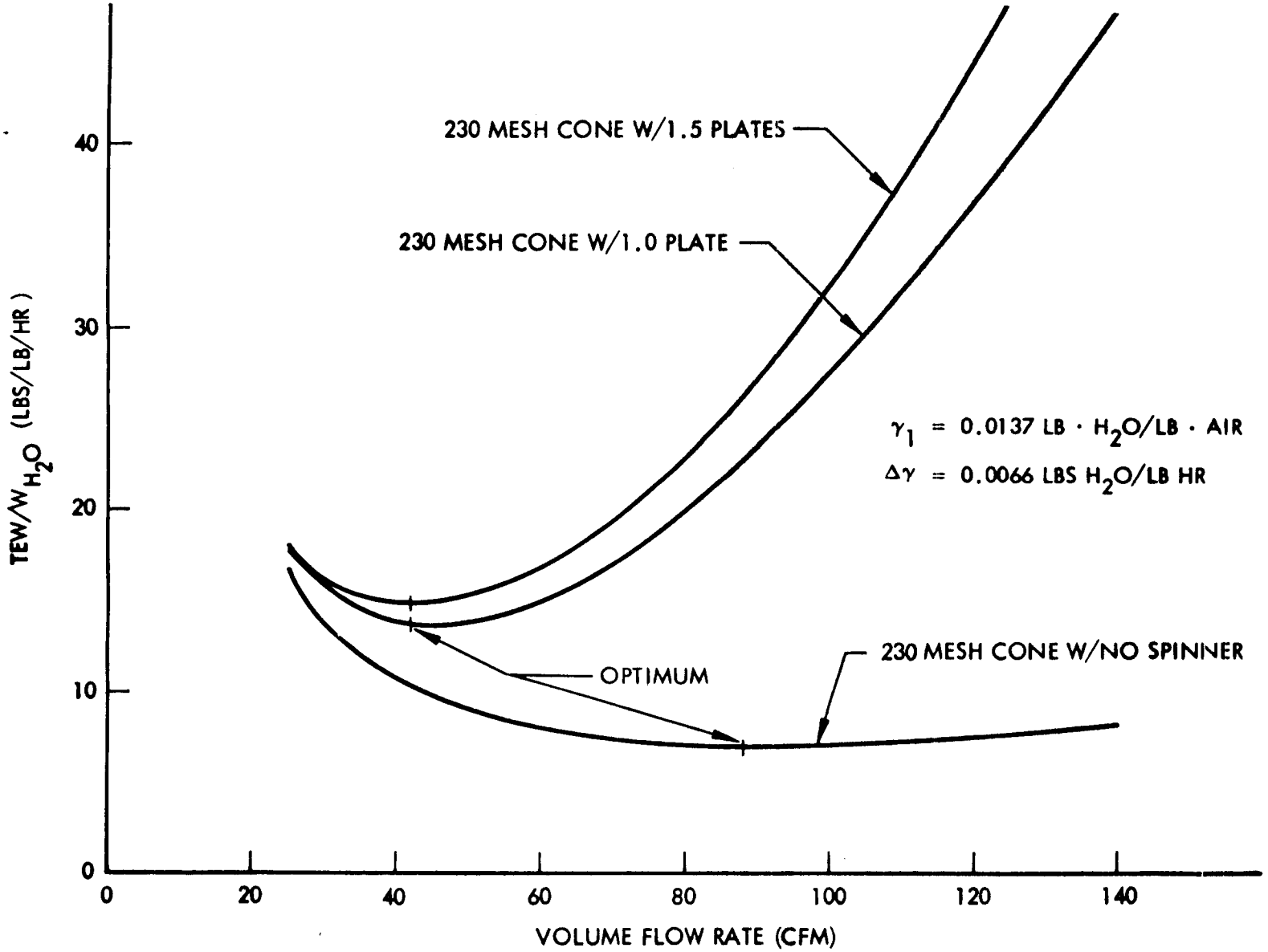

Fig. 26 - Spinner Selection

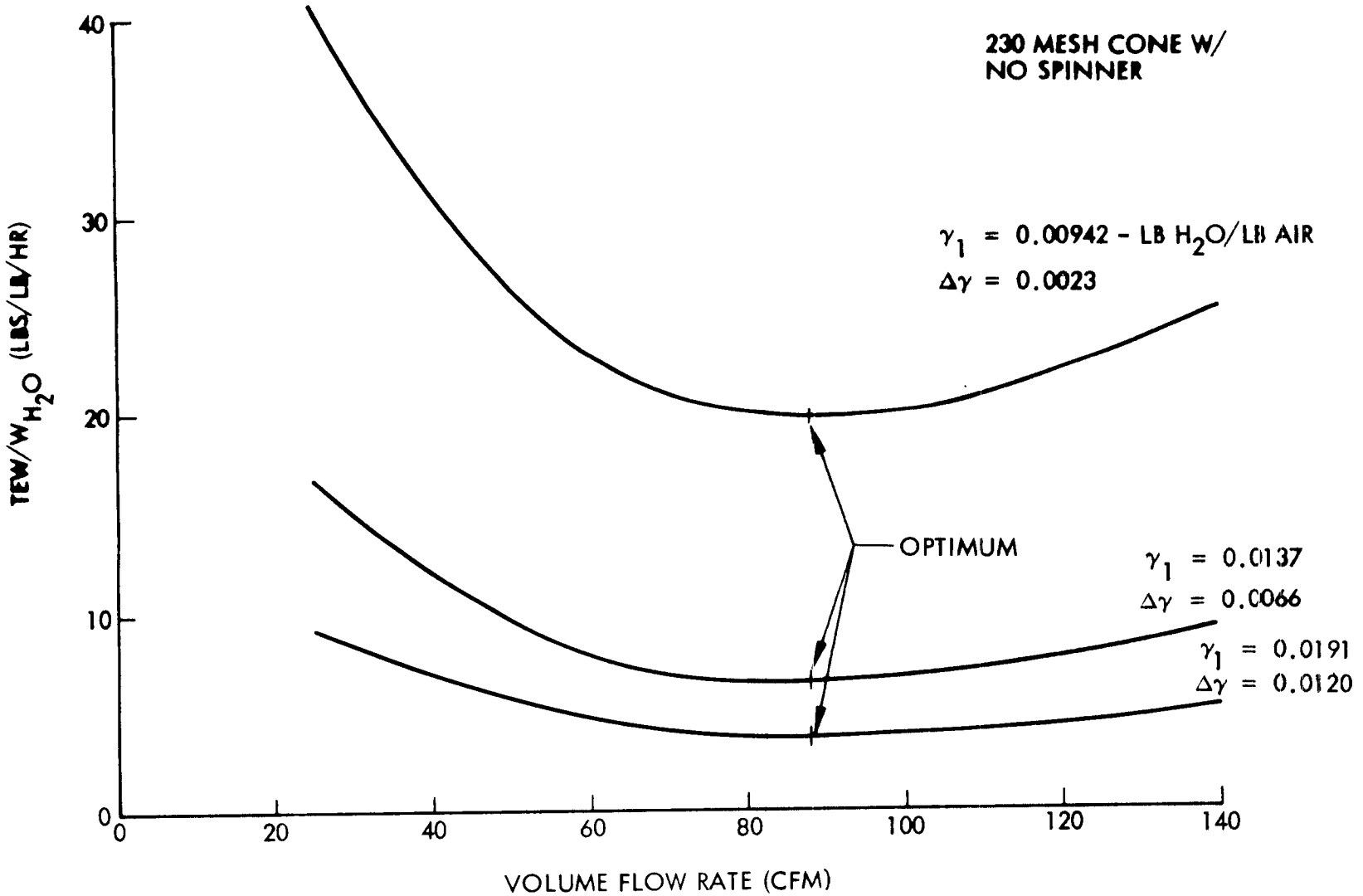

Fig. 27 - Effect of Water Removal

this theory to be in error within the range tested. The performance of the unit with the spinner in the water separator resulted in higher pressure loss, higher weight/performance penalty, and no improvement in performance. It was concluded that the water separator without the spinner was the optimum design configuration.

Optimum Water Removal Capability.- For the optimum configuration of the 230 mesh cone with no spinner, fig. 27 shows the effect of specific water removal rate on performance over the range of system air flows tested. This curve shows that the total equivalent weight per pound of water removed is least (optimum) at the maximum delta humidity (12) at an air flow of 88 cfm. The optimum system design, therefore, occurs at the point of maximum possible humidity difference consistent with system humidity control requirements.

Summary.- In summary, the optimum design characteristics for the tested humidity controlled water separator with a cone area of 28.9 in^2, fixed weight of 8.75 lbs., and a power penalty of 600 lbs/kw is a 230 mesh hydrophobic cone with no spinner configuration with an optimum flow of 88 cfm at the largest specific water removal rate allowed by vehicle design constraints. Based on this analysis, the following criteria apply to the development of an optimum water removal system whose performance is governed by humidity control requirements:

- Select 230 mesh hydrophobic cone with no spinner as optimum configuration.
- Design to maximum allowable cabin humidity and minimum allowable sink temperature.
- Establish vehicle power penalty and fan and motor efficiency for the system ΔP/flow requirements.
- Choose flow which results in minimum weight/power penalty.
- By imperical methods (using fig.24 to determine fixed weight), find optimum cone area at the design flow.

Normal vehicle ECS design specifications define values for minimum available sink temperatures and maximum water production rates and establish requirements for cabin relative humidity. From these values, system flow can be calculated directly with no penalty allowance for water separator efficiency. Water separator efficiency of 100 per cent is within system design capability. System design optimization utilizing the hydrophobic cone for water separation is then primarily one of weight and power of the moving force within the system.

Integration with Temperature Controlled System

In environmental control systems with relative humidity as a byproduct of temperature control requirements or a system with humidity control in combination with temperature control, system flow rates are generally in excess of that required to maintain the desired humidity control. In systems where flow requirements for humidity control are greater than the flow rates for the temperature control requirements, the design optimization is the same as discussed in the previous section. In either case, because the water separator performance efficiency has been demonstrated to be 100 per cent over the range of interest, the water separator penalties in the system design optimization are only those of power consumption, through pressure loss, weight and volume.

The selection of the optimum configuration for the hydrophobic cone and spinner shown in figs. 25 and 26 respectively are also applicable to the integrated temperature controlled system. Assuming a typical fixed thermal control flow requirement of 100 cfm and a vehicle power penalty of 600 lbs/kw, a plot of TEW (lbs) versus cone area (in^2) was made to determine the optimum cone area. This curve was based on the power consumption due to pressure drop, of the 230 mesh cone with no spinner at 100 cfm from fig. 17 and the fixed weight per cone area from fig.24. Figure 28 shows that the optimum TEW of 14.3 lbs, the cone area is 33.6 in^2. Based on this analysis, the following criteria apply to the development of any optimum water removal system whose flow is set by temperature control requirements:

- Select 230 mesh hydrophobic cone with no spinner as the optimum configuration.
- Establish the vehicle power penalty, fan and motor efficiency from the system Δ P/flow requirements.
- For the flow set by the temperature control requirements and the assumed system weight/power penalty (lbs/kw), determine the TEW (lbs) versus cone area relationship from the 230 mesh pressure loss characteristics (fig.17) and the water separator fixed weight per unit cone area (fig.24).
- Select the optimum hydrophobic cone area for the minimum TEW from the curve established in the preceding step.

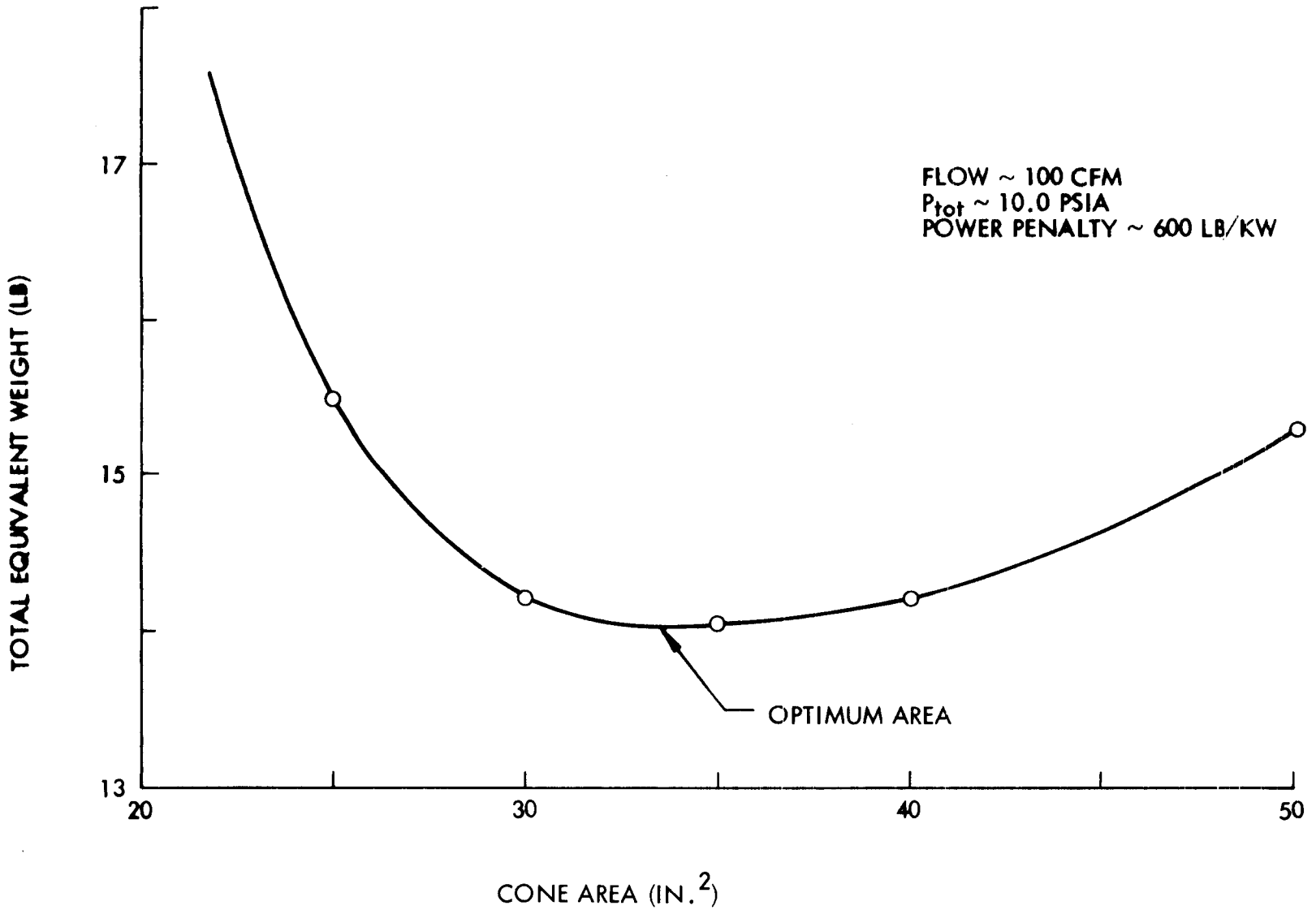

Fig. 28 - Typical Fixed Flow Optimization

CONCLUSIONS AND RECOMMENDATIONS

The following conclusions are based on the test and evaluation program conducted on the Lockheed Humidity Control System:

- The methodology developed in Appendix A and the reduced performance data from the test and evaluation program can be applied to establish optimum design criteria for other zero gravity systems utilizing the hydrophobic/hydrophilic water separator.

- The design concept of a hydrophobic cone with no moving parts as a water separator is valid as demonstrated in the test and evaluation program.

- The optimum configuration for the hydrophobic cone is a Teflon - coated 230 mesh (0.0014" diameter) wire screen, 45° cone angle with no spinner and no coalescer.

- Perform efficiencies of 100%, as demonstrated, are well within system operational and design capabilities.

- Pressure drop penalties across the hydrophobic cone are minimum, compared to other zero gravity water removal systems.

- Testing of the hydrophobic cones in the vertical mode under gravity conditions is valid for zero gravity application as it represents the maximum force of the water/air flow on the cone surface.

- The hydrophilic (sump) system tested was compatible with the water separator tested, however, no attempt was made to optimize the design or performance parameters of this system as gravity has a very beneficial effect on this component.

- The system responded rapidly to transient conditions demonstrating stable performance over a range of operating conditions with a step change input. However, response times are valid only for the volume of the test fixture.

- Based on design simplicity (no moving parts in the water separation mechanism) and performance repeatability, the Lockheed Humidity Control System is highly reliable.

- Maintainability is simple and pending endurance test demonstration and evaluation of mission requirements, maintenance requirements are comparatively low.

- Design and optimization procedures defined in the design criteria section are valid for preliminary design calculations over the range of data presented.

The positive results demonstrated in this program strongly imply that further development of the hydrophobic/hydrophilic humidity control system be undertaken. It is therefore recommended that:

- Endurance testing be conducted on the 230 mesh hydrophobic cone.
- Zero gravity tests be performed on a system to verify operation under zero gravity conditions.
- A man-rated humidity control system of flight configuration be designed, developed and qualified.

APPENDIX A

INITIAL HYDROPHOBIC/HYDROPHILIC HUMIDITY CONTROL SYSTEM

MODEL TRADE-OFF STUDY AND TEST PLAN

INTRODUCTION AND SUMMARY

Lockheed Missiles and Space Company is presently under contract to the NASA Langley Research Center to (1) develop an optimization trade-off methodology to establish requirements for experimental data, (2) develop a test plan directed toward obtaining the data required for the optimization analysis and (3) conduct the experiments defined in the test plan. This report presents the model trade-off study and the test plan.

The data generated during the experimental phase of this program will provide all of the necessary information to allow the optimization to be conducted.

MODEL TRADE-OFF STUDY
HYDROPHOBIC/HYDROPHILIC HUMIDITY CONTROL SYSTEM

The objective of the model trade-off study has been to establish a methodology for optimizing a hydrophobic/hydrophilic type water separator and to thereby identify the test data required to conduct the optimization. The methodology developed during the study is the subject of this report. The proposed three step plan is outlined below and then discussed in detail.

Step I **Optimize Design of Present System** - The more important physical design parameters (coalescer density and spinner configuration) will be varied and performance noted to support optimization of the laboratory unit under test.

Step II Rate Present System - The optimum flow rate and water removal rate of the present laboratory unit will be established. The methodology developed in accomplishing this task will serve as a basis for optimizing systems larger and smaller than the present unit.

STEP III Sizing of Systems Larger and Smaller Than the Present System - The data obtained in Steps I and II will be extrapolated to support optimization of any sized unit.

Step I Optimize Design of Present System

The basic elements of the humidity control system are the coalescer, spinner, and screen. Several characteristics of each of these elements can be varied with possible changes in system performance resulting. Possible variations in physical design of the unit are listed below.

Coalescer	Spinner	Screen
Type	Pitch	Mesh Size
Density	Number of Plates	Cone Angle
Length	Area	Area

Laboratory investigation of all combinations of these variables would result in a prohibitively large test program. In order to scope the program at a level consistent with the funded effort the two most important variables, coalescer density and spinner configuration were selected for optimization. The area of the unit is considered in Step III and will be discussed later. The wetting and pressure drop characteristics of various coalescer materials present an area of potential trade-off. The ability of a material to catch and hold water droplets will effect the design of the spinner and screen.

Increased coalescer length provides greater opportunity for water droplets to form prior to discharge from the coalescer, but also provides greater pressure drop. The number of spinner plates and spinner pitch affects system pressure drop and establish the amount of water removed from the airstream by centrifugal force which in turn affects screen design. Screen mesh and screen cone angle affect system pressure drop and the water removal efficiency. Increased cone angles will allow shorter unit design but must be offset by smaller screen mesh or increased screen diameter to prevent impact breakthrough. Although the most important variables are coalescer density and spinner configuration, a valuable addition to the current program would be the assessment of the effects of these other variables by test.

The first step in the currently funded effort is then based on optimizing the present design with respect to coalescer density and spinner configuration. The detailed plan for Step 1 is as follows:

1. For a pre-selected airflow (Q), cabin specific humidity (γ_1), and lowest feasible h/x exit specific humidity (γ_2), test the present system using three coalescer densities and with three spinner configurations (0, 1 and $1\frac{1}{2}$ spinner plates. Plot system's pressure drop (Δp) and water removal efficiency (η_R) vs. coalescer density with spinner configuration as a parameter.

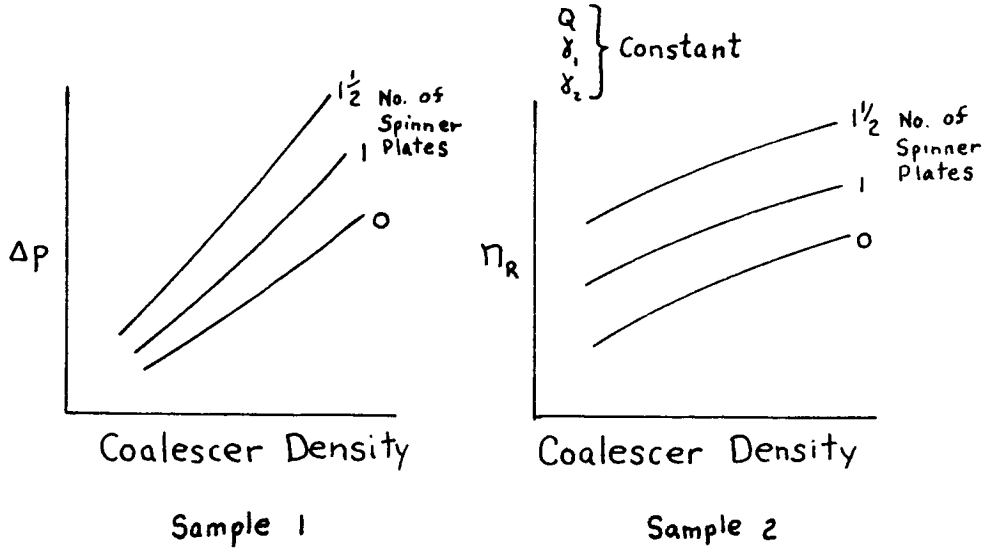

2. For the given Q, γ_1, γ_2 and using Sample 2, calculate the water removal rate ($\dot{\omega}_{H_2O}$)at various coalescer densities for the three spinner configurations.

$$\dot{\omega}_{H_2O} = Q\rho(\gamma_1 - \gamma_2)\eta_R$$

From Sample 1 obtain Δp and calculate the fan power

$$P_{fan} = Q\Delta p / \eta_{fan\text{-}motor}$$

3. Calculate the Total Equivalent Weight (TEW) of the system. TEW includes the fixed weight of the water separator and fan, and the power penalty for operation of the fan.

$$TEW = P_{fan}\left(^{weight}/_{Watt}\right) + W_{System}$$

The system fixed weight will reflect flight weight estimates and not the weight of the present test system.

4. Calculate TEW per pound of water removed and plot it against coalescer density with spinner configuration as a parameter. $TEW/\dot{\omega}_{H_2O}$ is the best measure of overall system optimization.

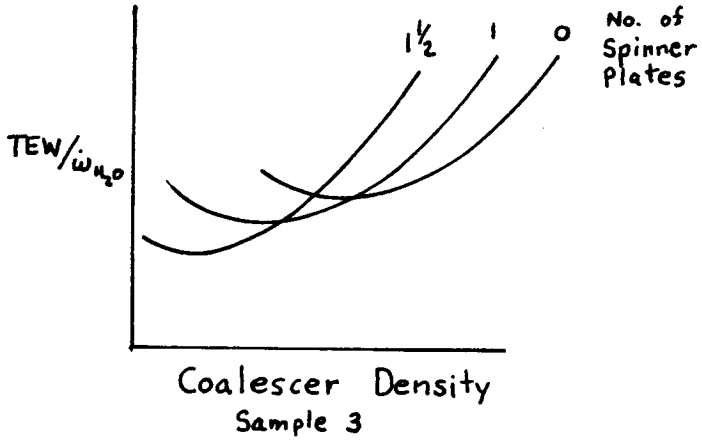

Sample 3

5. From Sample 3 select the coalescer density and spinner configuration that results in minimum $TEW/\dot{\omega}_{H_2O}$.

Coalescer densities to be tested will be selected to cover a wide range of interest. It is possible a minimum will not be identified after completion of Step I and that additional testing will be advisable. In that event IMSC will coordinate revisions in the test plan with LRC.

Step II Rate Present System

Having optimized the laboratory prototype with respect to physical design features, the next step in the program is to optimize it with respect to airflow rate and cabin and heat exchanger specific humidities. The end result of this optimization will be to establish a rating of the present

system (optimum water removal rate) and to thereby establish the basis for optimizing any sized system. The rating of the present system will be accomplished as follows:

1. Using the optimum coalescer density and spinner configuration from Step I, establish by test, system pressure drop and water removal efficiency as a function of Q and γ_1, for a fixed value of γ_2.

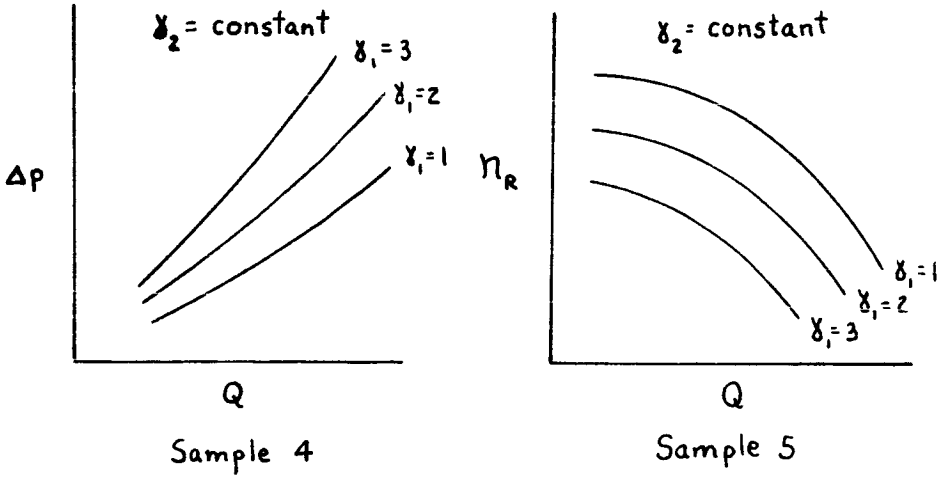

2. For each γ_1, and using at least 3 values of Q, obtain η_R from Sample 5 and calculate water removal rate.

$$\dot{\omega}_{H_2O} = Q\rho(\gamma_1 - \gamma_2)\eta_R$$

3. For each Q and γ_1, obtain Δp from Sample 4 and calculate fan power requirements.

$$P_{fan} = \frac{Q\Delta p}{\eta_{fan\text{-}motor}}$$

4. For each Q and γ_1, calculate $TEW/\dot{\omega}_{H_2O}$ based on the fan power and $\dot{\omega}_{H_2O}$ calculated above and an estimated flight system fixed weight. System weight must now include space radiator and heat exchanger weights which will vary with air flow rate.

5. Plot TEW/$\dot{\omega}_{H_2O}$ as a function of Q for each γ_1.

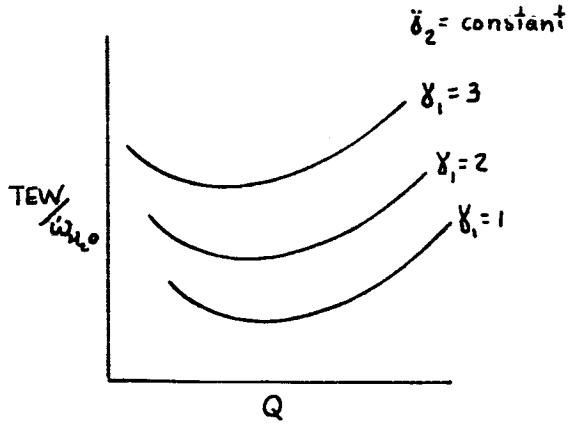

Sample 6

6. For a given γ_1, (Cabin temperature and relative humidity), the optimum flow rate can be obtained. $\dot{\omega}_{H_2O}$ can be calculated and for any given metabolic water production rate a "man-rating" can be established.

Heat exchanger outlet specific humidity has been held constant at the lowest possible value (dew point at approximately 38F). Use of this value is based on previously conducted trade-off studies that showed the lower the condensing temperature the lower the TEW/$\dot{\omega}_{H_2O}$. In order to check this calculation the effect of varying γ_2 will be determined by test. The testing will consist of three runs at three γ_2's, a preselected γ_1, corresponding to 75°F cabin temperature @ 50% relative humidity and a constant $\dot{\omega}_{H_2O}$ corresponding to the optimum flow rate obtained from Sample 6. Maintaining constant $\dot{\omega}_{H_2O}$ and γ_1, with increasing γ_2 will require airflow to be increased.

7. For the three γ_2's measure and record airflow and Δp (γ_1 and $\dot{\omega}_{H_2O}$ constant)

8. Calculate Fan Power and TEW/$\dot{\omega}_{H_2O}$

   $$TEW = P_{Fan}(Weight/_{Watt}) + W \text{ System}$$

   The system weight includes water separator weight, fan weight and space radiator system weight.

9. Plot TEW/$\dot{\omega}_{H_2O}$ as a function of γ_2.

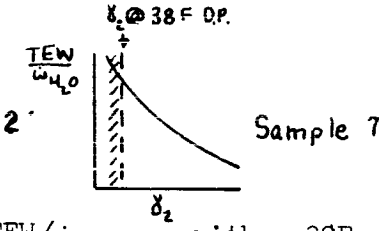

Sample 7

10. Select γ_2 corresponding to minimum TEW/$\dot{\omega}_{H_2O}$ with a 38F cutoff to prevent freezing in the heat exchanger.

Step III - Sizing of Systems Larger or Smaller Than the Present System

The information presented by Samples 4 and 5 can be presented parametrically to facilitate selection of an optimum water separator for any given number of men. Generalized plots of Samples 4 and 5 can be established by dividing Q by the coalescer area. Modifying these plots as such for optimization of all systems assumes that:

a. Coalescer density and spinner configuration established as optimum for the present system are optimum for all sized units.

b. Velocity and γ_1, are the only significant parameters for the determination of η_R and Δp once an optimum physical design (coalescer, spinner and screen) has been established.

These assumptions are considered to be reasonable. In order to verify their validity however, different sized units would have to be built and tested at the constant Q/A.

The following methodology is based on the two assumptions listed above:

1. Divide the airflow (Q) in Samples 4 and 5 by coalescer area (A) in order to generate Samples 10 and 11.

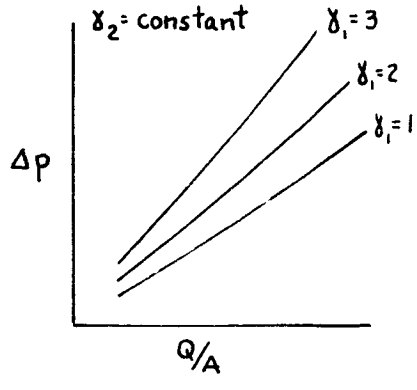

Sample 8

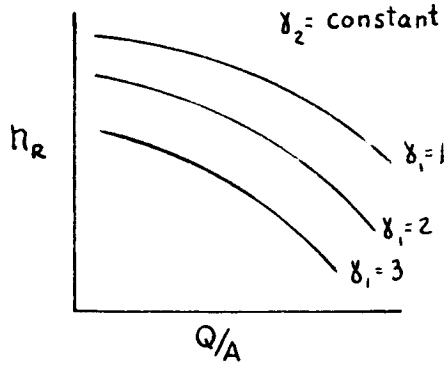

Sample 9

2. Estimate water separator system weight as a function of area (A) and plot as in Sample 10. The system weight will consist of the screen coalescer, spinner and duct.

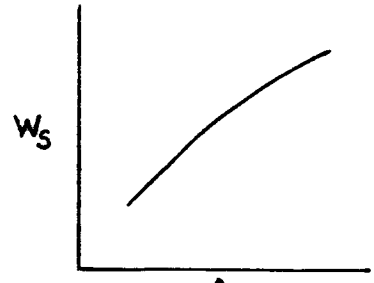

Sample 10

3. Using Sample 9 calculate required airflow for several values of Q/A for each γ_1, for $\dot{\omega}_{H_2O} = 1$. Also calculate (A) and P_{Fan}.

$$Q = \dot{\omega}_{H_2O} / \rho (\gamma_1 - \gamma_2) \eta_R$$

$$A = \frac{Q}{Q/A}$$

$$P_{fan} = \Delta P \, Q / \eta_{fan\text{-}motor}$$

4. Calculate $TEW/\dot{\omega}_{H_2O}$ from P_{Fan} Sample 10 and an estimate of radiator system weight

$$TEW/\dot{\omega}_{H_2O} = P_{Fan}(\text{Weight/Watt}) + W_{System}$$

System weight includes water separator weight, fan weight, and space radiator system weight.

5. Plot TEW/$\dot{\omega}_{H_2O}$ as a function of Q/A and γ_1 .

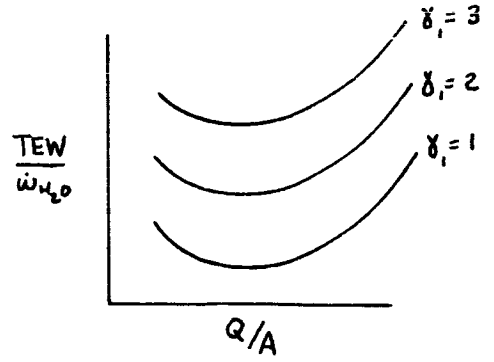

Sample 11

With the information presented by Samples 8, 9 and 11 the following method can be used for establishing the humidity control system design when γ_1, and $\dot{\omega}_{H_2O}$ are known. (γ_1 , and $\dot{\omega}_{H_2O}$ are independent variables generally known to the systems engineer). γ_2 has been established in the optimization of the laboratory system.

- o With γ_1 , and Sample 11 obtain optimum Q/A
- o With known Q/A and Sample 9 obtain η_R
- o Based on required $\dot{\omega}_{H_2O}$ and η_R calculate required Q

$$Q = \dot{\omega}_{H_2O} / \rho (\gamma_1 - \gamma_2) \eta_R$$

- o With known Q/A and Q calculate the area of the system

$$A = \frac{Q}{Q/A}$$

- o From A coalescer, spinner, screen and duct design can be established based on known coalescer type, density and length; spinner pitch and number of plates; and screen mesh size and cone angle.

TEST PLAN
HYDROPHOBIC/HYDROPHILIC HUMIDITY CONTROL SYSTEM

Steady State Test Plan

The steady state tests described herein are based on the model trade-off studies presented in previous section of this Appendix.

The present laboratory system shall be installed in the GFE test stand with the separator axis in a horizontal position. All tests shall be conducted with air at 10 psia utilizing the constant relative humidity controller as furnished to LMSC by LRC.

1. In order to support optimization of the physical design of the water separator system a series of nine test runs shall be made using three coalescer densities equal to 24.1, 48.4, and 72.5 pounds per cubic foot and three spinner configurations consisting of zero, one and one and one-half plates. Air flow rate (Q), cabin specific humidity γ_1, and water separator inlet specific humidity γ_2 shall be held constant at approximately the following values:

$$Q = 70 \text{ CFM}$$

$$\gamma_1 = 0.0137 \text{ lb. } H_2)/\text{lb air}$$

$$\gamma_2 = 0.0071 \text{ lb. } H_2O/\text{lb air}$$

During each of the nine test runs the following data shall be recorded:

- o System air flow (Q) CFM
- o Cabin Specific Humidity (γ_1) lb H_2O/lb air
- o Heat Exchanger Condensing Temperature (T_c)$^\circ$F
- o Water Separator Outlet Specific Humidity (γ_3) lb H_2O/lb air (γ_3) is measured downstream of the reheat heater where unremoved water droplets are re-evaporated)
- o System Pressure Drop (ΔP) $"H_2O$

NOTE: Separator water removal efficiency is established by γ_1, γ_2 and γ_3.

$$\eta_R = \frac{\gamma_1 - \gamma_3}{\gamma_1 - \gamma_2}$$

2. In order to provide data for rating the present system and optimizing other water separator systems, a series of nine test runs shall be made using the optimum coalescer density and spinner configurations established by the previous series of test runs. The nine test runs shall be conducted at approximately the following conditions: three air flows of 20, 70, and 120 CFM, and three values of γ_1 equal to 0.0191, 0.0137, and 0.0082 lb H_2O/lb air. γ_2 shall be held constant at approximately 0.0071 lb H_2O/lb air. Data taken during the tests shall be as listed for the previous set of runs.

3. In order to establish the affect of varying γ_2, two additional test runs shall be made holding $\dot{\omega}_{H_2O}$ constant at a value corresponding to the optimum air flow rate (Q) established as a result of the second series of tests and a γ_1 of approximately 0.0137 lb air H_2O/lb air. γ_2 values of approximately 0.0092 and 0.0116 lb H_2O/lb air shall be used. Air flow during the runs shall be adjusted to maintain $\dot{\omega}_{H_2O}$ constant and γ_1 at approximately 0.0137 lb H_2O/lb air.

APPENDIX B

HYDROPHOBIC/HYDROPHILIC

HUMIDITY CONTROL SYSTEM

MODIFIED STEADY STATE TEST PLAN

APPENDIX B

HYDROPHOBIC/HYDROPHILIC HUMIDITY CONTROL SYSTEM
MODIFIED STEADY STATE TEST PLAN

The steady state tests described herein are based on the model trade-off studies presented in the previous section of this Appendix.

The present laboratory system shall be installed in the GFE test stand with the separator axis in a vertical position. All tests shall be conducted with air at 10 psia utilizing the constant relative humidity controller as furnished to LMSC by LRC.

1. In order to support optimization of the physical design of the water separator system a series of 27 test runs shall be made using three screen apertures equal to .00148, .00178 and .00275 inches, three spinner configurations consisting of zero, one and one and one-half plates, and three air flow rate (Q) of 40, 70 and 100 cfm. The cabin specific humidity γ_1, and water separator outlet specific humidity γ_2 shall be held constant at approximately the following values:

$$\gamma_1 = 0.0137 \text{ lb } H_2O/\text{lb air}$$

$$\gamma_2 = 0.0071 \text{ lb } H_2O/\text{lb air}$$

During each of the twenty-seven test runs the following data shall be recorded:

- o System air flow (Q) cfm
- o Cabin Specific Humidity (γ_1) lb H_2O/lb air
- o Heat Exchanger Condensing Temperature (T_c) ^oF
- o Water Separator Outlet Specific Humidity (γ_3) lb. H_2O/lb air (γ_3 is measured downstream of the reheat heater where unremoved water droplets are re-evaporated)
- o System Pressure Drop (ΔP) "H_2O"

NOTE: Separator water removal efficiency is established by γ_1, γ_2, and γ_3.

$$\eta R = \frac{\gamma_1 - \gamma_3}{\gamma_1 - \gamma_2}$$

2. In order to provide data for rating the present system at off design conditions, a series of four test runs shall be made using the optimum screen aperture, spinner configuration, and flow rate established by the previous series of test runs. These test runs shall be conducted at approximately the following values of γ_1 equal to 0.0191 and 0.0082 lb H_2O/lb air. γ_2 shall be held constant at approximately 0.0071 lb H_2O/lb air. Data taken during the tests shall be as listed for the previous set of runs.

   In order to establish the affect of varying γ_2, test runs shall be made holding γ_1 at approximately 0.0137 lb H_2O/lb air. γ_2 values of approximately 0.0092 and 0.0113 lb H_2O/lb air shall be used.

APPENDIX C

OPERATION OF THE LOCKHEED HUMIDITY CONTROL SYSTEM

APPENDIX C

OPERATION OF THE LOCKHEED HUMIDITY CONTROL SYSTEM

GENERAL DESCRIPTION

The zero gravity humidity control system is designed to condense and remove water from an enclosed environment in order to prevent high humidity build up and to provide water for reuse. The humidity control system is presented schematically in fig. C-1.

Air is circulated through the humidity control system by a fan unit. The excess moisture in the air stream is condensed by the condensing heat exchanger to provide cabin humidity control. The coalescer, inside the water separator, ensures that the condensed moisture becomes droplets before leaving the coalescer. The centrifugal action generated by the static spinner will ensure that the water droplets pass over the hydrophilic sump and will minimize the impact of the water droplets on the hydrophobic surface. The hydrophobic surface allows the cooled air to pass but separates the water droplets.

The atmosphere is routed back to the cabin; the water, diverted to the hydrophilic sump, is withdrawn for storage. The hydrophilic sump allows the water to pass freely, but not the cabin atmosphere.

A bladdered-tank-type water delivery system is employed. A small air pump is controlled by the differential switch to provide the proper suction on the bladder and, thus, on the hydrophilic sump. By proper positioning of the 3-way vacuum and vent valves, the air-pump can withdraw water from the water separator or discharge water from the bladdered tank for use.

Four bosses are provided for pressure, temperature and air velocity monitoring during system operation.

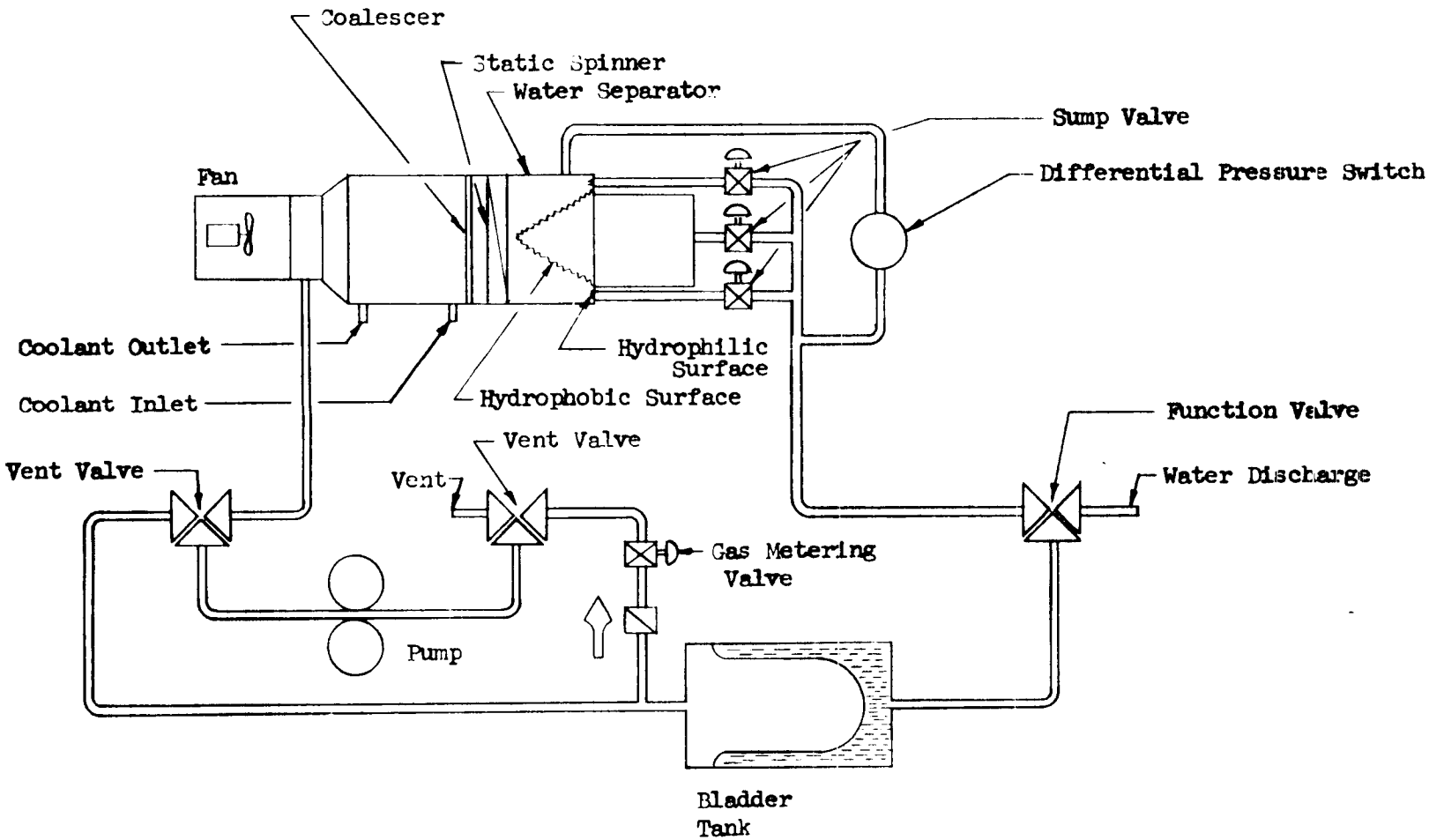

Fig. C-1 Humidity Control System Schematic

PREPARATION FOR USE AND CHECKOUT

Equipment required for operation of the Zero Gravity Humidity Control System

1. 115 VAC 60 cps Power Supply
2. 28 VDC Power Supply (10 AMP capacity)
3. Refrigeration system that will provide a continuous flow of 35°F coolant to the condensing heat exchanger
4. Air flow indicator

Preparation for Use and Checkout

Step	Procedure	Normal Indications	Notes
1	Turn pump and fan switches to off position	Off position indicated on control panel	
2	Connect system to interface equipment		Install system in test fixture
	a. Connect 28 VDC power supply	Meter on power supply to read max 28 V	Terminal board on chassis stand, Fan switch should be in off position
	b. Connect 115 VAC 60 cps power supply		Terminal board on chassis stand. Pump switch should be in off position
	c. Connect coolant lines to heat exchanger		Check for leaks
3.	Check cabling and fuses	Connectors in place and secure	Connector on different pressure switch and connector on sump pump housing fuse for fan

Step	Procedure	Normal Indications	Notes
4	Tighten and leak check all gas and water lines		Pressurize max 5 psi with dry nitrogen and check pressure decay
5	Close all sump valves	Turned clockwise to stop	Valves are metering valves and should be closed finger tight only
6	Close pump valve	Turned clockwise to stop	Valve is a metering valve and should be closed finger tight only
7	Instrumentation ports		If instrumentation is not used all unused ports should be plugged and leak checked.

OPERATION

The Humidity Control System controls for normal operation, are all contained within and on the unit itself. The water recovery system is depicted schematically on the control panel. The function and locations of each control and valve are described below.

Fan Switch

This switch is located on the control panel and indicates the ON or OFF condition of the blower.

Pump Switch

This switch is located on the control panel and has an automatic, OFF and manual position. The three conditions are indicated on the control panel.

Valves for the Water Recovery System

Function valve. - This valve determines the function of the system either to recover and store water or to expel water from the bladder tank to ambient or back through the sumps into the system. Operation and flow paths are depicted on the control panel.

Vent valves. - These valves are located on the control panel and are used to control the flow of air on the gas side of the bladder in bladder tank.

Bladder tank gas metering valve.- This valve is located over the bladder tank and regulates the rate of flow of gas removed by the pump during the water removal cycle.

Sump valves.- These three valves are located in front of the sump plate on the separator unit. There is one valve for each sump. These valves are used during the sump screen wetting procedure and for regulating the liquid flow from the water separator to the bladder tank.

Differential pressure switch.- This switch is located on the side of the separator unit. The switch senses the Δ P across the hydrophilic sump (gas side to liquid side) when there is sufficient Δ P the switch activates the pump which removes the liquid in the sump.

Operating Procedures

Valves on control panel shall always be operated in the following sequence. Close a vent, select a function, open a vent.

Step	Procedure	Normal Indications	Notes
1. Charge bladder tank with water	Open bladder tank metering valve 1/4 turn ccw. Set control panel valves as shown in fig. C-2. Attach function valve outlet to water supply. Close sump valves. Switch pump to ON position and fill bladder tank approx. 3/4 full; when bladder tank is 3/4 full turn pump switch to OFF	Water in bladder tank	Turn valves in right sequence
2. Wet sump screens	Change control panel valves to position shown in fig.C-3, Turn pump switch to ON position. Open one sump valve approx. $\frac{1}{4}$ turn ccw. Let sufficient water flow to wet screen and close valve. Follow the same procedure for all three sumps	Sump outlet tubes are filled with gas-free liquid	Turn control panel valves in right sequence
3. P switch	Set Δ P switch to 4 inches of water. Effective at the sump.	Read directly on switch adjustment screw	
4. HX	Flow coolant thru H-X at desired temp.	H-X body will become cool to the touch	Check inlet and outlet connection are correct for counter flow operation.

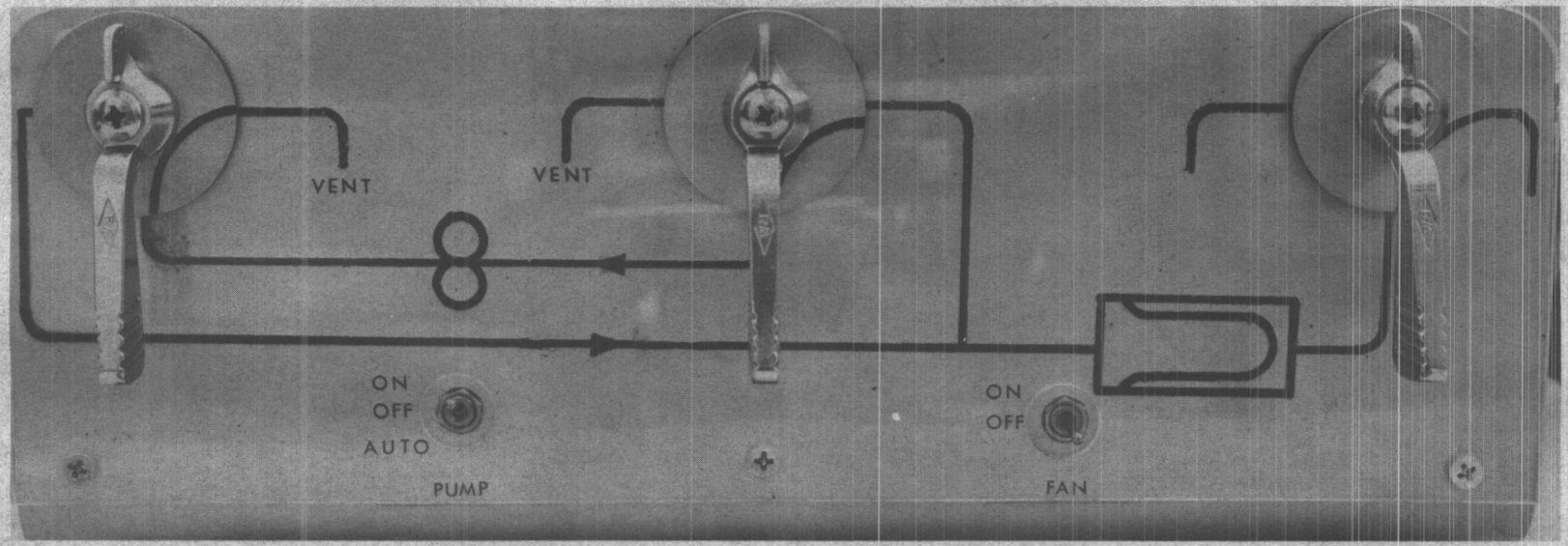

Fig. C-2 Valves Set to Charge Bladder Tank

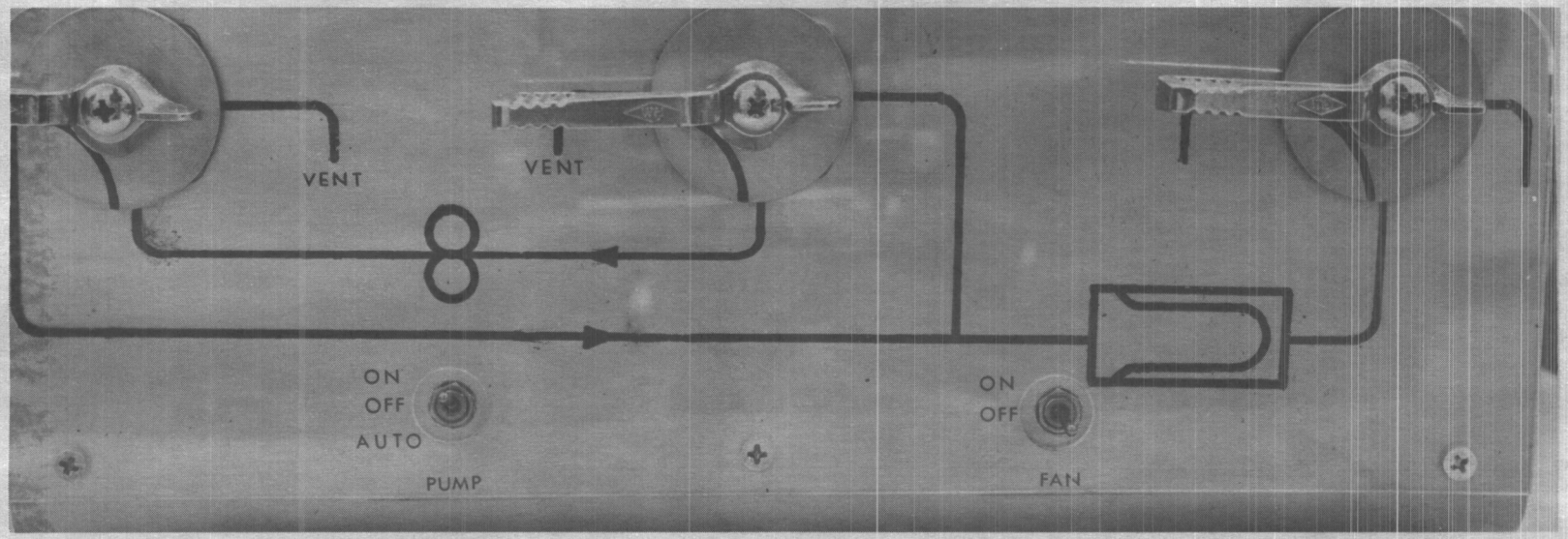

Fig. C-3 Valves Set to Wet Sump Screens

Step	Procedure	Normal Indications	Notes
5. Blower	Activate blower switch to ON position. Vary voltage on 28 VDC power supply to achieve correct air flow.		28 VDC max
6. Water	Set control panel as shown in fig. C-4. Activate pump switch to auto position. When light goes out, open desired sump valves 1/8 turn ccw and observe that water stays in outlet tube for that sump.		Operate control panel valves in proper sequence. If water leaves sump outlet tube, close sump valve and re-do Step 2.
7. Water Withdrawal	Close sump valves. Set control panel valves as shown in fig. C-5.		Operate control panel valves in proper sequence.

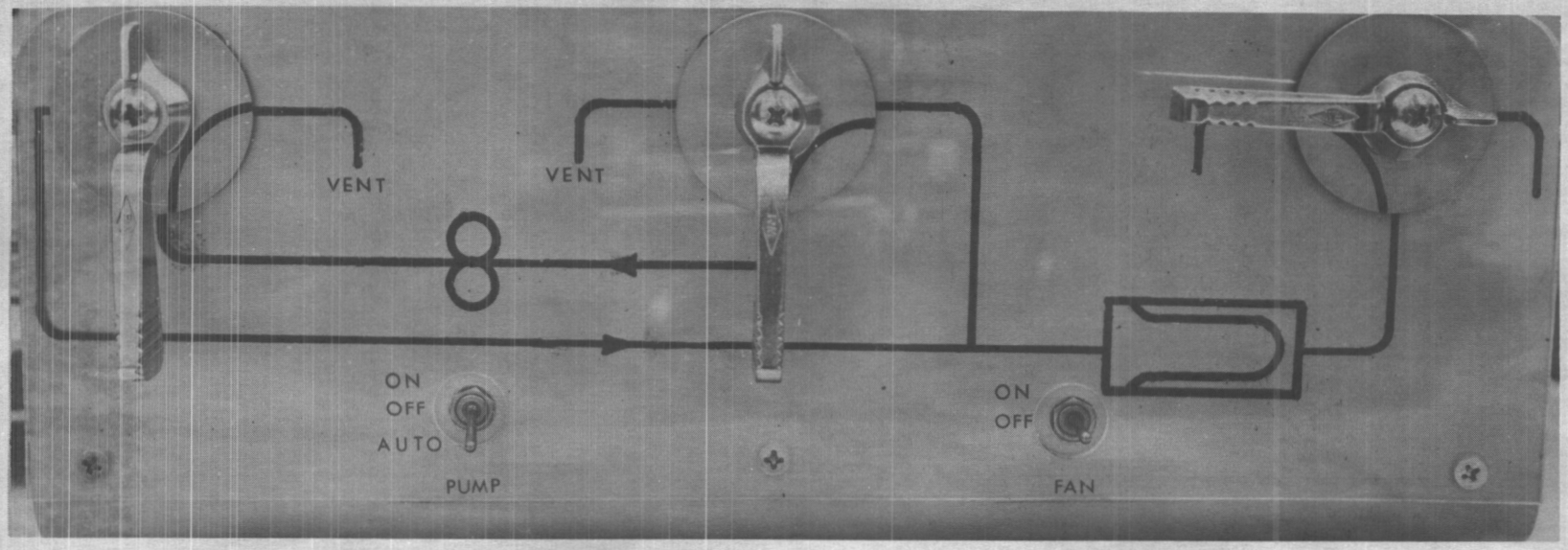

Fig. C-4 Valve Set to Remove Water From Sump and Store

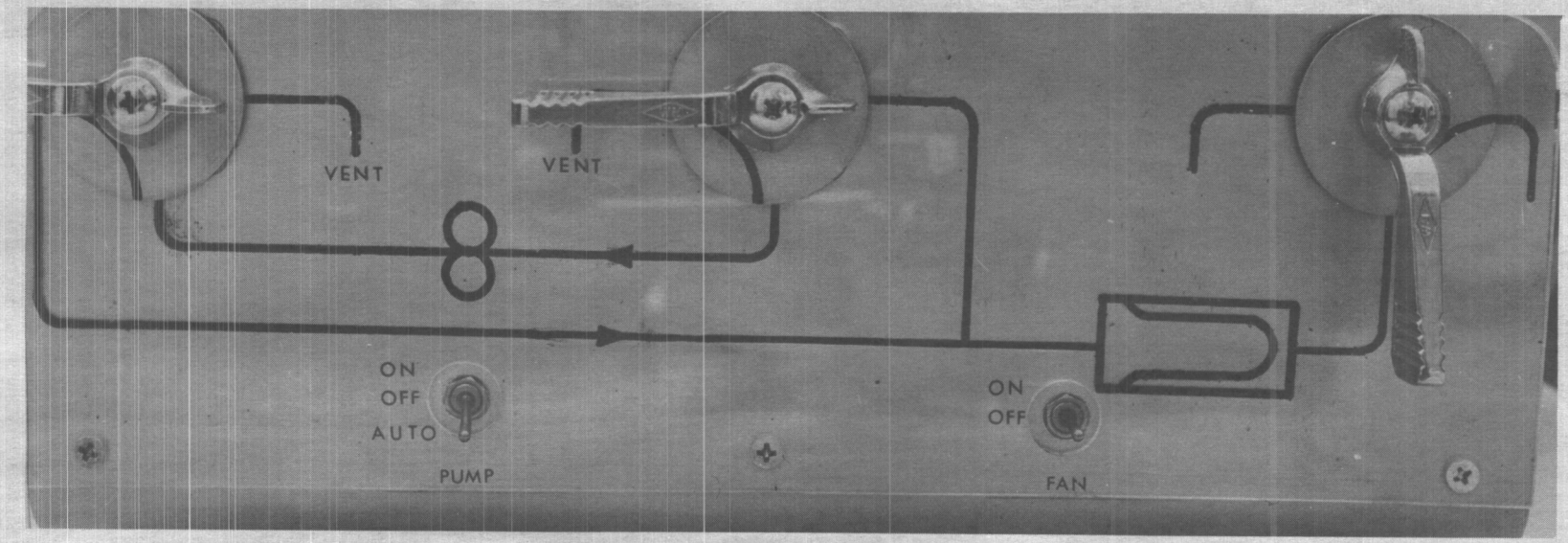

Fig. C-5 Valves Set for Water Withdrawal

APPENDIX D

TEST DATA FOR HYDROPHOBIC/HYDROPHILIC HUMIDITY CONTROL SYSTEM EVALUATION

PERTINENT UNITS FOR DATA IN APPENDIX D

Parameter	Units	Notes
1	millivolts	See fig. D-1 for conversion to ^{o}F dew point
2	millivolts	See fig. D-2 for conversion to ^{o}F dew point
3	millivolts	See fig. D-2 for conversion to ^{o}F dew point includes radiation loss to coolant fins
Thox	^{o}F	Includes radiator loss to coolant fins
Flow	ft/min	See fig. D-3 for conversion to CFM
Psys	in Hg	Represents level of test system pressure below ambient
P	inches water	Pressure loss across water separator

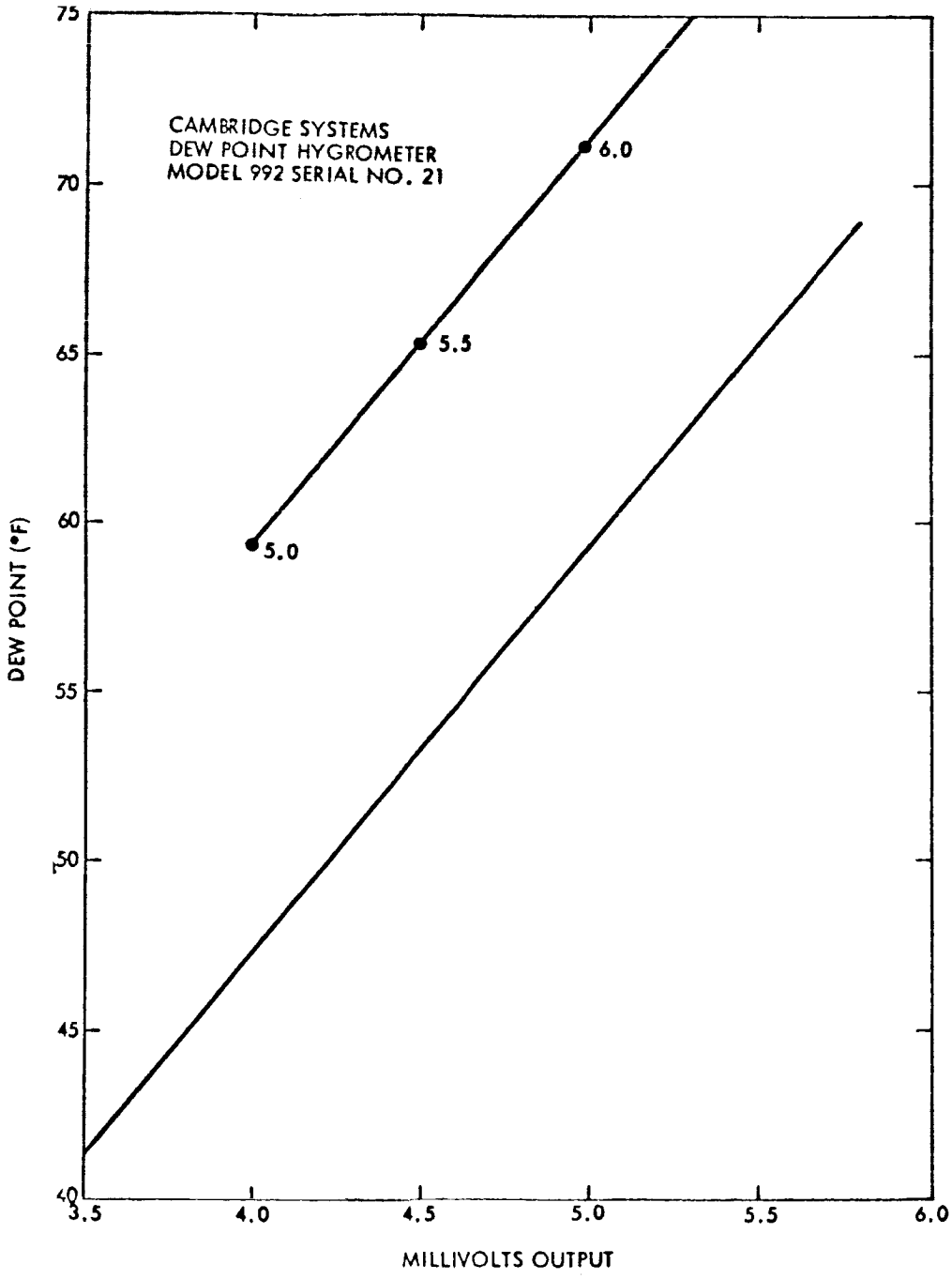

Fig. D-1 Inlet Dewpoint Conversion

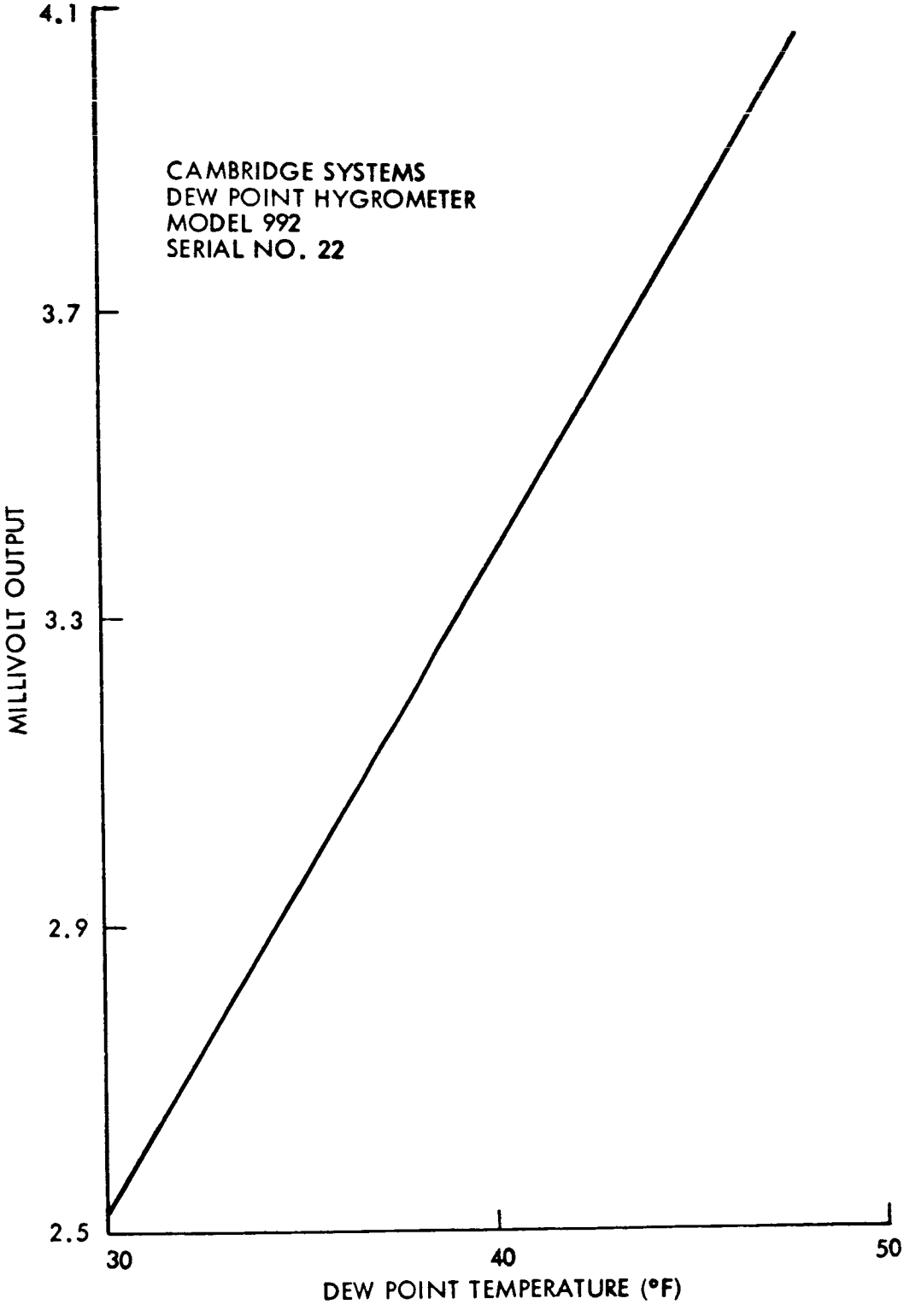

Fig. D-2 Outlet Dewpoint Conversion

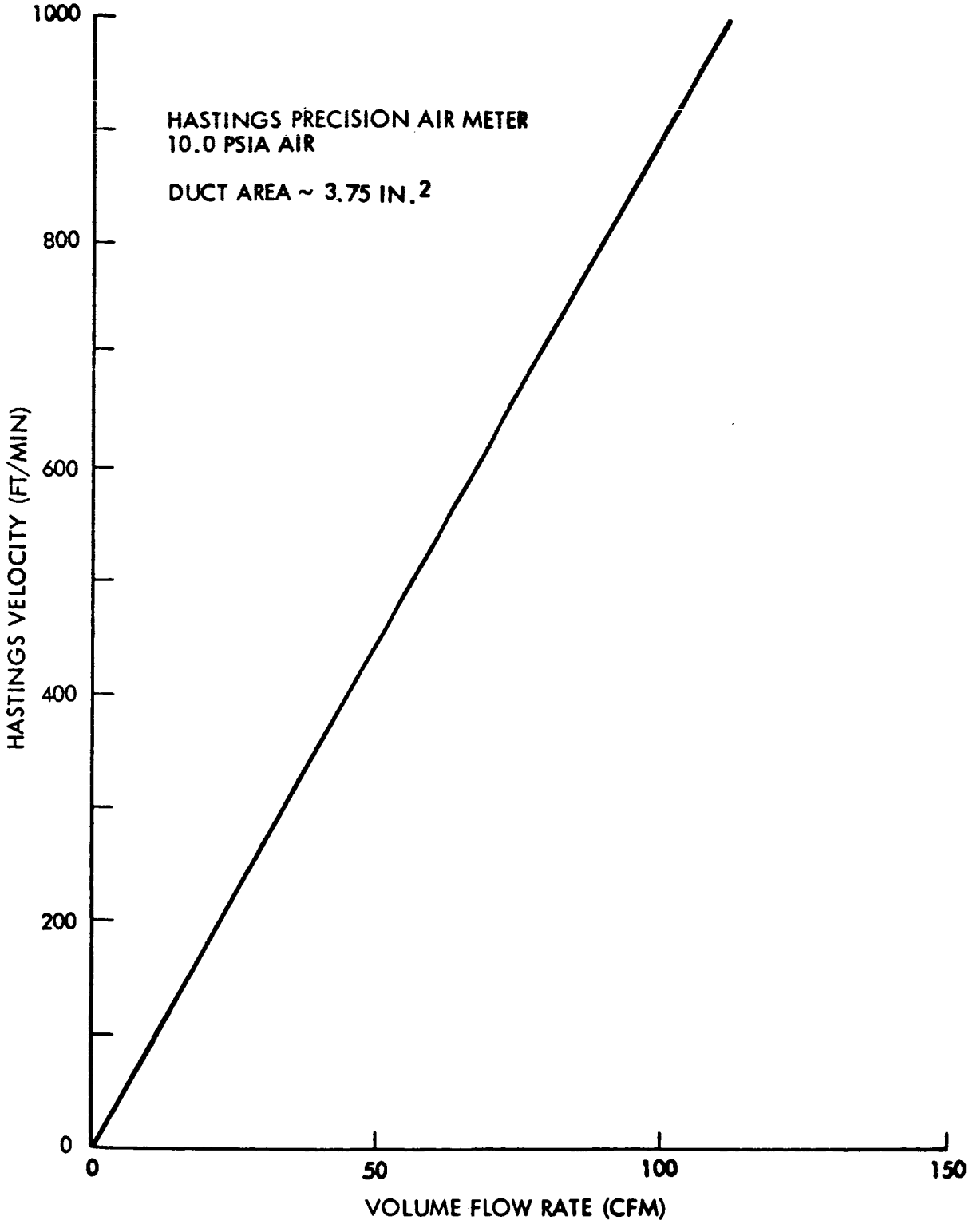

Fig. D-3 Flowrate Conversion

Run No. 1
Date - 9-27-66
Page - 2
Title - Typical Sump Performance Data

P (in H_2O) Switch Settings	Flow (cc/min)
6.5	15
8.0	33
10.0	66
12.0	92
8.0	33
11.0	air breakthrough
10.0	air breakthrough
9.0	air breakthrough
8.0	33 (no air flow)

Run No. - A1
Date - 10-3-66
Page - 5
Screen - 325 Mesh - Coarse Wire
Spinner - 1.5 turns
Coalescer - Low Density
Orientation - Horizontal
Title - Initial Horizontal Run - Low Flow

Time	γ_1	γ_2	γ_3	T_{HXO}	Flow	P_{SYS}	ΔP
4:43	4.55	3.44	3.43	35.3	630	-9.55	1.40

Run No. - A2
Date - 10-4-66
Page - 7
Screen - 325 Mesh - Coarse Wire
Spinner - 1.5
Coalescer - Low Density
Orientation - Horizontal
Title - Horizontal High Flow Run - Spinner Acting as Dam

Time	γ_1	γ_2	γ_3	T_{HXO}	Flow	P_{SYS}	ΔP
11:45	5.14	4.20	-	-	1010	-9.55	5.6

Run No. - A3
Date - 10-10-66
Page - 11
Screen - 325 Mesh - Coarse Wire
Spinner - 0 turns
Coalescer - Low Density
Orientation - Horizontal
Title - Horizontal Run - Postulate Gravity Acting as Separator

Time	γ_1	γ_2	γ_3	T_{HXO}	Flow	P_{SYS}	ΔP
11:04	5.15	4.04	4.05	43.5	1020	-9.5	.74
3:00	4.56	3.30	3.31	-	590	-9.55	.32

Run No. - A4
Date - 10-12-66
Page - 13 and 15
Screen - 325 Mesh - Coarse Wire
Spinner - 0 turns
Coalescer - Low Density
Orientation - Vertical
Title - Vertical Run - Postulate Heat Exchange as Coalescer

Time	γ_1	γ_2	γ_3	T_{HXO}	Flow	P_{SYS}	ΔP
10:52	2.10	4.35	4.33	46	1020	-9.5	1.66
2:50	55°	3.60	3.60	35.5	620	-9.5	.45

Run No. - A5
Date - 10-14-66
Page - 17
Screen - 325 Mesh - Coarse Wire
Spinner - 0 turns
Coalescer - None
Orientation - Vertical
Title - High Flow Run

Time	γ_1	γ_2	γ_3	T_{HXO}	Flow	P_{SYS}	ΔP
3:17	5.15	4.39	4.38	46.5	1020	-9.5	1.55
4:51	4.54	3.67	3.67	37	640	-9.5	.4

Run No. - A6
Date - 10-17-66
Page - 19
Screen - 325 Mesh - Coarse Wire
Spinner - 0 turns
Coalescer - None
Orientation - Vertical
Title - Full Run with Variable Specific Water Removal

Time	γ_1	γ_2	γ_2	T_{HXO}	Flow	P_{SYS}	ΔP
11:55	5.16	3.38	3.41		580	-9.6	.306
1:07	5.16	3.96	4.13		720	-9.5	.612
2:30	5.10	4.09	4.14		840	-9.55	.810
3:30	5.30	4.39	4.39	47.5	950	-9.5	1.10
4:25	5.50	4.69	4.75	52	1100	-9.5	2.14
5:40	5.15		3.64	-	580	-9.5	.356

Run No. - A7
Date - 10-18-66
Page - 21
Screen - 325 Mesh - Coarse Wire
Spinner - 0 turns
Coalescer - None
Orientation - Vertical
Title - High Flow Run - Effects of Specific Water Removal Rates

Time	γ_1	γ_2	γ_3	T_{HXO}	Flow	P_{SYS}	ΔP
10:55	3.36	3.34	3.35	-	910	-9.6	.608
11:35	3.70	3.54	3.56		900	-9.55	.628
1:05	4.05	3.76	3.73		950	-9.55	.678
1:55	4.7	4.03	4.01		950	-9.55	.750
2:40	5.3	-	4.29		890	-9.55	.928
3:05	5.72	4.48	4.53		910	-9.5	1.21
3:25	6.30	4.85	4.90		900	-9.5	1.63
4:40	5.50	4.81	4.85	53	1200	-9.45	4.2
5:00	4.90	4.14	4.14		890	-9.5	.840

Run No. - A8
Date - 10-19-66
Page - 23
Screen - 325 Mesh - Coarse Wire
Spinner - 0 turns
Coalescer - None
Orientation - Vertical
Title - Medium Flow Run - Effects of Specific Water Removal Rates

Time	γ_1	γ_2	γ_3	T_{HXO}	Flow	P_{SYS}	ΔP
11:15	3.17	3.08	3.10	-	600	-9.6	2.80
11:55	4.00	3.28	3.32	-	600	-9.55	.30
1:50	4.5	3.40	3.42	-	600	-9.55	.344
2:15	4.52	3.50	3.52		600	-9.55	.370
3:15	5.10	3.72	3.72		600	-9.55	.390
3:45	5.70	3.95	-		600	-9.55	.402

Run No. - B1
Date - 7-6-67
Page - 37
Screen - 230 Mesh
Spinner - 0 turns
Title - Standard Pressure Loss Run

Time	γ_1	γ_2	γ_3	T_{HXO}	Flow	P_{SYS}	ΔP
1:35	4.66	3.08	3.04	35	260	-9.5	.052
2:05	4.66	3.30	3.24	35	360	-9.5	.068
3:15	4.66	3.20	3.20	32	650	-9.5	0.146
4:15	4.66	3.23	3.25	32	890	-9.5	0.252
4:35	4.66	3.47	3.49	37	1100	-9.5	0.400
4:55	4.66	3.52	3.53	38	1150	-9.5	0.438

Run. No.- B2
Date - 7-27-67
Page - 51
Screen - 230 Mesh
Spinner - 0 turns
Title - Standard Pressure Loss Run

Time	γ_1	γ_2	γ_3	T_{HXO}	Flow	P_{SYS}	ΔP
2:15	-	3.08	3.05	90	280	-9.5"	0.053
2:50	4.70	3.13	3.11	115	350	-9.5"	0.064
3:00	4.70	3.25	3.20	108	640	-9.5	0.129
3:50	4.70	3.24	3.22	94	750	-9.5	0.197
4:10	4.70	3.23	3.23	87	900	-9.5	0.245
4:35	4.70	3.34	3.28	82	1000	-9.5	0.288

Run No. - B3
Date - 7-28-67
Page - 53
Screen - 230 Mesh
Spinner - 0 turns
Title - Standard Pressure Loss Run

Time	γ_1	γ_2	γ_3	T_{HXO}	Flow	P_{SYS}	ΔP
11:10	4.70	3.41	3.20	98	520	-9.5"	0.101
1:45	4.70	3.10	3.07	67	750	-9.5"	0.189
2:25	4.70	3.46	3.42	94	950	-9.5"	0.270
3:00	4.70	3.46	3.46	88	1100	-9.5	0.360
3:20	4.70	3.56	3.60	81	1180	-9.5"	0.485
4:30	4.70	3.90	3.95	90	1100	-9.5	0.412

Run No. - B4
Date - 7-12-67
Page - 41
Screen - 325 Mesh - Coarse Wire
Spinner - 0 turns
Title - Full Flow - 28 run

Time	γ_1	γ_2	γ_3	T_{HXO}	Flow	P_{SYS}	ΔP
1:40	4.47	3.55	3.58	38	1250	-9.5	2.505

Run No. - B5
Date - 7-13-67
Page - 43
Screen - 325 Mesh - Coarse Wire
Spinner - 0 turns
Title - Standard Pressure Loss Run

Time	γ_1	γ_2	γ_3	T_{HXO}	Flow	P_{SYS}	ΔP
11:00	4.70	3.23	3.26	32	470	-9.5	0.270
11:30	4.70	3.20	3.21	32	450	-9.5	0.262
2:15	4.70	3.19	3.19	32	660	-9.5	0.452
3:15	4.70	3.30	3.30	32	900	-9.5	0.930
4:40	4.70	3.37	3.40	32	1000	-9.5	1.260

Run No. - B6
Date - 7-14-67
Page - 45
Screen - 325 Mesh - Coarse Wire
Spinner - 0 turns
Title - Pressure Loss High Flow Runs

Time	γ_1	γ_2	γ_3	T_{HXO}	Flow	P_{SYS}	ΔP
10:30	4.70	3.45	3.47	38	1125	-9.5	1.550
4:00	4.70	3.47	3.53	37	1100	-9.5	1.619

Run No. - B7
Date - 10-17-66
Page - 19
Screen - 325 Mesh - Coarse Wire
Spinner - 0 turns
Title - Series I Standard Pressure Loss Run

Time	γ_1	γ_2	γ_3	T_{HXO}	Flow	P_{SYS}	ΔP
11:55	5.16	3.38	3.41	-	580	-9.6"	0.306
1:07	5.16	3.96	4.13	-	720	-9.6"	0.612
2:30	5.10	4.09	4.14	-	840	-9.55"	0.810
3:30	5.30	4.39	4.39	47.5	950	-9.5	1.10
4:25	5.50	4.69	4.75	52	1100	-9.5	2.14

Run No. - B8
Date - 7-18-67
Page - 47
Screen - 325 Mesh - Fine Wire
Spinner - 0 turns
Title - Standard Pressure Loss Run

Time	γ_1	γ_2	γ_3	T_{HXO}	Flow	P_{SYS}	ΔP
10:00	4.70	3.19	3.10	32	460	-9.5"	0.205
11:00	4.70	3.16	3.12	32	660	-9.5	0.287
11:14	4.70	3.19	3.15	32	680	-9.5	0.300
2:15	4.70	3.19	3.18	32	880	-9.5	0.432
3:25	4.70	3.24	3.27	35	1000	-9.5	0.560

Run No. - B9
Date - 7-19-67
Page - 49
Screen - 325 Mesh - Fine Wire
Spinner - 0 turns
Title - Pressure Loss High Flow Runs

Time	γ_1	γ_2	γ_3	T_{HXO}	Flow	P_{SYS}	ΔP
10:00	4.70	3.40	3.40	37	1100	-9.5	0.633
10:10	4.70	3.46	3.47	38	1200	-9.5	0.706

Run No. - B10
Date - 7-31-67
Page - 55
Screen - 230 Mesh
Spinner - 0 turns
Title - Pressure Loss Run High Inlet Humidity

Time	γ_1	γ_2	γ_3	T_{HXO}	Flow	P_{SYS}	ΔP
1:50	5.50	3.12	3.10	108	520	-9.5"	0.101
2:30	5.50	3.48	3.50	96	980	-9.5"	0.270
3:10	5.50	3.74	3.78	90	1090	-9.5"	0.370
3:50	5.50	3.47	3.41	106	750	-9.5"	0.201
4:30	5.50	3.96	4.00	88	1180	-9.5"	0.469

Run No. - B11
Date - 8-1-67
Page - 57
Screen - 230 Mesh
Spinner - 0 turns
Title - Pressure Loss Run High Inlet Humidity

Time	γ_1	γ_2	γ_3	T_{HXO}	Flow	P_{SYS}	ΔP
2:30	5.50	3.24	3.20	96	520	-9.5	0.106
3:00	5.50	3.21	3.18	92	750	-9.5	0.194
3:50	5.50	3.40	3.38	93	990	-9.5	0.310
4:20	5.50	3.58	3.59	88	1100	-9.5	0.380
4:50	5.50	3.44	3.45	84	1180	-9.5	0.445

Run No. - B12
Date - 8-8-67
Page - 65
Screen - 230 Mesh
Spinner - 0 turns
Title - Pressure Loss Run Low Inlet Humidity

Time	γ_1	γ_2	γ_3	T_{HXO}	Flow	P_{SYS}	ΔP
11:15	3.50	3.04	3.02	94	520	-9.5	0.102
11:30	3.50	3.06	3.05	86	750	-9.5	0.180
1:15	3.50	3.12	3.12	80	980	-9.5	0.300
2:00	3.50	3.27	3.29	80	1100	-9.5	0.401
2:10	3.50	3.27	3.30	79	1180	-9.5	0.485

Run No. - B13
Date - 8-9-67
Page - 63
Screen - 230 Mesh
Spinner - 0 turns
Title - Pressure Loss at Fixed Flow Variable Outlet Humidity

Time	γ_1	γ_2	γ_3	T_{HXO}	Flow	P_{SYS}	ΔP
11:30	4.70	4.22	4.21	96	950	-9.5	.286
1:00	4.70	4.22	4.23	95	950	-9.5	.288
1:10	4.70	4.07	4.08	94	950	-9.5	.288
1:20	4.70	3.96	3.96	88	950	-9.5	.290
1:30	4.70	3.86	3.89	83	950	-9.5	.289
1:50	4.70	3.76	3.76	82	950	-9.5	.288
2:05	4.70	3.70	3.70	76	950	-9.5	.288
2:10	4.70	3.56	3.57	75	950	-9.5	.288
2:20	4.70	3.42	3.41	69	950	-9.5	.288
2:40	4.70	3.27	3.29	69	950	-9.5	.298
2:50	4.70	3.25	3.27	70	950	-9.5	.295

Run No. - B14
Date - 8-10-67
Page - 69
Screen - --
Spinner - 1.5 turns
Title - Pressure Loss 1.5 Turn Spinner

Δ P	Flow	P_{SYS}
0.560	460	-9.5"
1.181	660	-9.5"
1.778	880	-9.5"
2.700	1000	-9.5"

Run No. - B15
Date - 8-10-67
Page - 69
Screen - --
Spinner - 1.0 turns
Title - Pressure Loss 1.0 Turn Spinner

Δ P	Flow	P_{SYS}
0.420	460	-9.5"
0.940	660	-9.5"
1.750	880	-9.5"
2.444	1000	-9.5"